EP/L014106/1

# Supergen Wind Hub

Sustainable Power Generation and Supply

- Wind Energy Technologies

D4.4: **Report on algorithms for wind turbine fault detection, with particular emphasis on fleet level damage model predictions**

| | | | |
|---|---|---|---|
| Delivered by: | Loughborough University | | |
| Author(s): | S J Watson, J Tautz-Weinert, R Ibrahim | | |
| Delivery date: | 23rd May 2017 | | |
| Distribution list: | Supergen Wind Hub Consortium | | |
| Version No | Status | Date | Checked by |
| 1 | Final | 23rd May 2017 | S J Watson |
| | | | |
| | | | |

This deliverable is provided in the form of several papers:

Tautz-Weinert J and Watson S J (2017). ‘Combining Model-based Monitoring and a Physics of Failure Approach for Wind Turbine Failure Detection’, 30th Conference on Condition Monitoring and Diagnostic Engineering Management (COMADEM 2017), 10th – 13th July 2017, School of Engineering, University of Central Lancashire, Preston, UK.

Tautz-Weinert J and Watson S J (2017). ‘Challenges in Using Operational Data for Reliable Wind Turbine Condition Monitoring’, The 27th International Ocean and Polar Engineering Conference, San Francisco, California, USA, 25 Jun 2017 - 30 Jun 2017.

Tautz-Weinert J and Watson S J (2017). ‘Condition monitoring of wind turbine drive trains by normal behaviour modelling of temperatures’, Conference for Wind Power Drives (CWD 2017), Aachen, $7^{th}$ - $8^{th}$ Mar 2017, pp 359-372.

Tautz-Weinert J and Watson SJ (2016). ‘Comparison of different modelling approaches of drive train temperature for the purposes of wind turbine failure detection’. Journal of Physics: Conference Series, 753, 072014.

Tautz-Weinert J and Watson S J (2016). ‘Using SCADA Data for Wind Turbine Condition Monitoring – a Review’. Accepted for publication in IET Renewable Power Generation. DOI: 10.1049/iet-rpg.2016.0248.

Ibrahim R K, Tautz-Weinert J and Watson S J (2016). ‘Neural Networks for Wind Turbine Fault Detection via Current Signature Analysis’. Proceedings of WindEurope Summit 2016, Hamburg, 27th – 30th September 2016.

Ibrahim, R and Watson, S J (2016). ‘Advanced Algorithms for Wind Turbine Condition Monitoring and Fault Diagnosis’. Proceedings of WindEurope Summit 2016, Hamburg, 27th – 30th September 2016.

Ibrahim R, Watson S J (2016). ‘Stator Winding Fault Diagnosis in Synchronous Generators for Wind Turbine Applications’. International Conference on Renewable Power Generation (RPG 2016 ), IET London: Savoy Place, UK, 21st – 23rd Sep 2016.

Ibrahim R, Daniyan A, Watson S J (2016). ‘Adaptive Fault Detection and Tracking for a Wind Turbine Generator using Kalman Filter’. 2nd International Conference on Offshore Renewable Energy - CORE 2016, 12th – 14th September 2016, Glasgow, UK.

# Advanced Algorithms for Wind Turbine Condition Monitoring and Fault Diagnosis

***Raed Khalaf Ibrahim and Simon Watson***
*Centre for Renewable Energy Systems Technology (CREST),*
*Wolfson School of Mechanical, Electrical and Manufacturing Engineering,*
*Loughborough University, UK.*
*R.Ibrahim@lboro.ac.uk, S.J.Watson@lboro.ac.uk*

***Abstract*—The work undertaken in this research focuses on advanced condition monitoring and fault detection methods for wind turbines (WTs). Fourier Transform (FFT) and Short Time Fourier transform (STFT) algorithms are proposed to effectively extract fault signatures in generator current signals (GCS) for WT fault diagnosis. With this aim, a WT model has been implemented in the MATLAB/Simulink environment to validate the effectiveness of the proposed algorithms. The results obtained with this model are validated with experimental data measured from a physical test rig. The detection of rotor eccentricity is discussed and conclusions drawn on the applicability of frequency tracking algorithms. The newly developed algorithms are compared with a published method to establish their advantages and limitations.**

***Index Terms*—Wind turbine, Generator, Condition monitoring, Current Signature, Fault signature, Fault detection, Diagnosis.**

## I. INTRODUCTION

Most components in wind turbines (WTs) are subjected to different sorts of failures during the operation, including blades, yaw systems, gearboxes rotor and shaft, bearings, generators, etc. The faulty component in WTs might change the main characteristics in the monitored signal. Traditionally, WTs condition monitoring system (CMS) is supervised using vibration signals but measuring such mechanical quantities is often expensive. Indeed, vibration sensors such as piezoelectric accelerometers and associated load amplifier are often expensive. Moreover, the ability of a clear detection of mechanical faults by vibration measurements potentially depends in the sensor locations [1]. For example, accelerometers need to be mounted near to each possible faulty component of the WT. To overcome this problem, the detection could be based on the measurement of stator currents which are already available for control purposes which means no additional sensors or data acquisition devices are needed [2]. However, there are challenges in using current measurements for WT CMS and fault detection. First, it is a challenge to extract WT fault signatures from non-stationary current measurements, due to variable-speed operating conditions of WTs. Moreover, the useful information in current measurements for WT usually has a low signal to noise ratio, and thus very difficult to extract without a dedicated signal processing.

CMS can be used to help schedule maintenance and reduce downtime [3]. However, many of these techniques evaluate WT state of health in terms of a binary state, i.e. either faulty or not. They provide technical insights and detect early abnormalities, but cannot forecast the expected degree of deterioration over a particular time frame [4]. For example, a gearbox is either broken and needs replacement or fixing, or it is fine until the next scheduled maintenance operation. CMS are carried out based using knowledge of the characteristics of signals obtained from a turbine. These signals are often non-stationary signals whose characteristics change over time due to the time-varying nature of machine operations and fault effects [5]. To date, the majority of signal processing techniques used in the condition monitoring of rotating machinery have been developed based on stationary signals and cannot reveal the time information of any frequency changes. To enable the benefits of a truly condition-based maintenance philosophy to be realized, robust, accurate and reliable algorithms, which provide maintenance personnel with the necessary information to make informed maintenance decisions, will be key. The work undertaken in this research focuses on advanced signal processing and statistical analysis techniques to lead to better remaining useful life prediction which will results in a much optimized maintenance schedule and less unscheduled maintenance events. The proposed method is based on time-frequency analysis to capture the fault frequencies from the measured signal and monitor the fault frequencies over time. This will provide the capability to potentially take historical and current data to create long-term forecasts of future asset conditions.

The following approach was taken in this paper:

- The data used in this work is recorded from a physical test rig at Durham University. Details of the data and test rig are presented in [4]. During the tests, rotor unbalance fault levels were implemented on the test rig by successively adding two additional external resistances to phase A of the rotor circuit through an external load bank. They correspond to two levels of rotor unbalance of 21% and 43%, respectively, given as a percentage of the rotor balanced phase resistance;
- A WT generator simulation model was also developed and validated with the experimental data in order to demonstrate the kind of results expected under a range of operating conditions. The model allows for certain nonlinear and time-varying characteristics and takes into account varying wind speeds similar to those experienced by WTs;
- Other aspects of this work are related to the use of the Gabor transform for time- frequency analysis. Another aspect is the observation of the change of the fault signature for different wind speed and fault level cases. This observation was connected theoretically with what is known as fault prognostics process;
- Finally, the Gabor transform for time- frequency analysis was proposed as a potential method for detecting early anomalies in WT generator operation;

## II. FAULT SIGNATURE ANALYSIS IN WIND TURBINE CURRENT SIGNALS

Mechanical faults such as unbalanced load and shaft misalignments essentially create a rotor eccentricity inside the motor [6]. These types of faults introduce sideband harmonics around the fundamental frequency in the motor current spectrum. Potentially, these fault signatures could be used to detect incipient failure if they can be clearly detected during the early stages of a developing fault. It has been reported that during a rotor eccentricity event, the sideband currents are given by [7]

$$f_{ecc,d} = \left(1 \pm \frac{k(1-s)}{p}\right).f \tag{1}$$

Where $f_{ecc,d}$ and $f$ are the rotor fault and fundamental frequency components for a doubly fed induction generator (DFIG), respectively, $k$ is an integer ($k$=1, 2, 3, ...) and $p$ the number of pole pairs.

## III. SIGNAL PROCESSING TECHNIQUES FOR FAULT DETECTION

Signal processing is used in WT fault studies and is becoming an important class of tools to facilitate the extraction of fault-related features in the monitored signals, and then, the fault detection can be automated via threshold comparison or probability analysis. The fault level and location can then be identified by a classification method, such as artificial neural networks, fuzzy logic, support vector machines, etc. A key aspect of a reliable and efficient condition monitoring technique in WTs is determining which parameters should be measured and to what accuracy, as well as which signal processing methods provide the best characterization and analysis of the signals to be investigated.

### A. Fast Fourier Transform

The Fast Fourier Transform (FFT) is one of the most well-known methods in the area of signal processing and has been widely used in fault diagnosis for Motors. The FFT algorithm is used to convert the time domain signal into a frequency domain signal in order to extract features related with characteristic defects. Fig. 1 shows a Fourier Transform of the stator current from the Durham test generator operating in a normal healthy state.

The upper plot is actual measured data and the lower plot is the WT generator simulation model set up using similar parameters to the test rig. The generator was driven close to a fixed rotational speed corresponding to a fixed wind speed, but with a degree of variation corresponding to a certain simulated level of wind turbulence.

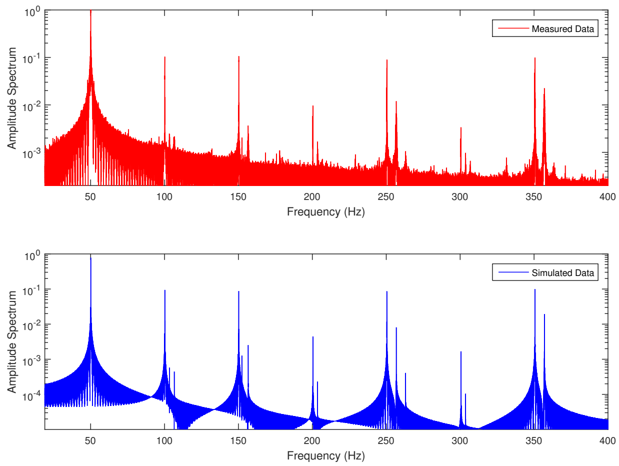


Fig. 1: The FFT of GCSs for the healthy case.

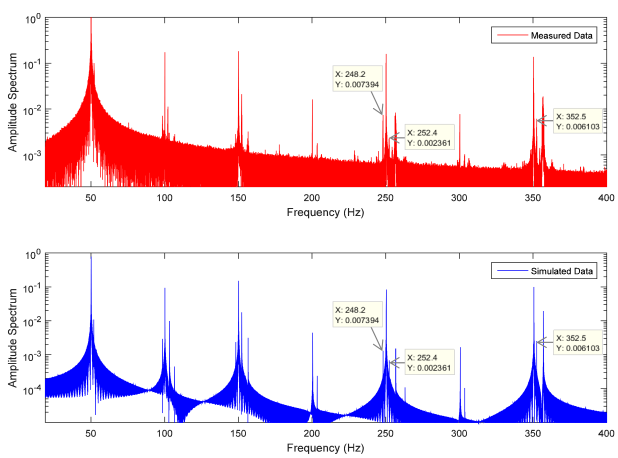


Fig. 2: The FFT of GCSs for the rotor unbalance case.

As can be seen in Fig. 1, there are unexpected harmonics around the even and odd harmonics even when operating in a healthy state (no unbalance). This might be caused by manufacturing and installation errors or might be frequency components that are apparent when the generator is first turned on. Fig. 2 shows a similar spectrum, but this time the rotor is subject to a degree of unbalance. Although the amplitudes of those frequency components in the rotor unbalance case shown in Fig. 2 are different from those in Fig. 1, it is difficult to distinguish the two cases. The fault signature frequencies are defined and labelled in Fig. 2 according to Equation (1).

### B. Short Time Fourier Transform (STFT)

The limitations of the direct application of the Fourier transform methods, and their inability to localize a signal in both the time and frequency domains, was realized very early on in the development of radar and sonar detection. The Hungarian electrical engineer and physicist Gabor Denes (Physics Nobel Prize in 1971 for the discovery of holography in 1947) was the first person to propose a formal method for localizing both time and frequency [8]. His method is known as the short-time Fourier transform (STFT), STFT of a continuous-time signal $x(t)$ is defined as:

$$STFT(f,\tau) = \int_{-\infty}^{\infty} x(t)g(t-\tau)e^{-j2\pi ft}\,dt \qquad (2)$$

where $g(t-\tau)$ is the window function whose position is translated in time by $\tau$. The integration over the parameter $\tau$ slides the time-filtering window along the entire signal in order to pick out the frequency information at each instant of time. Fig. 3 gives a clear illustration of how the time filtering scheme of STFT works. In this figure, the time filtering window is centered at  with a width $a$. Thus the frequency content of a window of time is extracted and  is modified to extract the frequencies of another window. The definition of the STFT captures the entire time-frequency content of the signal. Indeed, the STFT is a function of the two variables time and frequency.

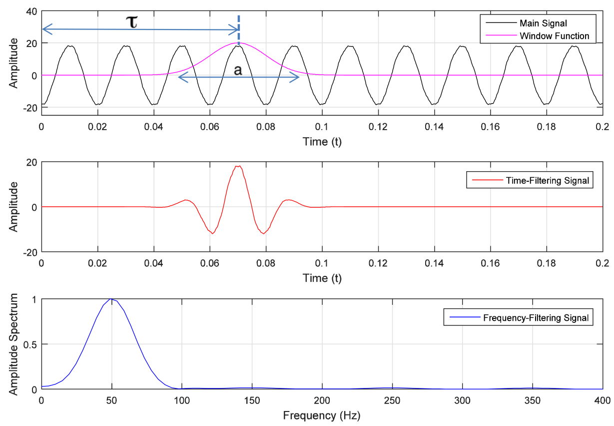


Fig. 3: Graphical illustration of the STFT for extracting the time-frequency content of a measured signal.

The key now for the STFT is to multiply the time filter function with the original signal in order to produce a windowed section of the signal. The Fourier transform of the windowed section then gives the local frequency content in time. Fig. 4 shows the generated spectrogram for the measured stator current signal for the healthy test rig generator. It is clearly seen that the measured time signal is comprised of various frequency components that are seen throughout the entire time.

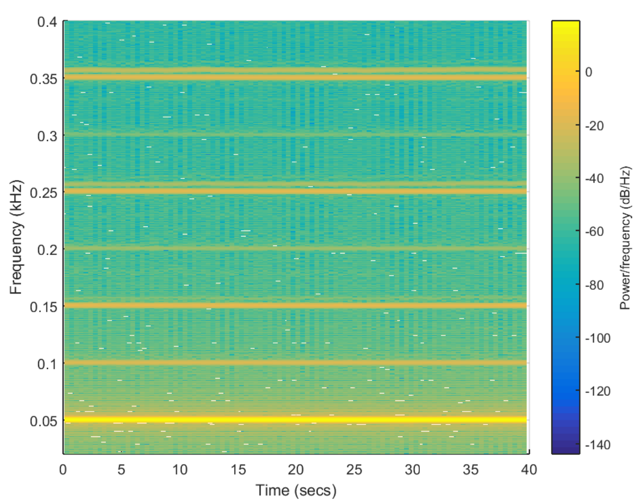


Fig. 4: The STFT of GCSs for the healthy case.

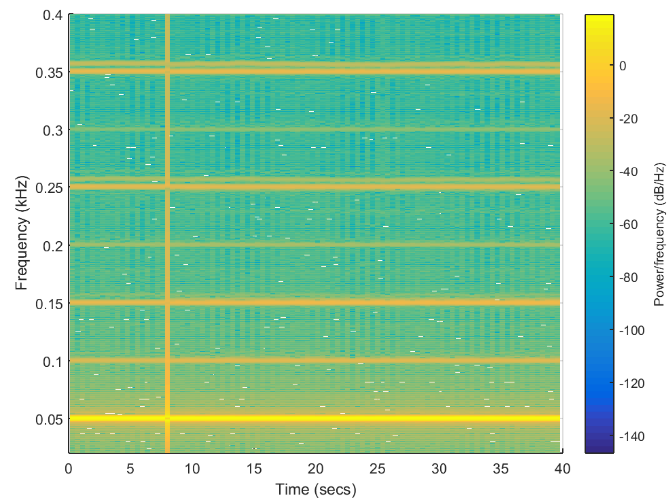


Fig. 5: The FFT of GCSs for the rotor unbalance case.

Figure 5 shows the stator current spectrogram after rotor unbalance conditions were applied. Although the fault characteristic frequency components are combined and buried in other dominant frequency components of the current signal that are irrelevant to the fault, the STFT captures the moment in time when the fault actually occurs at t=8 sec. This is clearly the main disadvantage of the STFT, and their capability to localize the frequency components of the measured signal in time domain, when compared to the Fourier transform. One could admit that this is a very apparent indication of the fault presence using this simple approach. In order to have a clear understanding of how we could use the STFT for faults prognosis, the same datasets are used again in the next example (Figure 6), this time after applying transient rotor unbalance fault from t=20sec to t=30 sec to see if we can still forecast the fault over time. What is shown here is that the fault signature frequencies are seen only during the time between (20-30 sec). So it is clear from this simulation, that the proposed method can be used to provide the capability to take historical and current data to create highly accurate long-term forecasts of future asset conditions.

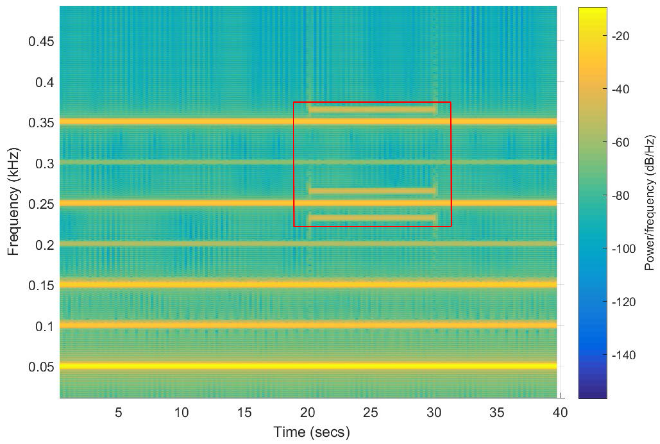


Fig. 6: The STFT of simulated GCSs for the transient fault.

## IV. Conclusion

A new approach based on time-frequency analysis of signals has been proposed, for fault diagnosis WTs to lead to better remaining useful life prediction which will result in a much optimized maintenance schedule and less unscheduled maintenance events. The simplest novelty in this work that the use of STFT for time- frequency analysis as a potential method for detecting and forecasting early abnormalities over a substantial time. Preliminary simulation results presented highlight its advantages over the conventional Fourier transform approach, and go on to indicate its potential and suitability.

## References


[1] Y. Amirat, M. Benbouzid, B. Bensaker, and R. Wamkeue, "Condition monitoring and ault diagnosis in wind energy conversion systems: a review," in *Electric Machines & Drives Conference, 2007. IEMDC'07. IEEE International*, vol. 2, pp. 1434–1439, IEEE, 2007.

[2] X. Gong and W. Qiao, "Current-based mechanical fault detection for direct-drive wind turbines via synchronous sampling and impulse detection," *Industrial Electronics, IEEE Transactions on*, vol. 62, no. 3, pp. 1693–1702, 2015.

[3] W. Qiao and D. Lu, "A survey on wind turbine condition monitoring and fault diagnosispart i: Components and subsystems," *IEEE Transactions on Industrial Electronics*, vol. 62, no. 10, pp. 6536–6545, 2015.

[4] J. Nilsson and L. Bertling, "Maintenance management of wind power systems using condition monitoring systemslife cycle cost analysis for two case studies," *IEEE Transactions on energy conversion*, vol. 22, no. 1, pp. 223–229, 2007.

[5] S. Nandi, H. A. Toliyat, and X. Li, "Condition monitoring and fault diagnosis of electrical motors-a review," *IEEE transactions on energy conversion*, vol. 20, no. 4, pp. 719–729, 2005.

[6] S. Nandi, H. Toliyat, and X. Li, "Condition monitoring and fault diagnosis of electrical motors-a review," *Energy Conversion, IEEE Transactions on*, vol. 20, pp. 719–729, Dec 2005.

[7] A. J. M. Cardoso *et al.*, "Discriminating the simultaneous occurrence of three-phase induction motor rotor faults and mechanical load oscillations by the instantaneous active and reactive power media signature analyses," *Industrial Electronics, IEEE Transactions on*, vol. 59, no. 3, pp. 1630–1639, 2012.

[8] S. F. Johnston, "Absorbing new subjects: holography as an analog of photography," *Physics in Perspective*, vol. 8, no. 2, pp. 164–188, 2006.

# Using SCADA Data for Wind Turbine Condition Monitoring – a Review

Jannis Tautz-Weinert*, Simon J. Watson

Centre for Renewable Energy Systems Technology, Wolfson School of Mechanical, Electrical and Manufacturing Engineering, Loughborough University, Loughborough, LE11 3TU, United Kingdom
*j.tautz-weinert@lboro.ac.uk

**Abstract:** The ever increasing size of wind turbines and the move to build them offshore have accelerated the need for optimised maintenance strategies in order to reduce operating costs. Predictive maintenance requires detailed information on the condition of turbines. Due to the high costs of dedicated condition monitoring systems based on mainly vibration measurements, the use of data from the turbine Supervisory Control And Data Acquisition (SCADA) system is appealing. This review discusses recent research using SCADA data for failure detection and condition monitoring, focussing on approaches which have already proved their ability to detect anomalies in data from real turbines. Approaches are categorised as (i) trending, (ii) clustering, (iii) normal behaviour modelling, (iv) damage modelling and (v) assessment of alarms and expert systems. Potential for future research on the use of SCADA data for advanced turbine condition monitoring is discussed.

## 1. Introduction

The global capacity of installed wind power stood at 432 GW at the end of 2015 [1]. The industry has long moved on from small clusters of turbines where maintenance access was relatively straightforward and the overhead of sending a maintenance team in at regular intervals was not excessive. In the case of offshore wind farms, in particular, the cost of maintenance relative to the levelised cost of energy (LCOE) is significantly increased compared to onshore. According to [2], the typical cost of operation and maintenance (O & M) as a fraction of the LCOE is between 18% and 23% compared to 12% for onshore with recent European offshore O & M costs amounting to between 40 and 44 Euros/MWh [3]. The restrictions imposed by the offshore environment as well as the increasingly large number of machines in a typical wind farm means that maintenance is moving to what in the past would have been scheduled or responsive to a regime that is more predictive and proactive. A key element in this move has been the more intelligent monitoring of wind turbine (WT) state of health, generally termed condition monitoring (CM).

So-called condition monitoring systems (CMS) have been developed by a number of manufacturers. These monitor several key parameters including drive train vibration, oil quality and temperatures in some of main subassemblies. Such systems are normally installed as additional ‘add-ons’ to the standard WT configuration. The significant costs of CMS – usually more than 11,000 Euros per turbine [4] – has deterred operators from installing these systems, although the financial benefit of early fault detection by CMS has been proven [5]. However, all large utility scale WTs have a standard Supervisory Control and Data Acquisition (SCADA) system principally used for performance monitoring. Such systems provide a wealth of data at normally 10-minute resolution, though the range and type of signals recorded can vary widely from one turbine type to another. As CM using SCADA data is a potentially low cost solution requiring no additional sensors, a number of approaches using these data for early failure detection have been developed in recent years.

A number of general literature reviews of WT CM have been conducted in the last decade to gather together information on new approaches and techniques. A comprehensive collection of CM techniques sorted by CM system and fault detection for different subsystems was provided by [6]. An overview of CM methodologies and signal processing techniques complemented by a fault tree analysis were given in [7]. A systematic literature review in [8] revealed the geographical contribution to this research topic and listed different approaches. An extensive review linked monitoring techniques with possible failures [9]. Considerations of the advantages, disadvantages, costs, online feasibilities, fault diagnosis abilities and deployment statuses of CM methodologies were discussed in [5]. The latest review considering complexity, capability, signal-to-noise ratio, sampling frequency and cost of multiple approaches was given in [10, 11]. However, to date, there has not yet been a detailed review of the use of SCADA data for the CM of WTs. In this paper, the use of SCADA data in this regard is covered including the potential for monitoring different subassemblies and the ways in which SCADA data are actually used to predict, diagnose and prognose failure.

In the next section, WT reliability and failure rates of subassemblies are briefly reviewed. The next and main part of this paper addresses the use of SCADA data for CM. The final section discusses the strengths and weaknesses of the different approaches reviewed and highlights areas for future research.

## 2. Failure statistics

Several surveys of WT failures have been conducted in the last two decades to identify failure rates and associated downtime for different subassemblies. However, the different taxonomies used by different turbine manufacturers, wind farm operators and researchers make comparisons between these surveys challenging.

The evaluation of 15 years of data from the German “250 MW Wind” programme [12] and >95% of all the turbines operating between 1997 and 2005 in Sweden [13] gave first insights into the reliability of the first onshore WTs. The German turbines had an average availability of about 98%. An average failure rate of 0.4 failures per turbine per year resulted in an average downtime of 130 hours per turbine per year for the Swedish turbines. A distinctive difference between failure rate and downtime distribution in subassembly groups was identified. The electrical and electronic control systems were identified as the most failure-prone, but gearbox and generator failures caused the longest downtime.

An evaluation of the Windstats newsletter providing statistics for turbines in Denmark and Germany for a similar time range revealed differences in failure rates of WTs in the two countries [14]. Higher failure rates for the German turbine population were traced back to the different age and the newer (but less mature) variable speed and pitch control technology employed in German turbines. The electrical system was the most failure-prone subassembly in the German turbine population, whereas the Danish population was mostly affected by yaw system and so-called “unclassified” failures. Records of the Chamber of Agriculture in Schleswig-Holstein, Germany, confirmed the failure rates for German WTs [15]. The different studies up to this time agreed that the gearbox had been the source of failure with the longest downtime [16]. An analysis of the first operating years of the UK Round 1 offshore wind farms revealed availabilities of only 80.2%. The main causes for this relatively low availability were found to be gearbox and generator bearing problems [17].

A more recent failure survey was conducted as part of the Reliawind project [18]. In this survey, 35,000 downtime events from 350 WTs were evaluated. The order of the subsystem failure rates was found to be led by the power module assembly followed by rotor module, control system, nacelle and drive train in descending order. The three most failure-prone subassemblies were identified as the pitch system, frequency converter and the yaw system. The downtime hierarchy was very similar to the failure rate order. This finding was in contrast to previous studies, which found that the gearbox was the greatest contributor to unscheduled turbine downtime.

A report from the National Renewable Energy Laboratory (NREL) in the US [19] stated that approx. 70% of gearbox failures were caused by bearing faults and approx. 26% by gear teeth faults based on a database of 289 failure events collected from 20 partners since 2009.

Carroll *et al.* [20] compared failure rates in the first five years of 1822 turbines with Doubly-Fed Induction Generators (DFIGs) with 400 turbines using a Permanent Magnet Generator (PMG) with a fully rated converter. For the PMG turbines, a lower generator failure rate was found to be accompanied by a much higher failure rate in the converter.

The most recent analysis of failure statistics from Carroll *et al.* [21] looked at data from around 350 relatively new offshore turbines from one manufacturer recorded over a 5 year period at 5-10 wind farms. The failure rates were highest for the pitch/hydraulic subassembly, followed by “other components” and the generator, but only those failures were considered where unscheduled maintenance visits were made. Analysis of the failure rate by year of operation showed a decrease in the first five years. A comparison with onshore turbines [20] suggested higher failure rates offshore, but not as high as expected given the different turbine populations and environmental characteristics. Analysis of average repair times, material costs and the number of required technicians indicated that blades, hub and gearbox were the most critical subassemblies in this context.

## 3. Review of approaches to utilise SCADA data for CM

This review focuses on CM approaches, which have already been applied using real data from operational WTs. Different methods have been developed, which are classified as (i) ‘trending’, (ii) ‘clustering’, (iii) ‘normal behaviour modelling’ (iv) ‘damage modelling’ and (v) ‘assessment of alarms and expert systems’. Class (v) covers how alarm logs and modelling results can be automatically interpreted. The usage of SCADA data for purposes besides CM is briefly outlined in (vi) ‘other applications’.

The parameters typically recorded by SCADA systems of geared-drive turbines are listed in Table 1. In general, SCADA records are 10-minute averages of 1 Hz sampled values. However, maximum, minimum and standard deviation are often recorded as well. The number of starts and stops and alarm logs recorded by the SCADA system can also be seen as part of CM [22]. Vibrations [4, 23], oil pressure level and filter statuses [24] could be recorded by a WT SCADA system too, but these are commonly recorded separately in a what might be termed a ‘dedicated’ CMS. There is no such thing as a standard set of monitoring equipment or measurement nomenclature for the different turbine populations seen today. Nevertheless, a general trend has been seen for the installation of more sensors in modern turbines. An overview of commercially available SCADA systems is given in [5, 25].

**Table 1** Basic SCADA parameters according to [4, 5, 22, 26–32].

| Environmental | Electrical characteristics | Part temperatures | Control variables |
|---|---|---|---|
| Wind speed | Active power output | Gearbox bearing | Pitch angle |
| Wind direction | Power factor | Gearbox lubricant oil | Yaw angle |
| Ambient temperature | Reactive power | Generator winding | Rotor shaft speed |
| Nacelle temperature | Generator voltages | Generator bearing | Generator speed |
| | Generator phase current | Main bearing | Fan speed / status |
| | Voltage frequency | Rotor shaft | Cooling pump status |
| | | Generator shaft | Number of yaw movements |
| | | Generator slip ring | Set pitch angle / deviation |
| | | Inverter phase | Number of starts / stops |
| | | Converter cooling water | Operational status code |
| | | Transformer phase | |
| | | Hub controller | |
| | | Top controller | |
| | | Converter controller | |
| | | Grid busbar | |

### *3.1. Trending*

Although WT SCADA systems have not been developed specifically for the purposes of CM, using SCADA data to monitor the health of turbines has been investigated as soon as optimising maintenance became a high priority in the wind industry. The main challenge lies in how to interpret trends given the variability in the operational conditions of modern WTs. A change in the value of a SCADA parameter is accordingly not necessarily evidence for a fault. One of simplest approaches is to collect data over a long period and monitor ratios of SCADA parameters and how they change over time. Past studies have involved trying to find early signs of degradation by using such trending approaches.

Research in the Condition Monitoring for Offshore Wind Farms (CONMOW) project carried out from 2002 to 2007 included SCADA CM techniques [33]. Simple trending methods e.g. using regression lines in scatter diagrams of temperature against power or three-dimensional visualisations including the ambient temperature were suggested. Manual interpretation of filtered SCADA data comparisons was seen as beneficial for detecting anomalies. Due to the lack of faults during the measurement campaign conducted on five turbines, detailed algorithms were not developed.

Kim *et al.* [34] investigated a Principal Component Analysis (PCA) trending approach with an auto-associative neural network. The structure of this network consisted of one input layer, a mapping layer, a bottleneck layer, a de-mapping layer and an output layer. After training with data from normal operation, the network produced a set of principal components, which were evaluated using the Q-statistic (a measure of uncaptured variation) and the Hotelling $T^2$ statistic (a measure of the model variation). Testing the approach using a known fault case from the 600kW Control Advanced Research Turbine 2 located at NREL proved the general ability to detect a failure thought no advance signs of the fault were detected. Testing using another control data set where no known faults occurred showed that false detections could occur.

Feng *et al.* [24, 35] showed that if the gearbox efficiency decreases, the gearbox temperature rise (compared to the ambient temperature) will increase. Example gearbox oil temperature trends from a case study of a 2 MW variable speed turbine are shown grouped by power bin in Fig. 1. The deterioration of the gearbox is already visible 6 months before a catastrophic planetary gear failure.

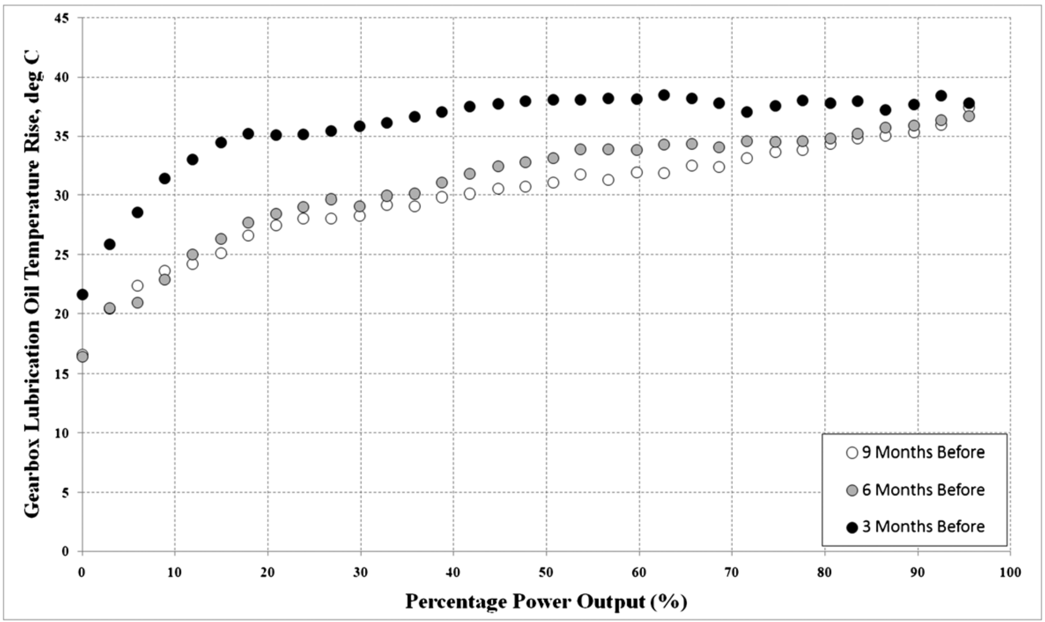


***Fig. 1.*** *Gearbox oil temperature rise by power bin during a developing failure from* [24].
*Reprinted from* [24], *Copyright 2012 with permission of John Wiley and Sons, Ltd.*

Yang *et al.* [4] proposed a trending method using bin averaging by wind speed, generator speed or output power. Two case studies with real turbines were analysed: a three-bladed turbine with a generator bearing failure; and a two-bladed turbine with a blade failure as shown in Fig. 2 (a) and (b), respectively. A CM quantifying criterion (denoted 'c') based on a correlation model of historic and present data was proposed as a way of detecting levels of damage, though the value of the criterion has a different scale depending on the damage mode and dependent parameter.

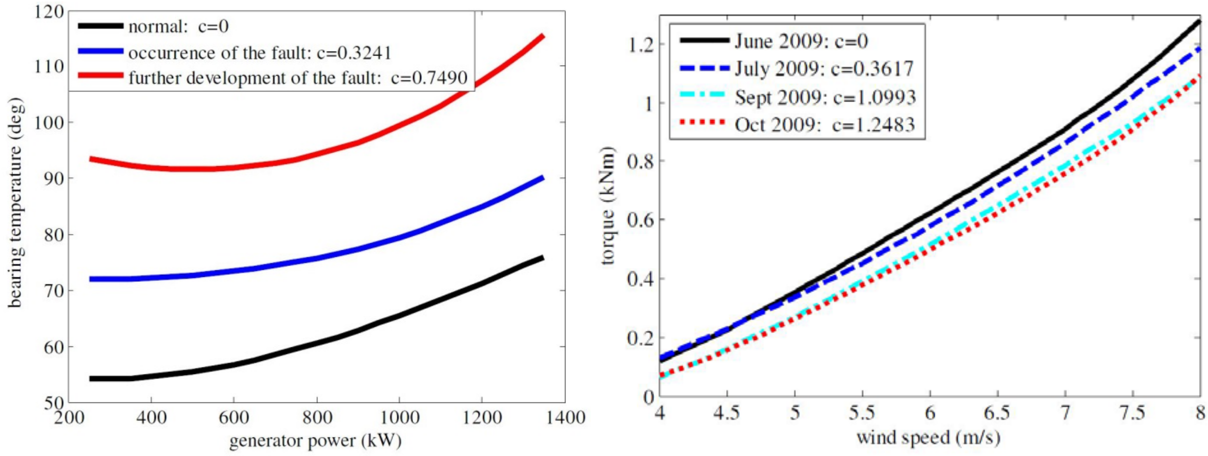


*a* *b*

***Fig. 2.*** *Generator bearing fault detected through generator bearing temperature and blade deterioration detected through generator torque for different stages of the faults. Additionally, a calculated CM fault severity parameter 'c' is shown* [4]*. Reprinted from* [4]*, Copyright (2013), with permission from Elsevier.*
a Generator bearing fault detection in filtered bearing temperature
b Blade deterioration detection in filtered torque (calculated from generator power and rotor speed).

Astolfi *et al.* [36] investigated trending of temperatures against the rated power over different time scales. Comparisons of results for a nine turbine onshore wind farm of 2 MW turbines were made. Historical and real time analyses helped the operator to detect problems.

Wilkinson *et al.* [31] investigated different methods of using SCADA data for CM. One approach included a simple comparison of temperature trends of different turbines in a particular wind farm. The authors ultimately dismissed this approach due to inaccuracy resulting from differing environmental conditions or operational modes in a wind farm.

Trending of SCADA parameters, especially drive train temperatures, can reveal the development of a failure using historical data. However, different studies have shown that changes in temperature are highly case-specific and require manual interpretation. Using a numerical description of the trend instead of visual interpretation of scatter diagrams did not prove to be beneficial. If trending is to be used for online monitoring, difficulties in the interpretation of changes and the setting of thresholds will most likely result in high uncertainties and possibly false alarms.

### *3.2. Clustering*

Visual interpretation of trends can be problematic if a large fleet of wind turbines operating under very different conditions is to be monitored cost-effectively. A next step in the evolution of CM with SCADA data was the application of clustering algorithms to automate the classification of 'normal' and 'faulty' observations.

Kusiak and Zhang [37, 38] analysed WT vibrations using SCADA records including drive train and tower acceleration. Vibrations were grouped by a modified k-means clustering algorithm conditioned on the wind speed. Abnormal vibrations were detected by measuring the Euclidean distance between data and cluster centroids built in an initial training period. Limitations in determining the boundaries of clusters and the missing description of temporal changes were acknowledged and subsequently a normal behaviour modelling approach was pursued.

Catmull [28] and Kim *et al.* [34] were the first to apply an artificial neural network (ANN) self-organising map approach to SCADA data. The method builds clusters by rearranging neurons on a regular grid during the training process in a way that neighbouring neurons denote similar input data. A unified distance matrix can be used to visualise the clustering. In combination with projections of parameters, this enables interpretation of the clustering. Fig. 3 shows a general example of a clustering with self-organizing maps. Catmull used only normal operational data for training and proposed the calculation of the distance between new input data and the best matching neuron, called quantisation error, for abnormality detection. Example applications of the method using data from WTs with a sensor error, reactive power loss and an unidentified generator failure showed a general ability to detect failures. Kim *et al.* used a training data set, which included failures. They were then able to assign subsequent WT failures to corresponding clusters. Wilkinson *et al.* [31] pursued Catmull's approach and presented some examples of detecting gearbox failures comparing the quantisation error for multiple turbines.

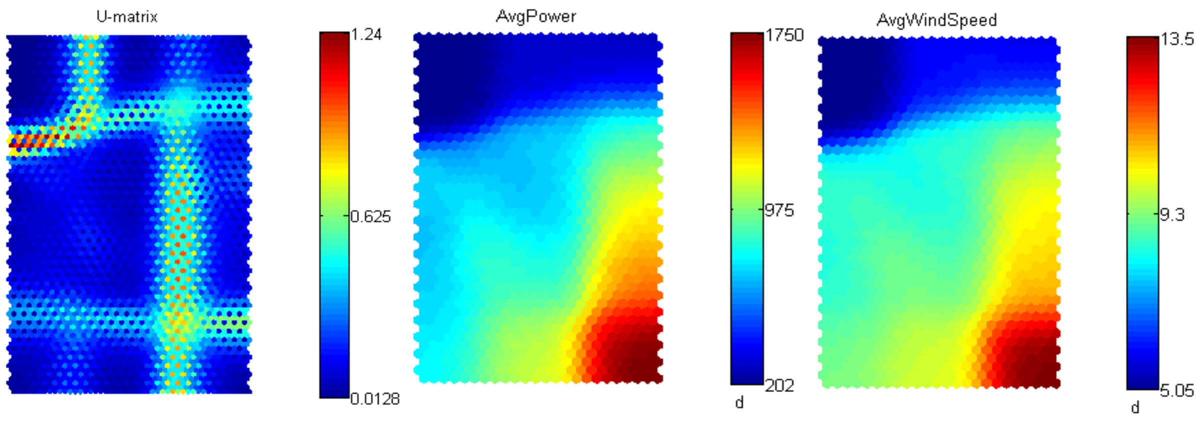


*a* *b* *c*

***Fig. 3.*** *General self-organizing map example from* [28] *showing in particular one cluster in the upper left and one in the lower right corner. Reprinted with permission of* [28]*. Copyright 2011, RES Offshore.*
a Unified distance matrix. Higher values indicate a greater Euclidean distance between the nodes.
b Power output component plane .
c Wind speed component plane.

From the evidence reviewed, the clustering of healthy and faulty observations has not shown a clear advantage in terms of CM compared to trending algorithms, as the interpretation of results is again difficult. In addition, using fault data for training is not necessarily feasible in an industrial setting.

### 3.3. Normal behaviour modelling (NBM)

NBM uses the idea of detecting anomalies from normal operation as used in the previous methods, but tries to empirically model the measured parameter based on a training phase. Fig. 4 illustrates the idea of model-based monitoring. The residual of measured minus modelled signal acts as a clear indicator for a possible fault: it is assumed to be approx. 0 with a given tolerance for normal conditions and not equal to 0 for changed conditions or failures. Two main concepts for NBM can be differentiated: Full Signal ReConstruction (FSRC), where only those signals, other than the target are used to predict the target, and AutoRegressive with eXogenous input modelling (ARX), where historic values of the target are also used.

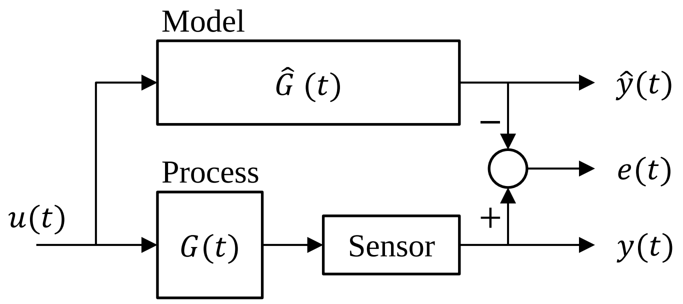


***Fig. 4.*** *Model-based monitoring with the input $u(t)$ for both the process $G(t)$ and its model $\hat{G}$, their outputs $y(t)$ and $\hat{y}(t)$, respectively, and the final error or residual $e(t)$. Sketch adapted from* [39].

*3.3.1. Linear and polynomial models:* The simplest form NBM is based on linear or polynomial models. Garlick *et al.* [39] used a linear ARX model to detect generator bearing failures in the bearing temperature. A cross-correlation analysis was conducted, i.e. the sample cross-correlation was computed as an estimate of the covariance between the target signal and each possible input. The correlation analysis determined that the generator winding temperature was the best exogenous input. Different numbers of polynomial parameters were investigated and evaluated with the coefficient of determination and Akaike's Information Criterion. 3 years of SCADA data for 12 turbines were evaluated with a three-parameter model trained with one day of data. Some of the detected anomalies were found to correlate with fault log reports.

Cross and Ma [23] investigated different NBM approaches using SCADA data from 26 turbines and 16 months of operation. Gearbox and generator winding temperatures were modelled using wind speed and active power in an ARX model. The coefficients of determination were only moderate for normal operation with 0.710 and 0.833 for the gearbox and winding temperature, respectively. No detailed study on linear models was conducted, as other approaches were considered as more suitable.

Wilkinson *et al.* [31] developed higher order polynomial FSRC models for NBM of drive train temperatures with different SCADA inputs based on correlation analysis and the physics of the system. Data from the same turbine, different turbines at the same site as well as different turbines at different sites were used. The developed algorithms were blind tested on 472 turbine years of data from five different wind farms. Examples of successful detection of gearbox and main bearing failures by modelling of a bearing or gearbox temperature with rotor speed, power output and the nacelle temperature were presented. Overall, 24 of 36 component failures were detected with only three false alarms with accuracy highly dependent on the wind farm. The algorithm resulted in detection of failures from one month to two years in advance.

Schlechtingen and Santos [40] developed a linear model based on up to 14 months of SCADA data from ten 2 MW offshore WTs. The linear FSRC model for the generator bearing temperature built with generator power output, nacelle temperature and shaft speed as inputs predicted the target temperature with an accuracy of ±4°C after filtering. A catastrophic generator bearing failure of one turbine was successfully detected as shown in Fig. 5. The use of daily averages of the residual was demonstrated to be plausible for the purposes of fault detection. The first alarm limit violation was 25 days prior to the damage.

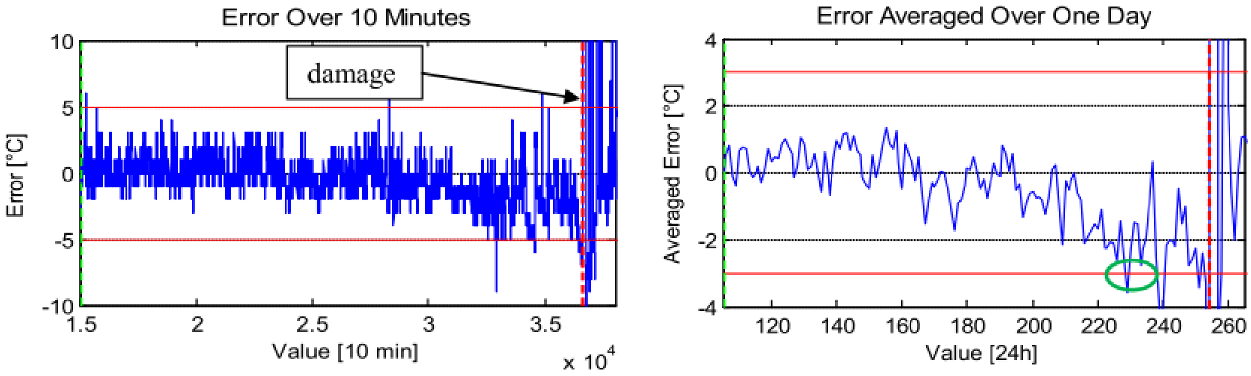


*a* *b*

***Fig. 5.*** *Regression based generator bearing temperature modelling showing a catastrophic failure* [40]. *If the residual of measurement minus modelled temperature ("error") is higher than the threshold, damage is likely. Reprinted from* [40], *Copyright (2010) with permission from Elsevier.*
a 10 minute prediction error
b Daily averaged prediction error

*3.3.2. Artificial Neural Network (ANN):* ANNs are a way of determining non-linear relationships between observations using training data. The basic architecture for modelling contains one input layer, a variable number of hidden layers and one output layer. Each layer consists of different numbers of neurons, which are fed by all inputs or other neuron outputs from the previous layer. The basic learning of the network involves the changing of input weights. Each neuron consists of a nonlinear transfer function to combine the inputs and an activation function deciding if output is generated. Common networks are feed-forward, i.e. only with links from lower to higher layers, in contrast to recurrent architectures [27, 41].

Garcia *et al.* [26] developed an intelligent system for predictive maintenance called SIMAP based on ARX NBM with ANNs. Table 2 shows the inputs used in this work for modelling of the gearbox bearing temperature, the cooling oil temperature and the difference in the cooling temperature before and after the gearbox determined by cross-correlation and impulse response analyses. A confidence level of 95% was proposed resulting in lower and upper bands for the detection of anomalies by comparison with measured values. Garcia *et al.* did not provide details of the ANN configuration and training algorithm or any results of a detailed case study.

**Table 2.** Inputs for ANN based modelling in SIMAP [26] Reprinted from [26],Copyright (2006) with permission from Elsevier.

| Model | Type | Inputs |
|---|---|---|
| Gearbox bearing temperature model | Multilayer perceptron | Gearbox bearing temperature (*t* - 1, *t* - 2) |
| | | Generated power (*t* - 3) |
| | | Nacelle temperature (*t*) |
| | | Cooler fan slow run (*t* - 2) |
| | | Cooler fan fast run (*t* - 2) |
| Gearbox thermal difference model | Multilayer perceptron | Gearbox thermal difference (*t* - 1) |
| | | Generated power (*t* - 2) |
| | | Nacelle temperature (*t*) |
| | | Cooler fan slow run (*t* - 2) |
| | | Cooler fan fast run (*t* - 2) |
| Cooling oil temperature model | Multilayer perceptron | Cooling oil temperature (*t* - 1) |
| | | Generated power (*t* - 2) |
| | | Nacelle temperature (*t*) |
| | | Cooler fan slow run (*t* - 2) |
| | | Cooler fan fast run (*t* - 2) |

Zaher *et al.* [27] investigated ANN based gearbox bearing and cooling oil temperature modelling and demonstrated its ability using 2 years of SCADA data for 26 Bonus 0.6 MW stall-regulated turbines. An ANN with 3 neurons in the hidden layer was presented as the best architecture. The inputs for the two investigated FSRC models were based on cross-correlation and included values from previous time-steps. Roughly 13,000 training data points were manually chosen to represent normal behaviour. Zaher *et al.* were able to detect a gearbox fault in one turbine with the trained model. Overheating problems were detected almost 6 months before the failure of one turbine. The interpretation of the highly fluctuating residual with several spikes was not conclusively explained, as no simple threshold would result in the depicted diagnosis.

Brandão *et al.* [42, 43] applied a FSRC ANN approach to gearbox and generator fault detection in a Portuguese wind farm with 13 turbines with 2MW rated power and an US farm consisting of 69 turbines with 1.5 MW rated power. The inputs were chosen based on cross-correlation and included appropriate delays. It was stated that at least 6 months' training data were needed, but details of settings were not provided. A fixed value of the mean absolute error was used as an alarm level, although this value was specific and not valid after maintenance actions.

Schlechtingen and Santos [40] compared a linear model (as described earlier) with two different ANN model configurations in a study of up to 14 months' SCADA data from ten 2 MW offshore WTs. The FSRC model used the generator stator temperature, nacelle temperature, power output and generator speed to predict the generator bearing temperature. The second model, an ARX approach, used additional historic values of the generator bearing temperature. A feed-forward network with one hidden layer with 5 or 6 neurons for FSRC and ARX modelling, respectively, was trained with three months of data. Input pre-processing was applied including: checking against the means of data ranges, checking for large changes in observations, normalisation of data, exclusion of records with missing data and lag removal based on cross-correlation. The accuracy of the FSRC model was comparable with the linear approach, whereas the ARX model showed errors of only $\pm 2$℃ most of the time. Using daily average prediction errors was demonstrated to be beneficial. All models were able to detect bearing damage prior to a catastrophic failure. The alarm was triggered earlier in the case of the ANN models compared to the linear model. A further disadvantage of the linear model was seen in a strong seasonality of the prediction error. Two other investigated bearing damage events were detected by the ANNs about 185 days ahead with up to 5 days difference between FSRC and ARX models. The FSRC model allowed easier identification of the bearing failures due to larger shifts in the mean. Another advantage of the FSRC model was seen in the possible identification of sensor problems due to the monitoring of absolute changes in the reconstructed signal. Higher false alarm rates were expected for the FSRC model, however.

Kusiak and Verma [44] studied bearing fault detection using four months' SCADA data in 10 s resolution from 24 1.5 MW turbines. The input parameters for the FSRC model were selected firstly using physical understanding of the system and next by one of three data mining algorithms: wrapper with genetic search, wrapper with best first search and boosting tree algorithm. The differences between the five tested ANN configurations were in the number of neurons (5-25) and activation functions (tanh, exponential, identity, logistics). The best configuration consisted of 18 neurons, logistic hidden activation and identity output activation. NBM was successfully demonstrated and abnormal bearing behaviour during one week of data for one turbine was analysed.

Kusiak and Zhang [37, 38] modelled WT drive train and tower accelerations from SCADA data at 10 s resolution. Two fault code situations were studied using a few days of data from six variable speed 1.5 MW turbines. The models used for fault detection were ANN, ANN ensemble, boosting regression tree, support vector machine, random forest with regression, standard classification and regression tree and k-nearest-neighbour ANN. Modelling used several time-steps of wind speed, 'wind deviation' (assumed to stand for yaw error), blade pitch angle, generator torque and previous time-steps of the target variable as inputs using an ARX approach. Details of the algorithm settings were not provided, but results under normal conditions showed that the ANN and the ANN ensemble performed best for modelling drive train and tower acceleration, respectively. In a second approach, the accelerations were successfully modelled with inputs from two different turbines (here called virtual sensor concept). Detection of two anomalies in the data set was demonstrated.

Z.-Y. Zhang *et al.*[45] applied ARX ANN modelling to the main shaft rear bearing temperature in direct-drive turbines. Based on approx. one year of data from two 3 MW turbines in a 17 WT farm, a failure in one turbine was detected three months ahead with a model using output power, nacelle temperature and turbine speed as exogenous inputs. The anomaly threshold was set to 1.5°C for the residual and was validated with normal operation from a second turbine.

Li *et al.* [46] built a monitoring system utilising an ANN for modelling component temperatures, power output and rotor speed based on data from 34 1.5 MW turbines. Temperatures were modelled in an ARX approach using current wind speed, ambient temperature and the output power as exogenous inputs. The authors stated that a specific model needs to be tuned to each individual turbine and is influenced by seasonal variations of wind speed and ambient temperature. A mean absolute error for normal conditions of 0.67– 0.91°C was stated. Failure detection using a 'health degree' measure utilised penalty factors for residuals in the outer regions of a probability distribution. Sun *et al.* [32] investigated a revised system with additional models trained using either samples from a time period one year before or measurements on other turbines. Although the traditional models trained with up-to-date data of the same turbine perform best, the other models were beneficial in anomaly detection, where their prediction errors were weighted based on the accuracy under normal conditions. Two case studies highlighted the advantages of the anomaly detection system compared to simple residual thresholds or single-model based assessment. A further 14 fault cases were identified with 93.25% detection accuracy.

Cross and Ma's [23] second approach to NBM used ANN. The gearbox bearing temperature, generator winding temperature and active power output were predicted in an ARX approach using wind speed as an exogenous variable. Ten neurons with a sigmoidal transfer function were applied in the hidden layer. NBM with ANN resulted in high coefficients of determination significantly outperforming two other investigated approaches, namely linear and state dependent parameter modelling. In a multivariate setting with the active power as a second exogenous input, the state dependent parameter modelling was more accurate, however.

Bangalore and Tjernberg [47] applied an ANN for NBM of gearbox bearing temperatures in an ARX configuration. The selection of the training data was automated by using filtering and selection [48]. Self-evolution by automatically updating the ANN after maintenance actions was suggested [49]. Anomalies were detected by considering residual and target distributions from the training period in a Mahalanobis distance. Five ANNs were built to model temperatures of five bearings in a common gearbox based on data from an onshore 2 MW turbine. All ANNs used power, gearbox oil temperature, nacelle temperature and the rotational speed as inputs as well as up to two additional temperatures of the other investigated bearings. The Mahalanobis distance was averaged over three days and compared with a threshold defined by training results. A recorded gearbox failure due to spalling in one bearing was successfully detected by the approach one week before the vibration-based CM system identified the failure. Comparison with root mean square errors emphasised the advantage of the Mahalanobis distance in detecting anomalies earlier.

*3.3.3. Fuzzy system:* A fuzzy inference system evaluates inputs with if-then rules based on fuzzy logic, i.e. degrees of truth instead of Boolean logic (true/false). Membership functions define how inputs are mapped to a fuzzy value. If-then rules are built of two parts: the 'if' – the 'antecedent' with the evaluation of the input membership(s) and the 'then' – the 'consequence' applying the rule and returning a fuzzy output or an output as a function of the inputs (Sugeno fuzzy model) [50].

Schlechtingen *et al.* [30] proposed an Adaptive Neuro-Fuzzy Inference System (ANFIS) for NBM. ANFIS can be described as network-based learning of membership functions of fuzzy inference systems. Three years of SCADA data from 18 onshore 2 MW turbines were used as the basis of this research. Two rules with generalised normal distribution membership functions were applied for each input. Depending on the target variable and its physical properties, reconstruction with signals of a different sensor type or of the same type (cross prediction, e.g. temperature of another phase of the generator) were chosen. The resulting 45 models are visualised in Fig. 6. Hybrid gradient descent and least squares estimation learning was used for training. A comparison with ANN modelling similar to the approach described above by the same authors [40] showed that the prediction accuracy in terms of the standard deviation of the error was comparable.

ANFIS required less time for training, however. For failure diagnosis, the prediction errors were averaged to daily values and compared with a probability limit of 0.01%. An alarm was raised when at least three daily values violated the threshold within a week. Successful detection of a hydraulic oil leakage, gearbox oil temperature increases, converter fan malfunctions, an anemometer offset and a controller malfunction were demonstrated [51].

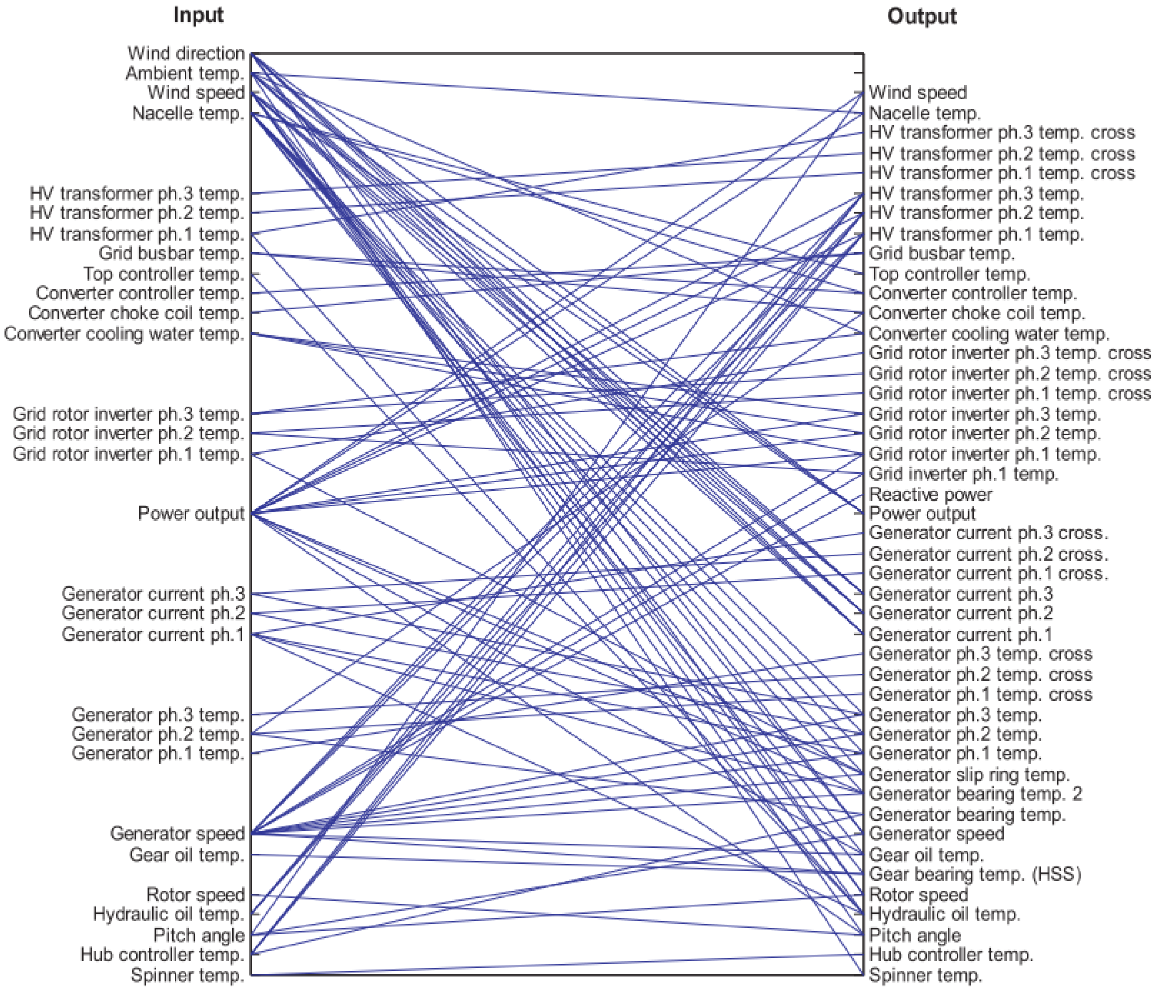


***Fig. 6*** *Fuzzy modelling, input and outputs from* [30]. *Reprinted from* [30], *Copyright (2013) with permission from Elsevier.*

*3.3.4. Other methodologies:* Wang and Infield [52] proposed a non-parametric, non-linear state estimation technique (NSET) for NBM using SCADA data. This approach was based on an estimation of the target value by using a state memory matrix of inputs. The NSET algorithm uses a product of the memory matrix and a weighting vector to estimate each new operational state. The weighting vector was determined using a least squares approach for minimising the residuals of estimated and measured output utilising a Euclidean distance operator. The input variables considered for building the state memory matrix were chosen using physical understanding of the system and correlation analysis. A data selection algorithm was applied to reduce the number of states for each variable. Welchs's t-test, as a distance measure for samples with different variances, or a one-sided hypothesis test was used for anomaly detection.

In a case study, Wang and Infield investigated gearbox failures using 3 month of SCADA data from 10 turbines. Data from different turbines were used for training (7 turbines), validation (1 turbine) and testing data (2 turbines with failures). The target gearbox cooling oil temperature was modelled with the gearbox bearing temperature, the power output, the nacelle temperature and the oil temperature itself. Using this approach, alarms were reported almost a month before the final gearbox failures. A comparison with a four-input four-output ANN approach similar to [26, 27] demonstrated better performance for the NSET. Guo [53] investigated NSET to model a generator bearing temperature, but did not actually apply the approach to failure detection.

Butler *et al.* [54] presented modelling based on sparse Bayesian learning of a configuration equivalent to ARX to predict the main bearing temperature. The model was defined as a weighted sum of radial basis functions. A threshold based on the residual distribution was used to detect fault conditions. The authors presented an estimation of remaining useful life with Particle Filtering (or Sequential Monte Carlo) methods.

Cross and Ma [23] applied, as a third approach, a quasi-linear State Dependent Parameter (SDP) model for NBM. The coefficients of determination were high for normal operations, i.e. 0.983 and 0.997 for the gearbox temperature and generator winding temperature, respectively. A three-dimensional surface built using the prediction model acted as an adaptive threshold for failure detection with fuzzy rules.

*3.3.5. Discussion:* Multiple studies have proven that NBM can be used to detect failures. Although the concept of evaluating a residual of measured minus modelled signal provides a failure indicator which is easy to interpret, the dependency on training data and manually set thresholds can result in undetected changes or frequent false alarms. The usage of a confidence factor based on training duration and accuracy as suggested in [31] might help to improve anomaly detection and assessment. Different NBM concepts as ARX and FSRC, different techniques based on linear models, ANN, ANFIS etc. and different anomaly detections as simple thresholds, Mahalanobis distance or health degree approaches have been tested, but sufficiently comprehensive comparisons are needed to evaluate which solution is best. Additionally, there is a need for a universal strategy to select inputs for NBM.

### *3.4. Damage modelling*

The NBM approaches described above tend to be 'black-box' based with little or no insight into the physical processes which drive failure. Instead of comparing measured signals with empirical models of normal behaviour, interpreting measured signals using physical models can potentially better represent damage development and give more accurate results.

Gray and Watson [55] presented a Physics of Failure approach for damage calculation and failure probability estimation, i.e. developing a damage model based on a physical understanding of the particular failure mode of interest. For failure modes, which manifest themselves through accumulated damage, such as fatigue, the probability of an imminent breakdown can be estimated. The approach was applied in a field study using two years of SCADA data from a wind farm consisting of 160 fixed-speed 1 MW turbines in order to study gearbox failures. A Lundgren-Palmgren damage model for gearbox bearings was proposed and linear damage accumulation assumed. Constants were calibrated by comparison of the assumed design lifetime and the actual lifetime of the failed bearings. An assessment of the resulting damage in the full turbine distribution for the wind farm revealed that the failed turbines show higher damage values than 75% of the population, see Fig. 7. The widely distributed values showed that it would be difficult to accurately predict which turbines were about to fail, but nonetheless could be used to help prioritise maintenance actions within a large fleet of turbines. The approach was also applied to yaw failures for the same wind farm [29].

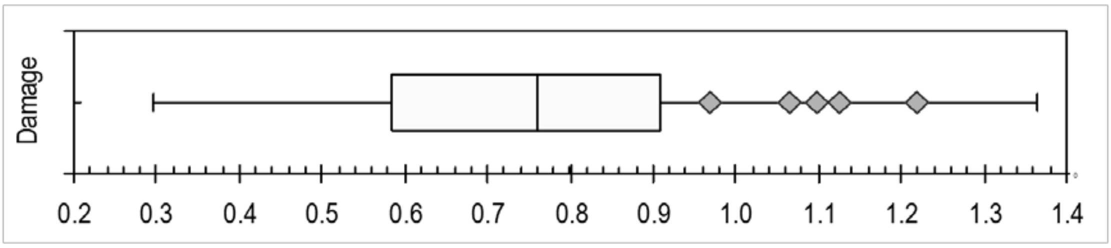


***Fig. 7.*** *Calculated bearing damage for 160 turbines from* [55]*. Box plot with extrema, quartiles and diamond symbols for failed turbines. Reprinted from* [55]*, Copyright 2009 with permission of John Wiley and Sons, Ltd.*

Breteler *et al.* [56] generated a general framework for a Physics of Failure approach as illustrated in Fig. 8. An additional load generator module was proposed to consider external factors. A gearbox failure in a helical gear due to bending fatigue of a gear tooth was investigated in a case study. Laser measurements of the misalignments were used to calculate loads using a finite element method calculation. Number of cycles and forces were calculated from averaged ten minute SCADA power output and generator speed measurements. The resulting remaining lifetime showed large differences not only between reference state and failure, but also between three different turbines.

Qiu *et al.* [57, 58] built a theoretical model for a turbine with gearbox and a DFIG based on thermodynamic principles and combined it with temperature trending approaches. Steady-state rotor aerodynamics was combined with simplified rigid drivetrain dynamics and an electromagnetic torque formula. In a case study of a 1.5 MW turbine, a gearbox gear teeth failure, a generator ventilation fault and generator winding unbalance were examined. SCADA data trends were used to validate the simulated degradation as shown in Fig. 9. Diagnostic rules were determined for the investigated faults based on the power transmission efficiency and generator winding or lubricant temperature gradients.

Borchersen and Kinnaert [59] developed a mathematical model for three generator coil temperatures. The model for the switching generator cooling and heating system was built without knowledge of the actual system. Parameters were found by applying an extended Kalman filter. The anomaly detection utilised residuals of model parameters for the different coils with a cumulative sum algorithm. In a case study with 3 years of SCADA data from 43 offshore turbines, 16 out of 18 cooling faults were successfully detected with only one false alarm.

Comparing measured signals with physical turbine or damage models has been successfully applied to fault detection, although challenges to get sufficient detection accuracy remain. Due to a lack of studies with sufficiently large numbers of failures, different failure modes or different turbines, the potential for using damage modelling in CM is not yet fully established.

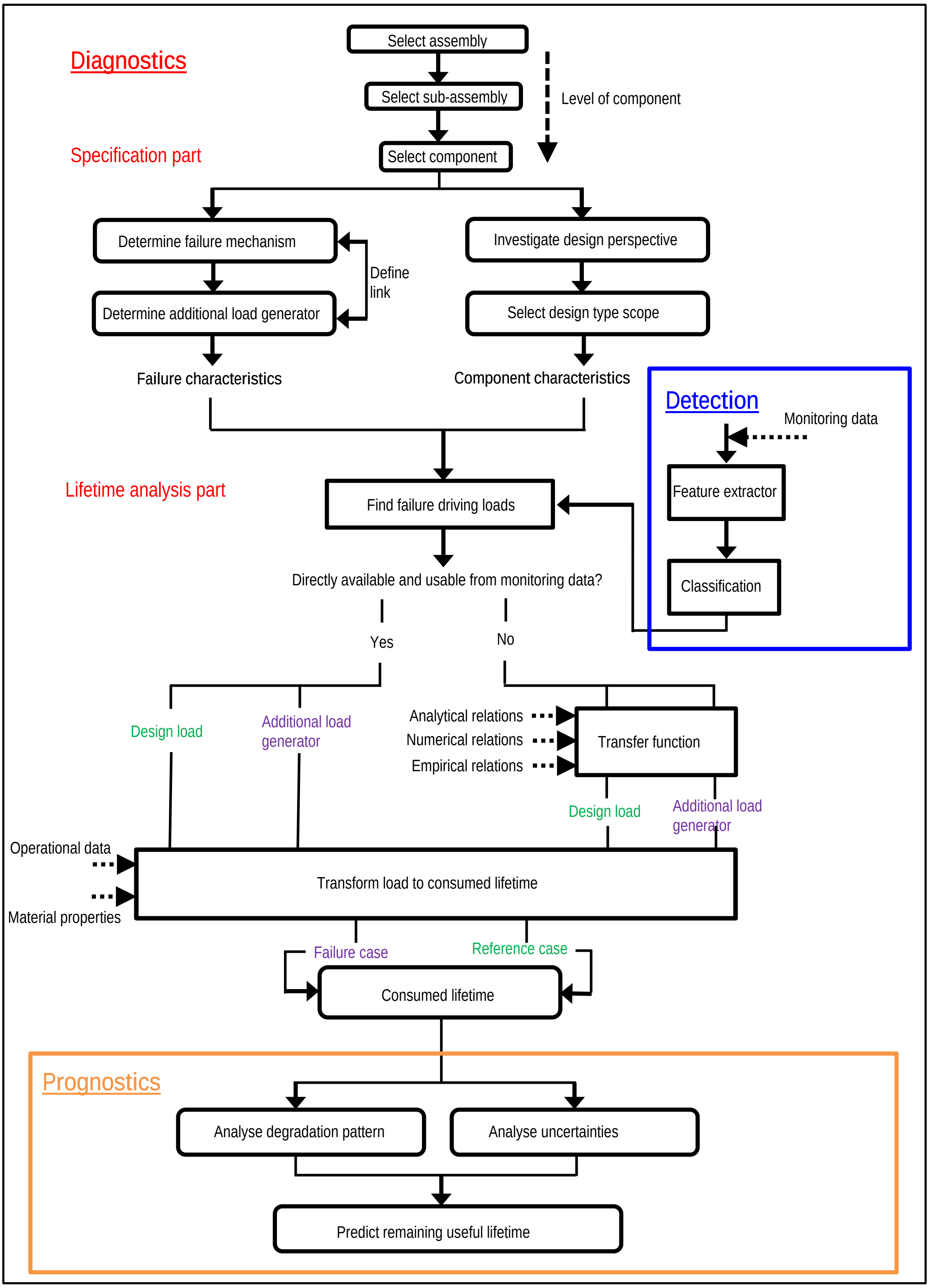


***Fig. 8.*** *Flowchart of Physics of Failure approach from* [56].
*Redrawn with permission of* [56] *Copyright 2015, MECAL IX.*

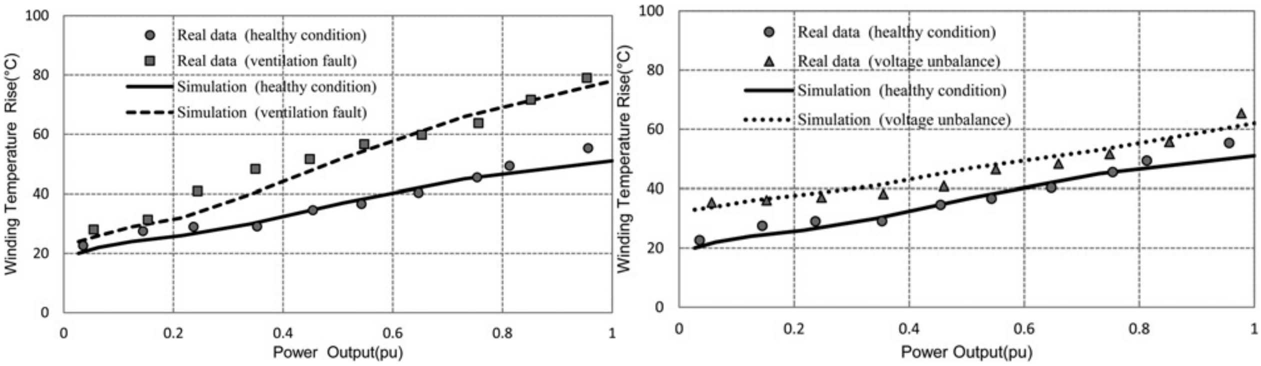


*a* *b*

***Fig. 9.*** *DFIG degradation simulation in comparison with case study result from* [58] *Reprinted from* [58], *Copyright 2014, The IET.*
a Ventilation fault.
b Voltage unbalance.

### 3.5. Assessment of alarms and expert systems

Different systems have been proposed in order to better interpret outputs from SCADA control alarms or NBM results.

*3.4.1. Status code processing:* Qiu *et al.* [60] developed two approaches to reduce SCADA alarms based on up to two years of data from two different wind farms with more than 400 turbines in total and two different manufacturers. The different types of alarms were classified as general, system operation, environmental and communication/connection/software alarms. The average alarm rate was about 10-20 per ten-minute interval, but high maximum rates of up to 1500 alarms per ten minutes occurred. Remotely resetting was possible for only about 24% of the alarms (considering only one turbine type). An alarm time-sequence analysis was used to identifying cases where one alarm triggered another. In a second approach, probabilities were analysed using Bayes' theorem and probabilistic patterns were compared using a Venn diagram. An example probability analysis is given in Fig. 10. Although the time-sequence analysis was found to be useful when few data were available, root causes were better identified with the probability based analysis.

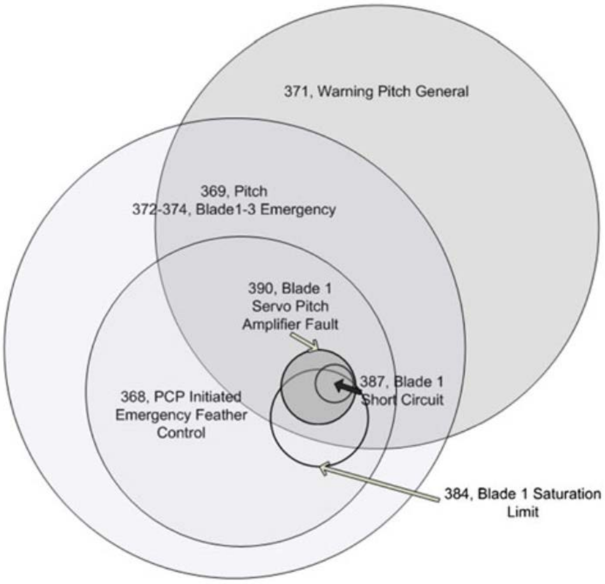


***Fig. 10.*** *Probability based Venn diagram analysis of pitch malfunction from* [60]*. The different circles represent alarms, intersections denote simultaneously occurring alarms. Here, the alarm 387 seems to be the origin of all other alarms. Reprinted from* [60]*, Copyright (2011) with permission from John Wiley and Sons, Ltd.*

Chen *et al.* [61] utilised a binary ANN to map from alarm pattern to faults. A hidden layer size of 50 neurons was found to be optimal in the prediction of a pitch fault. The training data included 221 alarm patterns of 31 SCADA alarms from one turbine with an electrical pitch system. Tests using alarms from four other turbines showed a detection accuracy of only 8-47%. The training data dependency of this approach was highlighted and possible extrapolation errors discussed.

Chen *et al.* [62] continued the probabilistic approach [60] and proposed a Bayesian network to find root causes. Good reasoning capabilities were demonstrated with the same data. An example is given in Fig. 11.

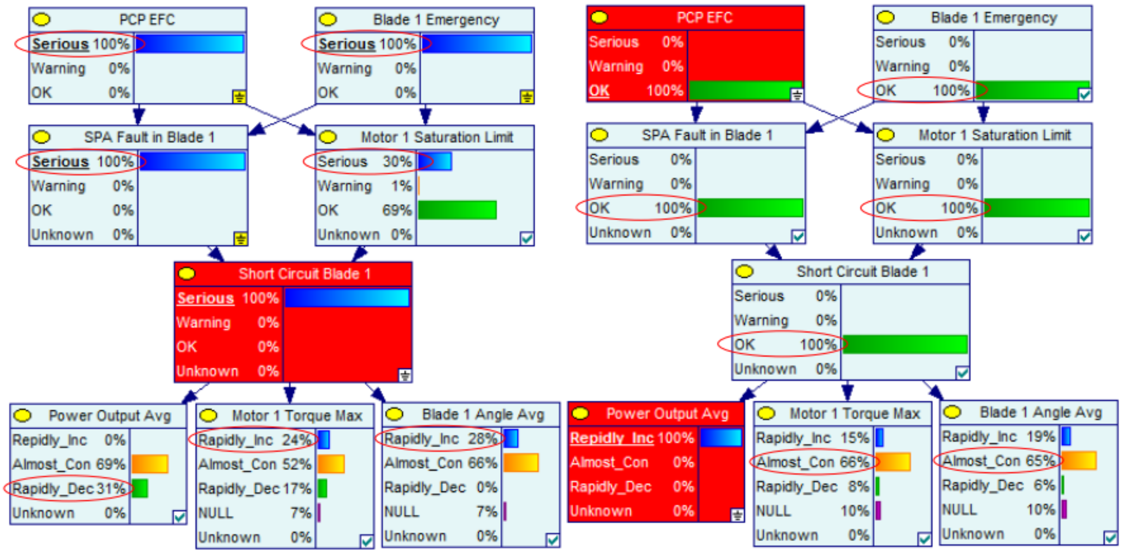


*a* *b*

***Fig. 11.*** *Examples of Bayesian network reasoning from* [62]. *Reprinted with permission of* [62]. *Copyright 2012, Durham University.*
a With pitch fault.
b Without pitch fault.

Godwin and Matthews [22] post-processed SCADA status codes for the purpose of pitch fault detection. The expert system developed based on logical rules learned using a RIPPER algorithm was able to concentrate the amount of information.

Kusiak and Li [63] predicted status codes, their severity and specific code types (in this case, a malfunction of the diverter) by mapping codes to wind speed and power output. Training and testing data were taken from three months of SCADA data with five-minute resolution from four turbines. Neural Network Ensemble, Standard Classification, Regression Tree and Boosting Tree Algorithm Difference methods were found to extract the required information best. Faults were predicted 60 minutes ahead.

Chen *et al.* [64] utilised an a priori knowledge-based ANFIS to detect pitch faults. Based on six fault cases from two turbines, a knowledge base was built by finding relationships between rotor speed, blade angle, pitch motor torque and power output. This knowledge was included in the ANFIS structure to supplement modelling in cases of insufficient training data. Testing with maintenance records of 28 months from 26 turbines in a Spanish farm demonstrated the advantage of this approach compared to simple alarm counting. For a 21 days' prognostic horizon, the model detected 62.2% of the cases that required maintenance. Tests using data from a US wind farm with 160 fixed speed 1 MW turbines resulted in less accurate fault prognosis, however [65]. Unclear maintenance reports, missing torque signals and curtailments due to low grid demands were seen as causes.

The evaluation of status codes for CM has been proven to be beneficial for better alarm assessment. However, the lack of any details concerning algorithms used in recent commercial products and the differences in status code generation of different software manufacturers hinders any clear assessment of the progress achieved in this field.

*3.4.2. Using expert systems to interpret alarms or modelling results:* Garcia *et al.* [26] applied an expert system to assess the output of their ANN modelling. Manually implemented fuzzy rules were used to diagnose causes of anomalies. The evolution of health was proposed to be used as a method for the prediction of remaining lifetime. Planning of maintenance as well as evaluation of its effectiveness and cost were also discussed. Failure history needed to be available for proper training of the system.

Cross and Ma [23] applied fuzzy inference to their temperature modelling. Trapezoidal and triangular membership functions based on fixed values for the residual size and duration were used to generate a three-stage status output.

Schlechtingen *et al.* [30] proposed an expert system to process their ANFIS modelling results. Prediction errors were passed to a fuzzy inference system only if three anomalies were detected by the daily probability threshold during one week. Triangular membership functions defined by occurrence probabilities and manual definitions in a master threshold table were used. Manually implemented fuzzy rules generated three stage condition statements as well as potential root causes, as shown in Fig. 12.

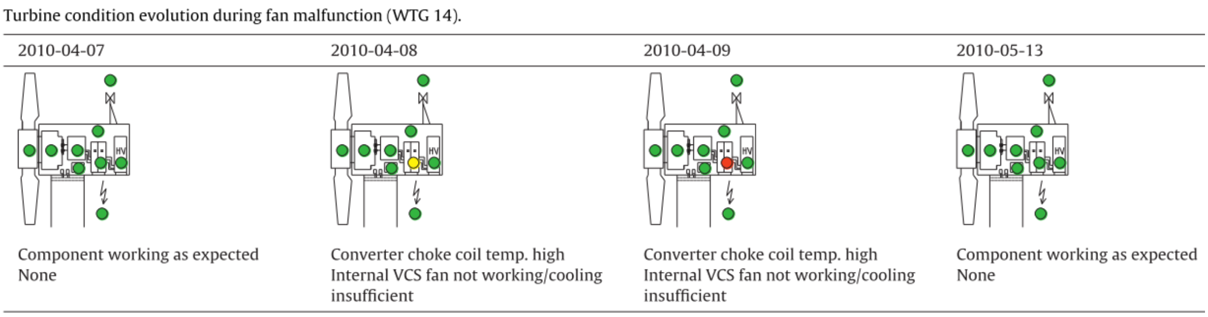


***Fig. 12.*** *Example of fuzzy expert system output from* [51] *giving component status as green (ok), yellow (warning) and red (alarm) and possible root cause. Reprinted from* [51], *Copyright (2014) with permission from Elsevier.*

H. Li *et al.* [66] proposed a fuzzy assessment system, which was tested on a 850 kW variable speed turbine. A deterioration degree was defined using polynomial functions up to third order of the wind speed for setting normal limits of temperatures. Trapezoidal and triangular membership functions were used with weights for different temperatures to build a fuzzy synthetic assessment system with linguistic results from “excellent” to “danger”. A case study was presented including normal operation, a gearbox fault and a stop due to a high generator winding temperature.

J. Li *et al.* [46] and Sun *et al.* [32] used a similar framework of fuzzy synthetic evaluation to assess the results from several ANN models for different targets or based on different training data. Nine different faults were used for the allocation of the abnormal level indices to fuzzy memberships. The implementation of weights considered the share of each ANN model in the 'health degree' [46] and/or the prediction accuracy under normal conditions of the ANN models [32].

De Andrade Viera and Sanz-Bobi [67] proposed a risk indicator concept based on their ANN modelling [26]. Residuals of modelling were integrated over time, if the residual was outside a confidence band. Results of different ANN models were combined in a weighted sum based on quality of models. A cost-effective maintenance model was proposed adapted to the ongoing observed life with a variable threshold depending on a risk indicator growth rate.

Gray *et al.* [68] suggested abductive diagnosis to link SCADA errors or modelling results with expert knowledge. Assessed failure modes, their location, operational mode and resulting indicator changes were used to create a so-called Propositional Horn Clause Abduction Problem which is able to provide fault diagnoses using a computational process.

The usage of expert systems clearly simplifies the interpretation of NBM results. Health degrees or risk indicators can play an important role in integrating SCADA CM approaches in maintenance strategies.

### *3.6. Other applications*

Other applications of SCADA data beside classical CM include: power curve analyses, modelling and monitoring, e.g. with k-nearest-neighbour [69], copula estimation [70], k-nearest-neighbour, cluster centre fuzzy logic, ANN and ANFIS [71], ANN and Gaussian processes [72], linear and Weibull profiles definitions [73] or with stochastic methods [74]. Further references can be found in dedicated power curve modelling reviews, e.g. [75]. Spare part demand forecasting was investigated with a proportional hazards model utilising counts of temperature threshold violations from SCADA data [76]. More general load and structural health monitoring can also employ SCADA data as an additional source of information, e.g. [74, 77, 78].

## 4. Discussion and conclusion

Different approaches to utilise SCADA data for CM of WTs are reviewed in this paper grouped as (i) trending, (ii) clustering, (iii) NBM, (v) damage modelling and (vi) assessment of alarms and expert systems.

The simple trending of SCADA data has demonstrated good abilities to detect anomalies. Case specific configuration and interpretation seem to be required, however. Automated monitoring based on trending will most likely struggle to be accurate enough and avoid false alarms.

Clustering, as a more advanced technique of finding the differences between normal operation and anomaly, has the same disadvantage. Additionally, extensive historical failure data are required, if the methods are able to reliably diagnose failures. It is unlikely that the full range of fault stages will be available in any training data period in practice.

NBM has been the focus of recent research using SCADA data for CM due to the advantage of relatively easy anomaly detection using the residual of modelled minus measured variables after training under normal conditions. Models based on polynomial equations, ANN, ANFIS or NSET demonstrated good failure detection abilities. However, comprehensive comparisons of the techniques are lacking in order to be able to assess which technique is best. From the different studies, it is hard to assess whether a good accuracy and fault detection is based on a certain technique, on the NBM concept being ARX or FSRC, or even on further detailed settings. However, it is not satisfactorily shown that the (computational) effort of machine learning techniques like ANN, ANFIS or NSET is reasonable as only one case study compares linear modelling with ANN [40]. On the other hand, most publications criticising ANN training as too time-consuming do not consider the ongoing improvements in computational resources in common desktop computers. There is lack of published NBM performance metrics for different case studies in order to be able to properly evaluate required effort and performance in terms of normal behaviour prediction, true failure detections and false alarms for all of the techniques.

The damage modelling approaches show potential for CM of WTs focussing on physical causes of failures. However, the development of reliable and accurate damage models for all failure modes of a WT will be a very difficult task. As only a few studies have been published in this area, the feasibility of using such models for online monitoring of different turbines, possibly from different manufacturers and in different locations, cannot be assessed yet.

Status code processing with probabilistic approaches or physical rules shows promise to condense a large number of alarms into helpful information. However, the studies reviewed do not discuss recent industrial developments, which might have already solved problems discussed. Expert systems with fuzzy inference can be used to automate interpretation of modelling results and deliver easy to understand outputs.

Complete asset monitoring and maintenance planning will require assessment of monitoring alarms and decision making as supported by such systems.

This review focuses on techniques which have been already applied to real SCADA data. Table 3 gives a summary of the reviewed SCADA CM approaches with respect to WT type described by rated power, the amount of data expressed in WT years, the number of investigated failures or anomalies and the subassembly or part of interest. It can be seen, that nearly all research has been based on relatively old WT technology with WTs in the range 1-2MW. The majority of the case studies reviewed based their results on a relatively small amount of data, with less than 30 WT years of SCADA data. Only four case studies were based on more than 10 failures. Most of the approaches focused on detecting failures in gearboxes or bearings.

Based on the presented review of recent CM approaches with SCADA data, future research should initially address the following:

- comparing the prediction accuracy of different approaches as many publications have claimed to have the best solution for SCADA CM, but do not comprehensively compare them with other techniques;
- validating approaches on modern multi-MW WTs, because all studies up to date have used relatively old turbines
- testing approaches using data from a range of different wind farms and turbine types as most studies have only considered one farm or one WT manufacturer

For future studies, emphasis should be put on providing sufficient metrics, true and false failure detection rates, advance detection times and computational effort to allow better comparison between SCADA analysis techniques. In terms of data-driven training, the demonstration of a few successful failure detections alone is not sufficient as the practical use is determined by the reliability of the approach, i.e. in particular the detection rate and false alarms for new data.

Further potential is seen in future research concerning:

1) NBM:
   - comparing ARX and FSRC concepts independent of modelling technique
   - finding sufficient training length and universal input selection algorithm
   - validating ANN training and updating algorithm [48] on bigger scale and for other techniques
   - evaluating NSET with more data
   - testing of linear, ANN or NSET modelling for multiple targets beside temperatures as done with ANFIS [30]

- comparing different anomaly detection techniques such as using a Mahalanobis distance [47], a health degree based on probability [32, 46], multiple alarms over a given period[30], etc., independent of modelling technique
- investigating “black-box” information from models: do the model parameters provide helpful information?

2) Damage modelling:
   - testing and validating damage models with different turbines
   - investigating possible merging of Physics of Failure models with “black box” NBM
   - developing new damage models for turbine components not yet studied
   - using high resolution SCADA data for damage modelling to provide higher damage accumulation accuracy
3) Assessment of alarms and status codes:
   - applying status code processing approaches to subassemblies besides the pitch system
   - investigating current state-of-the art in industrial SCADA processing systems

**Table 3.** Summary of different SCADA CM approaches and WT type investigated, data used, number of anomalies and subassembly of interest. Only approaches in the focus of a paper and with at least one investigated failure from real data are listed.

| Category | | First approach | Second approach | Third approach | Fourth approach | Fifth approach |
|---|---|---|---|---|---|---|
| Trending | | [24] 1 : | [36] 3 : | [4] 2 : | | |
| Clustering | | [28] 3 : | [34] 1 : | | | |
| NBM: | Linear and polynomial | [39] 3 : | [31] 36 : | | | |
| | ANN: FSRC | [43] 8 : | [40] 5 : | [44] 5 : | [45] * 1 : | |
| | ANN: ARX | [27] 3 : | [40] 5 : | [38] 1 : | [46] [32] 25 : | [47] 1 : |
| | ANFIS / NSET | [51] 31 : | [52] 2 : | | | |
| Damage modelling | | [55] [29] 10 : | [56] 3 : | [58] 3 : | [59] 18 : | |
| Status code processing | | [60] : | [61] [62] : | [63] : | [64] [65] & : | |

**Legend:**

WT type: : undefined : < 1.5 MW: : 1.5-2.5 MW (exception: * 3.0 MW)

Amount of data: : undefined : ≤ 3 WT years : ≤ 30 WT years : ≤ 300 WT years : ≥ 300 WT years

The superscript depicts the investigated number of failures or anomalies.

Failing part / subassembly: : Gearbox : Pitch or yaw system : Generator : Bearing : Other

## Acknowledgements

This project has received funding from the European Union's Horizon 2020 research and innovation programme under the Marie Sklodowska-Curie grant agreement No 642108 (project AWESOME).

## References

[1] Global Wind Energy Council: 'Global Wind Statistics 2015', http://www.gwec.net/wp-content/uploads/vip/GWEC-PRstats-2015_LR_corrected.pdf, accessed 29 March 2016

[2] Tavner, P.: 'Offshore Wind Turbines: Reliability, availability and maintenance' (The Institution of Engineering and Technology, London, 2012)

[3] Milborrow, D.: 'The tide turns on offshore maintenance costs', http://www.windpoweroffshore.com/article/1314299/tide-turns-offshore-maintenance-costs, accessed 29 March 2016

[4] Yang, W., Court, R., Jiang, J.: 'Wind turbine condition monitoring by the approach of SCADA data analysis'*Renew. Energy*, 2013, **53**, pp. 365–376.

[5] Yang, W., Tavner, P.J., Crabtree, C.J., Feng, Y., Qiu, Y.: 'Wind turbine condition monitoring: technical and commercial challenges'*Wind Energy*, 2014, **17**, (5), pp. 673–693.

[6] Hameed, Z., Hong, Y.S., Cho, Y.M., Ahn, S.H., Song, C.K.: 'Condition monitoring and fault detection of wind turbines and related algorithms: A review'*Renew. Sustain. Energy Rev.*, 2009, **13**, (1), pp. 1–39.

[7] García Márquez, F.P., Tobias, A.M., Pinar Pérez, J.M., Papaelias, M.: 'Condition monitoring of wind turbines: Techniques and methods'*Renew. Energy*, 2012, **46**, pp. 169–178.

[8] Purarjomandlangrudi, A., Nourbakhsh, G., Esmalifalak, M., Tan, A.: 'Fault Detection in Wind Turbine: A Systematic Literature Review'*Wind Eng.*, 2013, **37**, (5), pp. 535–548.

[9] Tchakoua, P., Wamkeue, R., Ouhrouche, M., Slaoui-Hasnaoui, F., Tameghe, T.A., Ekemb, G.: 'Wind Turbine Condition Monitoring: State-of-the-Art Review, New Trends, and Future Challenges'*Energies*, 2014, **7**, (4), pp. 2595–2630.

[10] Qiao, W., Lu, D.: 'A Survey on Wind Turbine Condition Monitoring and Fault Diagnosis - Part I: Components and Subsystems'*IEEE Trans. Ind. Electron.*, 2015, **62**, (10), pp. 6536–6545.

[11] Qiao, W., Lu, D.: 'A Survey on Wind Turbine Condition Monitoring and Fault Diagnosis - Part II: Signals and Signal Processing Methods'*IEEE Trans. Ind. Electron.*, 2015, **62**, (10), pp. 6546–6557.

[12] Hahn, B., Durstewitz, M., Rohrig, K.: 'Reliability of wind turbines - Experience of 15 years with 1500WTs', in 'Wind Energy' (Springer, 2007), pp. 329–332

[13] Ribrant, J., Bertling, L.M.: 'Survey of failures in wind power systems with focus on Swedish wind power plants during 1997-2005'*IEEE Trans. Energy Convers.*, 2007, **22**, (1), pp. 167–173.

[14] Tavner, P.J., Xiang, J., Spinato, F.: 'Reliability analysis for wind turbines'*Wind Energy*, 2007, **10**, (1), pp. 1–18.

[15] Spinato, F., Tavner, P.J., van Bussel, G.J.W., Koutoulakos, E.: 'Reliability of wind turbine subassemblies'*IET Renew. Power Gener.*, 2009, **3**, (4), p. 387.

[16] Pinar Pérez, J.M., García Márquez, F.P., Tobias, A., Papaelias, M.: 'Wind turbine reliability analysis'*Renew. Sustain. Energy Rev.*, 2013, **23**, pp. 463–472.

[17] Feng, Y., Tavner, P.J., Long, H.: 'Early experiences with UK round 1 offshore wind farms'*Proc. Inst. Civ. Eng. - Energy*, 2010, **163**, (4), pp. 167–181.

[18] Wilkinson, M., Harman, K.: 'Measuring wind turbine reliability, results of the reliawind project', in 'EWEA Annual Conference 2011' (2011)

[19] Sheng, S.: 'Report on Wind Turbine Subsystem Reliability - A Survey of Various Databases'*NREL/PR-5000-59111,National Renew. Energy Lab.*, 2013.

[20] Carroll, J., McDonald, A., McMillan, D.: 'Reliability Comparison of Wind Turbines With DFIG and PMG Drive Trains'*IEEE Trans. Energy Convers.*, 2015, **30**, (2), pp. 663–670.

[21] Carroll, J., McDonald, A., McMillan, D.: 'Failure rate, repair time and unscheduled O&M cost analysis of offshore wind turbines'*Wind Energy*, 2015, **17**.

[22] Godwin, J.L., Matthews, P.: 'Classification and Detection of Wind Turbine Pitch Faults Through SCADA Data Analysis'*Int. J. Progn. Heal. Manag.*, 2013, **4**, p. 11.
[23] Cross, P., Ma, X.: 'Model-based and fuzzy logic approaches to condition monitoring of operational wind turbines'*Int. J. Autom. Comput.*, 2015, **12**, (1), pp. 25–34.
[24] Feng, Y., Qiu, Y., Crabtree, C.J., Long, H., Tavner, P.J.: 'Monitoring wind turbine gearboxes'*Wind Energy*, 2013, **16**, (5), pp. 728–740.
[25] Crabtree, C.J., Zappalá, D., Tavner, P.J.: 'Survey of Commercially Available Condition Monitoring Systems for Wind Turbines' (2014)
[26] Garcia, M.C., Sanz-Bobi, M.A., del Pico, J.: 'SIMAP: Intelligent System for Predictive Maintenance Application to the health condition monitoring of a windturbine gearbox'*Comput. Ind.*, 2006, **57**, (6), pp. 552–568.
[27] Zaher, A., McArthur, S.D.J., Infield, D.G., Patel, Y.: 'Online wind turbine fault detection through automated SCADA data analysis'*Wind Energy*, 2009, **12**, (6), pp. 574–593.
[28] Catmull, S.: 'Self-Organising Map Based Condition Monitoring of Wind Turbines'*EWEA Annu. Conf. 2011*, 2011.
[29] Watson, S.J., Kennedy, I., Gray, C.S.: 'The use of physics of failure modelling in wind turbine condition monitoring', in 'EWEA Annual Conference 2011' (2011), pp. 309–312
[30] Schlechtingen, M., Santos, I.F., Achiche, S.: 'Wind turbine condition monitoring based on SCADA data using normal behavior models. Part 1: System description'*Appl. Soft Comput.*, 2013, **13**, (1), pp. 259–270.
[31] Wilkinson, M., Harman, K., van Delft, T., Darnell, B.: 'Comparison of methods for wind turbine condition monitoring with SCADA data'*IET Renew. Power Gener.*, 2014, **8**, (4), pp. 390–397.
[32] Sun, P., Li, J., Wang, C., Lei, X.: 'A generalized model for wind turbine anomaly identification based on SCADA data'*Appl. Energy*, 2016, **168**, pp. 550–567.
[33] Wiggelinkhuizen, E., Verbruggen, T., Braam, H., Rademakers, L., Xiang, J., Watson, S.: 'Assessment of Condition Monitoring Techniques for Offshore Wind Farms'*J. Sol. Energy Eng.*, 2008, **130**, (3), pp. 031004–1–031004–9.
[34] Kim, K., Parthasarathy, G., Uluyol, O., Foslien, W., Sheng, S., Fleming, P.: 'Use of SCADA data for failure detection in wind turbines', in 'ASME 5th Int. Conf. Energy Sustain.' (2011), pp. 2071–2079
[35] Feng, Y., Qiu, Y., Crabtree, C., Long, H., Tavner, P.: 'Use of SCADA and CMS signals for failure detection and diagnosis of a wind turbine gearbox'*EWEA Annu. Conf. 2011*, 2011.
[36] Astolfi, D., Castellani, F., Terzi, L.: 'Fault Prevention and Diagnosis Through Scada Temperature Data Analysis of an Onshore Wind Farm'*Diagnostyka*, 2014, **15**, (2), pp. 71–78.
[37] Kusiak, A., Zhang, Z.: 'Analysis of Wind Turbine Vibrations Based on SCADA Data'*J. Sol. Energy Eng.*, 2010, **132**, (3), p. 031008.
[38] Zhang, Z., Kusiak, A.: 'Monitoring Wind Turbine Vibration Based on SCADA Data'*J. Sol. Energy Eng.*, 2012, **134**, (2), pp. 021004–1–021004–12.
[39] Garlick, W.G., Dixon, R., Watson, S.J.: 'A Model-based Approach to Wind Turbine Condition Monitoring using SCADA Data'*20th Int. Conf. Syst. Eng.*, 2009.
[40] Schlechtingen, M., Santos, I.F.: 'Comparative analysis of neural network and regression based condition monitoring approaches for wind turbine fault detection'*Mech. Syst. Signal Process.*, 2010, **25**, pp. 1849–1875.
[41] Du, H.: 'Data mining techniques and applications: an introduction' (Cengage Learning EMEA, 2010)
[42] Brandão, R.F.M., Carvalho, J. a. B., Barbosa, F.P.M.: 'Neural Networks for Condition Monitoring of Wind Turbines'*Int. Symp. Mod. Electr. Power Syst. Wroclaw, Pol.*, 2010.
[43] Brandão, R.F.M., Carvalho, J.A.B.: 'Intelligent System for Fault Detection in Wind Turbines Gearbox', in 'PowerTech' (2015)
[44] Kusiak, A., Verma, A.: 'Analyzing bearing faults in wind turbines: A data-mining approach'*Renew. Energy*, 2012, **48**, pp. 110–116.
[45] Zhang, Z.-Y., Wang, K.-S.: 'Wind turbine fault detection based on SCADA data analysis using ANN'*Adv. Manuf.*, 2014, **2**, (1), pp. 70–78.
[46] Li, J., Lei, X., Li, H., Ran, L.: 'Normal Behavior Models for the Condition Assessment of Wind Turbine Generator Systems'*Electr. Power Components Syst.*, 2014, **42**, (11), pp. 1201–1212.

[47] Bangalore, P., Tjernberg, L.B.: 'An Artificial Neural Network Approach for Early Fault Detection of Gearbox Bearings'*IEEE Trans. Smart Grid*, 2015, **6**, (2), pp. 980–987.
[48] Bangalore, P., Tjernberg, L.B.: 'An approach for self evolving neural network based algorithm for fault prognosis in wind turbine', in '2013 IEEE Grenoble Conference' (IEEE, 2013).
[49] Bangalore, P., Tjernberg, L.B.: 'Self evolving neural network based algorithm for fault prognosis in wind turbines: A case study', in '2014 International Conference on Probabilistic Methods Applied to Power Systems (PMAPS)' (IEEE, 2014).
[50] Jang, J.-S.R., Sun, C.-T., Mizutani, E.: 'Neuro-fuzzy and soft computing : a computational approach to learning and machine intelligence' (Prentice Hall, 1997)
[51] Schlechtingen, M., Santos, I.F.: 'Wind turbine condition monitoring based on SCADA data using normal behavior models. Part 2: Application examples'*Appl. Soft Comput.*, 2014, **14**, (1), pp. 447–460.
[52] Wang, Y., Infield, D.: 'Supervisory control and data acquisition data-based non-linear state estimation technique for wind turbine gearbox condition monitoring'*IET Renew. Power Gener.*, 2012, **7**, (4), pp. 350–358.
[53] Guo, P.: 'Wind turbine generator bearing condition monitoring with NEST method'*Proc. 2012 24th Chinese Control Decis. Conf. CCDC 2012*, 2012, (Cm), pp. 235–239.
[54] Butler, S., O'Connor, F., Farren, D., Ringwood, J. V.: 'A feasibility study into prognostics for the main bearing of a wind turbine'*Proc. IEEE Int. Conf. Control Appl.*, 2012, pp. 1092–1097.
[55] Gray, C.S., Watson, S.J.: 'Physics of Failure approach to wind turbine condition based maintenance'*Wind Energy*, 2010, **13**, (5), pp. 395–405.
[56] Breteler, D., Kaidis, C., Loendersloot, R.: 'Physics based methodology for wind turbine failure detection , diagnostics & prognostics', in 'EWEA 2015 Annual Event' (2015)
[57] Qiu, Y., Zhang, W., Cao, M., Feng, Y., Infield, D.: 'An Electro-Thermal Analysis of a Variable-Speed Doubly-Fed Induction Generator in a Wind Turbine'*Energies*, 2015, **8**, (5), pp. 3386–3402.
[58] Qiu, Y., Feng, Y., Sun, J., Zhang, W., Infield, D.: 'Applying thermophysics for wind turbine drivetrain fault diagnosis using SCADA data'*IET Renew. Power Gener.*, 2016, pp. 1–8.
[59] Borchersen, A.B., Kinnaert, M.: 'Model-based fault detection for generator cooling system in wind turbines using SCADA data'*Wind Energy*, 2016, **19**, (4), pp. 593–606.
[60] Qiu, Y., Feng, Y., Tavner, P., Richardson, P., Erdos, G., Chen, B.: 'Wind turbine SCADA alarm analysis for improving reliability'*Wind Energy*, 2012, **15**, (8), pp. 951–966.
[61] Chen, B., Qiu, Y.N., Feng, Y., Tavner, P.J., Song, W.W.: 'Wind turbine SCADA alarm pattern recognition'*IET Conf. Renew. Power Gener. (RPG 2011)*, 2011, pp. 363–368.
[62] Chen, B., Tavner, P., Feng, Y., Song, W., Qiu, Y.: 'Bayesian network for wind turbine fault diagnosis', in 'EWEA 2012 Copenhagen, Denmark' (2012)
[63] Kusiak, A., Li, W.: 'The prediction and diagnosis of wind turbine faults'*Renew. Energy*, 2011, **36**, (1), pp. 16–23.
[64] Chen, B., Matthews, P.C., Tavner, P.J.: 'Wind turbine pitch faults prognosis using a-priori knowledge-based ANFIS'*Expert Syst. Appl.*, 2013, **40**, (17), pp. 6863–6876.
[65] Chen, B., Matthews, P.C., Tavner, P.J.: 'Automated on-line fault prognosis for wind turbine pitch systems using supervisory control and data acquisition'*IET Renew. Power Gener.*, 2015, **9**, (5), pp. 503–513.
[66] Li, H., Hu, Y.G., Yang, C., Chen, Z., Ji, H.T., Zhao, B.: 'An improved fuzzy synthetic condition assessment of a wind turbine generator system'*Int. J. Electr. Power Energy Syst.*, 2013, **45**, (1), pp. 468–476.
[67] De Andrade Vieira, R.J., Sanz-Bobi, M. a.: 'Failure risk indicators for a maintenance model based on observable life of industrial components with an application to wind turbines'*IEEE Trans. Reliab.*, 2013, **62**, (3), pp. 569–582.
[68] Gray, C.S., Koitz, R., Psutka, S., Wotawa, F.: 'An Abductive Diagnosis and Modeling Concept for Wind Power Plants'*IFAC-PapersOnLine*, 2015, **48**, (21), pp. 404–409.
[69] Kusiak, A., Zheng, H., Song, Z.: 'Models for monitoring wind farm power'*Renew. Energy*, 2009, **34**, (3), pp. 583–590.
[70] Gill, S., Stephen, B., Galloway, S.: 'Wind Turbine Condition Assessment Through Power Curve Copula Modeling'*IEEE Trans. Sustain. Energy*, 2012, **3**, (1), pp. 94–101.
[71] Schlechtingen, M., Santos, I.F., Achiche, S.: 'Using data-mining approaches for wind turbine power curve

monitoring: A comparative study'*IEEE Trans. Sustain. Energy*, 2013, **4**, (3), pp. 671–679.
[72] Papatheou, E., Dervilis, N., Maguire, A.E., Worden, K.: 'Wind Turbine Structural Health Monitoring: A Short Investigation Based on SCADA Data'*EWSHM - 7th Eur. Work. Struct. Heal. Monit.*, 2014.
[73] Long, H., Wang, L., Zhang, Z., Song, Z., Xu, J.: 'Data-Driven Wind Turbine Power Generation Performance Monitoring'*IEEE Trans. Ind. Electron.*, 2015, **62**, (10), pp. 6627–6635.
[74] Wächter, M., Lind, P.G., Hernandez, I.H., *et al.*: 'Efficient load and power monitoring by stochastic methods', in 'EWEA 2015 Annual Event' (2015)
[75] Lydia, M., Kumar, S.S., Selvakumar, A.I., Prem Kumar, G.E.: 'A comprehensive review on wind turbine power curve modeling techniques'*Renew. Sustain. Energy Rev.*, 2014, **30**, pp. 452–460.
[76] Tracht, K., Goch, G., Schuh, P., Sorg, M., Westerkamp, J.F.: 'Failure probability prediction based on condition monitoring data of wind energy systems for spare parts supply'*CIRP Ann. - Manuf. Technol.*, 2013, **62**, (1), pp. 127–130.
[77] Obdam, T.S., Rademakers, L.W.M.M., Braam, H.: 'Flight Leader Concept for Wind Farm Load Counting: Offshore Evaluation'*Wind Eng.*, 2010, **34**, (1), pp. 109–122.
[78] Smolka, U., Cheng, P.W.: 'On the Design of Measurement Campaigns for Fatigue Life Monitoring of Offshore Wind Turbines'*Twenty-third Int. Offshore Polar Eng. Conf.*, 2013, **9**, pp. 408–413.

# Combining Model-based Monitoring and a Physics of Failure Approach for Wind Turbine Failure Detection

J. Tautz-Weinert[1], S. J. Watson[1]

[1] Centre for Renewable Energy Systems Technology, Loughborough University, Loughborough LE11 3TU, UK

## ABSTRACT

Condition monitoring of wind turbines with only operational data has received more attention in the last decade due to the advantage of freely available data without extra equipment needed. Although the operational data recorded by the Supervisory Control And Data Acquisition (SCADA) system are intended for performance monitoring and typically stored only every 10 minutes, information on the turbine's health can be extracted. A major focus is here on the temperature signals of mechanical parts such as drivetrain bearings. Despite the fact that absolute temperatures rise very late in the case of a failure, the temperature behaviour might change well in advance. Model-based monitoring is a tool to detect these small changes in the temperature signal affected by varying load and operation. Data-driven models are trained in a period where the turbine can be assumed to be healthy and represent the normal operation thereafter. Degradation and imminent failures can be detected by analysing the residual of modelled and measured temperatures. However, detecting failures in the residual is not always straightforward due to possibly unrepresentative training data and limited capabilities of this approach. A different way of using SCADA data lies in the estimation of damage accumulation with performance parameters based on the Physics of Failure methodology. A combination of model-based monitoring with damage calculation based on a Physics of Failure approach is proposed to strengthen the failure detection capabilities. The monitoring performance is evaluated in a case study with SCADA data from a wind farm.

*Keywords: wind turbines, SCADA, physics-of-failure, condition monitoring, machine learning.*

*Corresponding author: J. Tautz-Weinert (email: j.tautz-weinert@lboro.ac.uk)*

## 1. INTRODUCTION

With the exponential growth of wind energy in the last decades, the demand for optimised asset management of wind turbines has slowly evolved. In the early days of wind energy, scheduled and corrective maintenance were the appropriate measures for easy-to-access onshore farms and small turbines. With the move offshore and turbine capacities in the multi-MW category in recent years, the more complicated accessibility and significant financial losses for any downtime demand an optimised maintenance strategy. Condition-based or predictive maintenance as a proven strategy in other industries, promises to increase the efficiency of maintenance by optimising the point of intervention based on the condition of the system and risks of imminent failures.

Condition-based maintenance requires adequate measurements and monitoring techniques to reveal the health of the turbine and probabilities of upcoming failures. Due to the complexity of a wind turbine, a single measurement cannot cover the monitoring of all possible structural, mechanical and electrical failures. Failure analyses showed that the gearbox and generator are the most critical subassemblies in terms of failure rate and the corresponding downtime [1,2]. Accordingly, research and industry have focused on condition monitoring of the underlying mechanical failure mechanisms in wind turbine drive trains, although structural health monitoring of the blades, tower and foundation and detection of faults in the power converter, pitch and yaw systems have also been investigated. Potential measurements were found as vibration, acoustic emission, strain, torque, temperatures or oil parameters combined with signal processing techniques such as filtering, synchronous sampling, Hilbert transform, Wavelet transform, Fast Fourier Transform and many others [3,4].

More recently, the use of the operational data recorded by the Supervisory Control And Data Acquisition (SCADA) system has been investigated due the availability of such data without additional sensor installations. While these data are mainly intended for monitoring the performance of turbines in terms of power production, availability, possible misalignment and similar, several different applications to condition monitoring have been identified. Alarm logs in SCADA data might be analysed to find the root causes of events [5,6]. However, the most promising information for drive train condition monitoring lies in the temperature signals as mechanical degradation shows in increased thermal losses [7]. Drive train temperatures in wind turbines fluctuate with changing wind speed, rotational speed and loading. Accordingly, absolute temperature thresholds are known to give late alarms in contrast to vibration-based condition monitoring systems [3]. To overcome this drawback, model-based monitoring can reveal hidden trends in the temperature time series. Due to the complexity of wind turbine systems, data-driven learning is preferred to analytical building of models. Inputs for modelling drive train temperatures might be other temperatures, control signals as the power output or rotational speed or even the history of the target in a partly autoregressive approach. Modelling of the temperatures has been investigated with simple linear sums of inputs [8], artificial neural networks (ANNs) [9,10], adaptive neuro-fuzzy inference systems [11] or state estimation techniques [12]. A previous comparative study of the authors showed that most of the (non-autoregressive) techniques result in similar accurate prediction with slight advantages of ANNs [13].

In contrast to the model-based monitoring investigating temperature signals, the Physics of Failure approach tries to analyse the operational statistics derived from SCADA data in order to estimate the damage accumulation. In a case study with a big farm, it has been demonstrated that turbines with gearbox problems might be identified by their operational statistics [14].

In this paper, a combination of model-based monitoring with statistical analyses as used in the Physics of Failure approach is discussed and tested in a case study with data from an onshore wind farm.

## 2. MONITORING WIND TURBINE DRIVE TRAINS WITH OPERATIONAL DATA

The SCADA system in wind turbines usually measures multiple parameters with a sampling frequency of 1 Hz. Due to the fact that these measurements are originally intended for long-time performance monitoring, usually only averages and possibly extrema and standard deviations of ten minutes are recorded. The number and selection of measured signals depends on the turbine manufacturer or SCADA system provider, but wind speed and direction, pitch and yaw angles, rotational speed, power output and ambient temperature are always monitored. Additionally, temperatures of parts in the drive train are often measured – although with different levels of detail, e.g. only a generator and a gearbox temperature in one setup or more than twenty temperatures at different locations at the shaft in a more detailed configuration. The numerical SCADA data are supplemented by the alarm log listing all fault events happening during the operation.

### 2.1. Normal behaviour modelling of SCADA temperatures

Model-based monitoring [8–13] tries to identify anomalies in a system by comparing measured parameters with outputs of a model of the system. This kind of monitoring is able to highlight slight changes in measured signals affected by complex interaction of loading and heat transfers as in the wind turbine drive train. The model needs to predict the fluctuations of the temperature accurately enough to allow the residual of measured and modelled temperature to act as an indicator for possible degradation and imminent failure, as sketched in Figure 1.

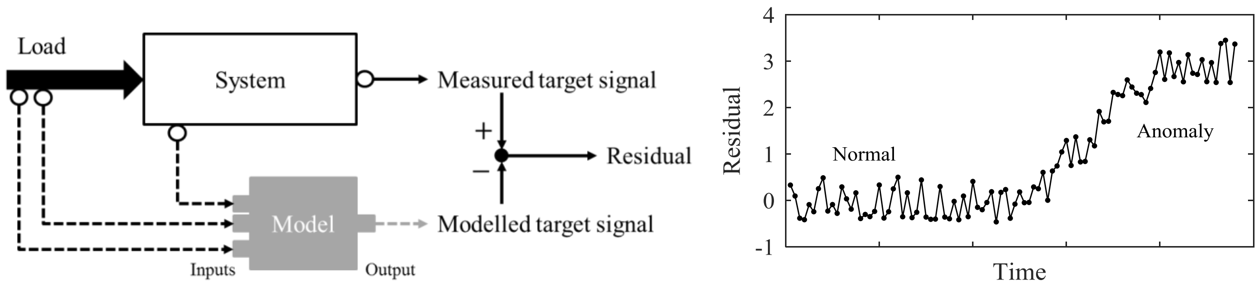


Figure 1.Sketch of model-based monitoring and indication of anomalies in the residual.

Although the basic heat generation in the drivetrain can be traced back to mechanical losses proportional to the acting wind and the rotational speed, the system is affected by more complex interaction of sub-systems, the ambient temperature and cumulative effects which make analytical modelling difficult. In contrast, data-driven modelling requires only a representative training period to learn the relationship. During this training phase the system needs to be in normal condition to enable detecting anomalies thereafter based on the difference to this behaviour. ANNs are a tool to learn and represent non-linear relationships inspired by the human brain. A common feedforward ANN trained by Levenberg-Marquardt backpropagation consists of one input layer, one or more hidden layers with a specified number of neurons and the output layer. Each neuron sums the weighted outputs of the previous layers and uses a non-linear activation function, typically a hyperbolic tangent, to generate an output. For the application of modelling a drivetrain temperature, a single linear output is used.

The inputs for modelling can be chosen based on the understanding of the system (also called domain knowledge) or based on the properties of the signals, e.g. the correlation of signals. Although using partly autoregressive modelling might increase the accuracy of prediction, this will not necessary improve the anomaly detection capability as the prediction is influenced by the target signal and could adapt to changes in the behaviour.

Wind turbine drivetrains usually consist of main bearings, main shaft, a gearbox build of a planetary and two parallel stages, the generator shaft and generator and multiple bearings. All possible target temperatures have to be monitored as behavioural changes might not only show up in the nearest sensor, but also in other signals.

Any significant maintenance or replacement will alter the behaviour of the system. Accordingly, normal behaviour models need to be re-trained after such events.

The model-based monitoring of drivetrain temperatures aims to detect slow degradation due to mechanical wear in bearings and gears. Early identification of these problems will enable the operator to optimise the maintenance scheduling and prevent long downtimes. However, challenges in representative training and limited detection capabilities result in significant uncertainties of this monitoring approach.

## 2.2. Physics of Failure

The Physics of Failure approach [14] aims to estimate damage accumulation based on a simplified physical model and operational statistics derived from SCADA data. Maintenance is to be targeted based on probabilities of failures. The basis of a Physics of Failure approach is a system analysis which includes a detailed system definition, potential failure modes with their causes and damage driving operating conditions. A damage accumulation model has to be built for each of the identified potential failure modes. Gray and Watson [14] gathered failure root causes of wind turbine gearboxes and derived several performance parameters from SCADA data to identify failure modes in a case study. The farm-wide comparison of the parameters such as average wind speed, rated power hours, brake application count, yaw movement, low speed and high power and rated speed hours, rotor starts and power dynamic, indicated that the failing turbines were affected by 'high cycle fatigue due to poor contact between roller and raceway occurring at conditions of high stationary power' [14]. A bearing damage model based on Lundberg-Palmgren's bearing life formulae and linear Palmgren-Miner damage accumulation was proposed and applied using the SCADA signals power and rotational speed to approximate the bearing load. The damage model was only calibrated with the observed failures, but the resulting damage values of the failing turbines were clearly higher than the 75% percentile of the farm. However, in terms of indicating problems in certain turbines, the farm-wide comparison of the rated power hours gave similarly helpful information. Accordingly, evaluating performance parameters can be prioritised over developing full damage models.

## 3. CASE STUDY

In this study, data from 12 turbines in an onshore UK wind farm with a capacity of approx. 1-3 MW are analysed. The SCADA records are available from a period of 2.5 years and consist of signals in 10 minute resolution as listed in Table 1, available as averages (mean) and partly maximums (max), minimums (min) and standard deviations (std). No detailed specification of sensor types or locations is available. The temperature signals are numbered, but lack a descriptive labelling.

Table 1: Case study SCADA signals

| **Parameter** | **Signal** |
|---|---|
| Wind speed | Mean, max, min, std |
| Wind, nacelle and relative direction | Mean |
| Pitch angle | Mean |
| Generator speed | Mean, max, min, std |
| Electrical power | Mean, max, min, std |
| Power factor, frequency | Mean |
| Voltage and current per phase | Mean |
| 16 temperatures | Mean |
| Active time for line, turbine, wind, ambient temperature, yaw motion | Seconds of 600 |

The investigated turbines were affected by several drivetrain subassembly or part replacements, which are gathered from a commented stoppage list as the only maintenance documentation. Five gearbox replacements, three generator replacements and six bearing replacements took place. Sufficient details to describe the failure are only given for one gearbox replacement, where gear teeth broke on the intermediate speed stage gear. Only three of the investigated turbines did not undergo any major replacement.

Due to the missing temperature labels in this case study, the different failing parts cannot be targeted directly by normal behaviour modelling. Instead, all temperature signals are analysed and possibly helpful targets identified. Pre-processing is applied in terms of a validity check and removal of a complete sample if invalid values are found. ANN models with 20 neurons in one hidden layer are trained with data representing 3 months. Five inputs are automatically selected on the basis of the strongest correlation in the training phase. Re-training of models after major replacements or obvious system modifications is implemented. Residuals are filtered for steps > 5°C in the target, model prediction or residual. To reduce the fluctuations, residuals are smoothed by calculating the median of each 288 samples (two days). Warnings are generated based on a threshold representing 2% exceeding probability derived from a fitted Gaussian distribution to the residual from the training period. Alarms are raised only if more than 3 of possibly 10 warnings occur in a moving window.

As a first step of the Physics of Failure approach, performance parameters are defined as given in Table 2. Due to the distribution of replacements in time, analysing statistics of the whole data as done in [14] would not be helpful. In contrast, the parameters are calculated for each month accumulating all data up to this date. Adequate normalisation is chosen to enable comparing of parameters from different data size. It has to be noted that the small number of turbines in this case study impedes any statistical analysis.

Table 2: Definition of performance parameters for failure analysis. All parameters (except TUS) are calculated for operation only by requiring power mean > 10%.

| **Parameter** | **Definition** | **Normalisation / scaling** |
|---|---|---|
| Wind speed (WS) | Average of wind speed mean | 1.0 to 1.5 rated wind speed |
| Turbulence (TU) | Average of wind speed std | 0 to 1.5 rated wind speed * 10 |
| Turbulence in standstill (TUS) | Average of wind speed std (power < 10%) | 0 to rated wind speed * 10 |
| Rated power (RP) | Count if power mean > 90% | Ratio: divide by sample size |
| High wind speed (HW) | Count if wind speed max > rated wind speed | Ratio: divide by sample size |
| Power factor inverse (PF) | 1 – average of power factor mean | *100 |
| Power dynamic (PD) | Average of power std | 0 to rated power * 10 |
| High rotational speed (HS) | Count if generator speed mean > 90% | Ratio: divide by sample size |

# 4. RESULTS

## 4.1. Model-based monitoring

Two temperatures are identified to relate to gearbox failures. The advance detection of problems is demonstrated in Figure 2 and 3. Gearbox problems are detected 39, 66, 75, 78 and possibly 492 days in advance for the five gearbox replacements, respectively. However, if the approach is applied to all turbines, a significant number of alarms is issued without known gearbox problems, see Figure 4. The alarms might be false or indicate other unreported problems. If the generator failures are to be detected, using another temperature shows good indication for the two replacements in the same turbine. However, the number of alarms in other turbines without generator replacement is high, see Figure 5. The alarm distribution over time indicates here a seasonal pattern visible in most turbines. Additionally, it seems possible, that some alarms might indicate gearbox problems. No clear alarm pattern is found in any of the temperatures for the bearing replacements.

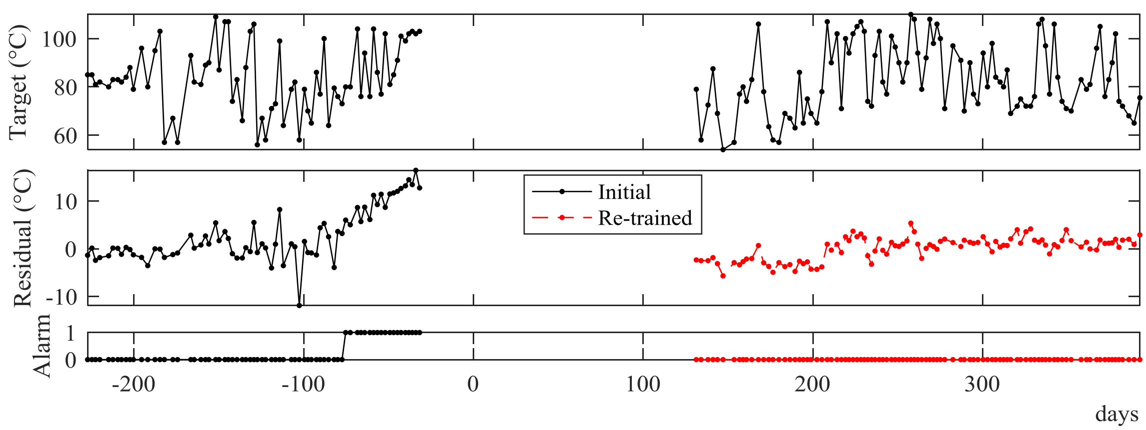


Figure 2. Detection of a gearbox problem with the time axis referring to the replacement date (temperature A, turbine 12).

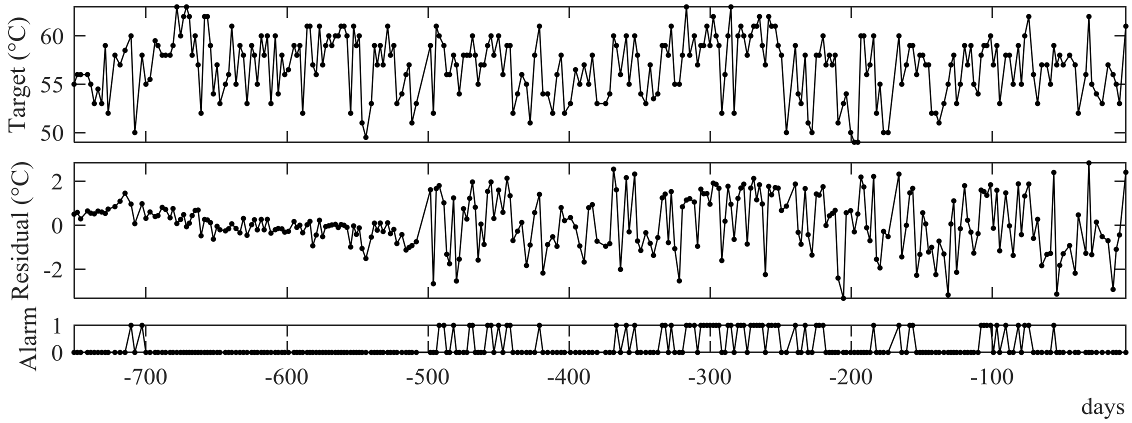


Figure 3. Detection of a gearbox problem with the time axis referring to the replacement date (temperature B, turbine 2).

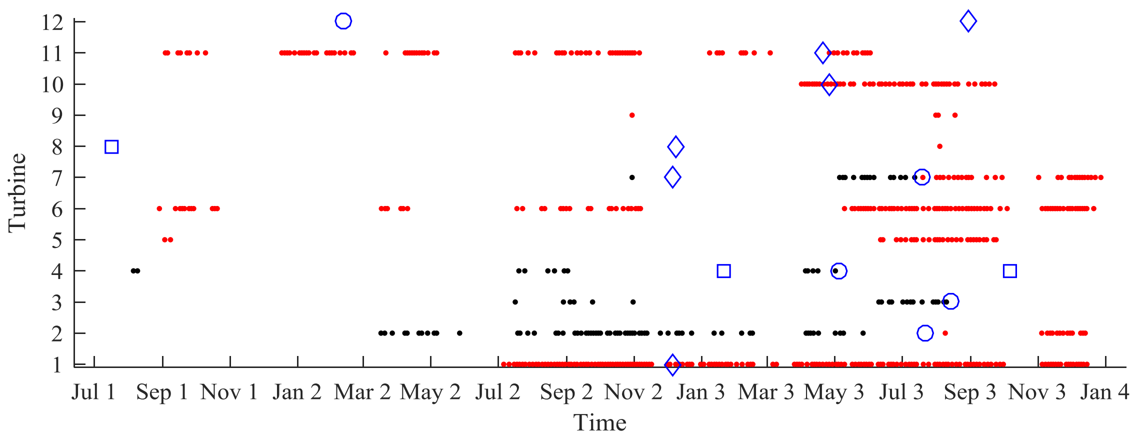


Figure 4. Alarms for gearbox problems in all turbines based on temperature B. Unrelated alarms are marked red, gearbox replacements with a circle, generator and bearing replacements with a square and asterisk, respectively.

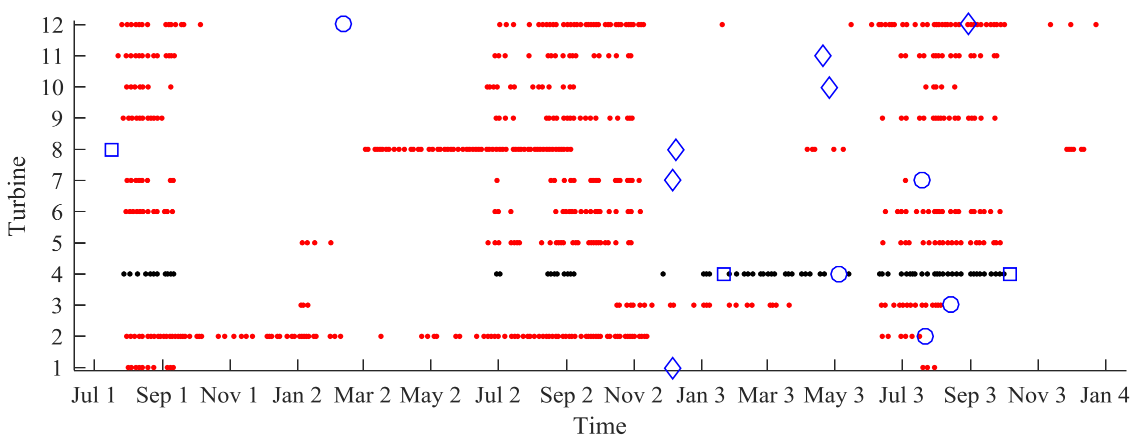


Figure 5. Alarms for generator problems in all turbines based on temperature C. Unrelated alarms are marked red, generator replacements with a square, gearbox and bearing replacements with a circle and asterisk, respectively.

## 4.2. Operational statistics

The analysis of the defined performance parameters showed that the whole farm is affected by changing operation during the whole 2.5 years of data as the parameter values from all turbines clearly vary with time. As there is no common pattern, it is most likely that the reported replacements of gearboxes, generators and bearings have diverse causes and failure modes. Examples are given in Figure 6 and 8 for selected dates with highlighted replacements happening in this month. The generator problem in turbine 4, Figure 6a, seems to be related to relative high wind speed and accordingly rated power operation and high speed. Noticeably, the reactive power generation was exceptionally high in this time in several turbines including the failing one (average power factor of 0.9947). The bearing replacements, Figure 6b and Figure 7a, are found with various parameter values. Although most of the replacements show low or average parameter values, some are linked to high turbulence in operation. A high turbulence could also be the driver of the two gearbox replacements in Figure 7b.

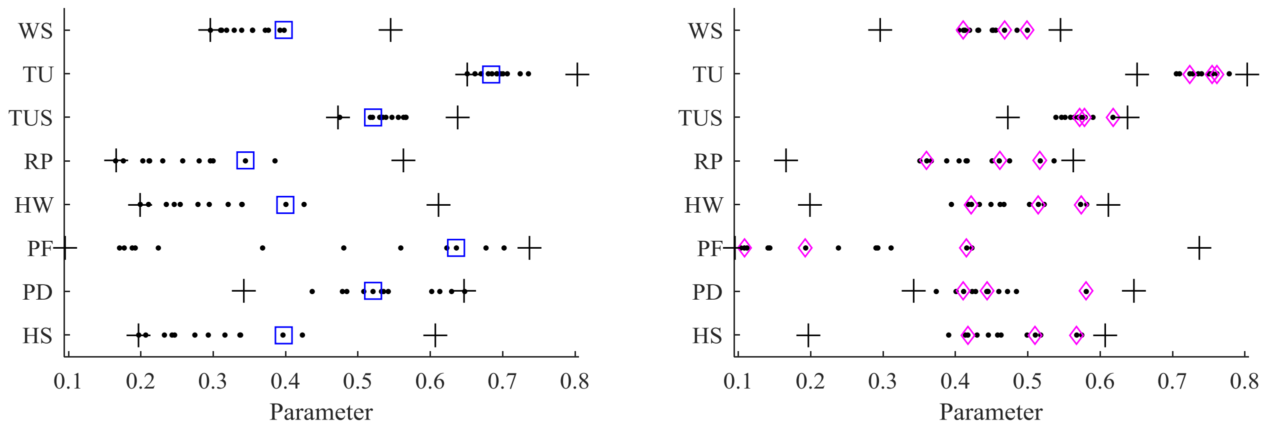


(a) (b)

Figure 6. Performance parameters for all turbines in July year 1 (a) and December year 2 (b). Generator and bearing replacements marked with square and diamond, respectively. The extrema of the parameters from all months are marked with a plus symbol.

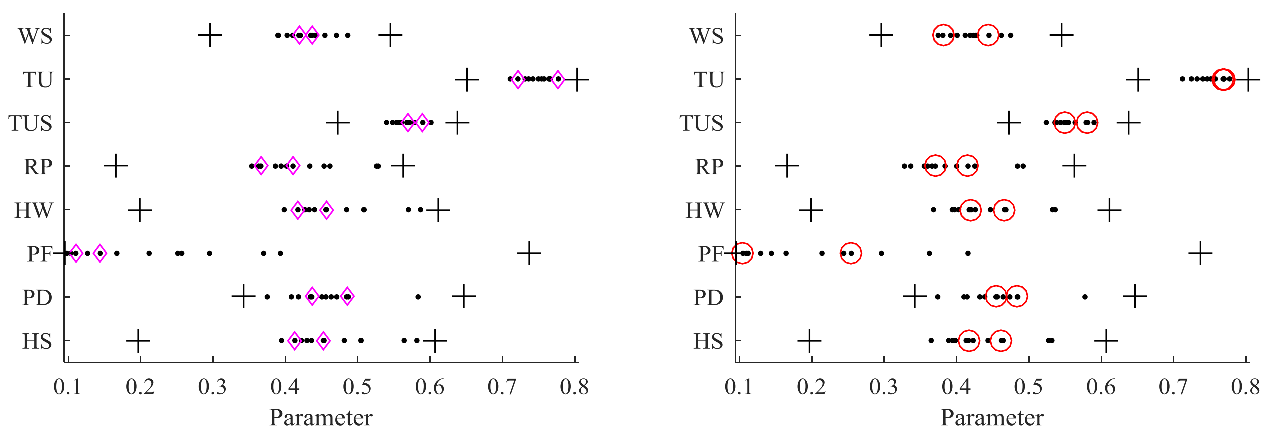


(a) (b)

Figure 7. Performance parameters for all turbines in April year 3 (a) and July year 3 (b). Bearing and gearbox replacements marked with diamond and circle, respectively. The extrema of the parameters from all months are marked with a plus symbol.

# 5. CONCLUSION

Operational data from wind turbines could build an alternative and complement of dedicated vibration measurements. Model-based monitoring is a way to detect anomalies in the behaviour of wind turbine drive train temperature signals to detect mechanical degradation and possible failures. In contrast, the statistical analysis used in the Physics of Failure approach tries to identify turbines at risk by evaluating the damage drivers with performance parameters. A combination of the two approaches is proposed to increase the reliability of monitoring.

In a case study, both approaches are applied with the aim of finding early indications for several gearbox, generator and generator bearing replacements. In the model-based monitoring with ANNs and thresholds based on the residual distribution from training, early alarms for all gearbox replacements are issued. Similarly, generator problems in one turbine show up if using another temperature signal. However, many unrelated or possibly false alarms in turbines without reported problems of this type reveal challenges in getting reliable monitoring. The evaluation of the performance parameters results in the conclusion that different damage drivers and failure modes were involved. Particular high values in turbulence, reactive power generation and wind speed are found to correlate with some of the failed turbines. Although the properties of the case study limit the capabilities of both approaches, it can be seen that the combination of model-based monitoring and statistical analysis of SCADA data increases the knowledge of the system's condition.

In future works, the performance parameter values of this farm shall be compared to farms with similar settings. However, a thorough evaluation of the benefit of combining the two monitoring approaches will need better case data with a bigger farm size, more fault-free turbines and sufficient documentation.

## ACKNOWLEDGEMENTS

This project has received funding from the European Union's Horizon 2020 research and innovation programme under the Marie Sklodowska-Curie grant agreement No 642108 (project AWESOME, http://awesome-h2020.eu/).

## REFERENCES

[1] Carroll, J., McDonald, A., McMillan, D. (2015) Failure rate, repair time and unscheduled O&M cost analysis of offshore wind turbines. Wind Energy 17:1107–19. doi: 10.1002/we.1887.

[2] Reder, M., Gonzalez, E., Melero, J.J. (2016) Wind Turbine Failure Analysis - Targeting current problems in Failure Data Analysis. J Phys Conf Ser 753. doi: 10.1088/1742-6596/753/7/072027.

[3] Tchakoua, P., Wamkeue, R., Ouhrouche, M., Slaoui-Hasnaoui, F., Tameghe, T.A., Ekemb, G. (2014) Wind Turbine Condition Monitoring: State-of-the-Art Review, New Trends, and Future Challenges. Energies 7:2595–630. doi: 10.3390/en7042595.

[4] Qiao, W., Lu, D. (2015) A Survey on Wind Turbine Condition Monitoring and Fault Diagnosis - Part II: Signals and Signal Processing Methods. IEEE Trans Ind Electron 62:6546–57. doi: 10.1109/TIE.2015.2422394.

[5] Qiu, Y., Feng, Y., Tavner, P., Richardson, P., Erdos, G., Chen, B. (2012) Wind turbine SCADA alarm analysis for improving reliability. Wind Energy 15:951–66. doi: 10.1002/we.513.

[6] Gonzalez, E., Reder, M., Melero, J.J. (2016) SCADA alarms processing for wind turbine component failure detection. J Phys Conf Ser 753. doi: 10.1088/1742-6596/753/7/072019.

[7] Feng, Y., Qiu, Y., Crabtree, C.J., Long, H., Tavner, P.J. (2013) Monitoring wind turbine gearboxes. Wind Energy 16:728–40. doi: 10.1002/we.1521.

[8] Schlechtingen, M., Ferreira Santos, I. (2011) Comparative analysis of neural network and regression based condition monitoring approaches for wind turbine fault detection. Mech Syst Signal Process 25:1849–75. doi: 10.1016/j.ymssp.2010.12.007.

[9] Bangalore, P., Tjernberg, L.B. (2015) An Artificial Neural Network Approach for Early Fault Detection of Gearbox Bearings. IEEE Trans Smart Grid 6:980–7. doi: 10.1109/TSG.2014.2386305.

[10] Sun, P., Li, J., Wang, C., Lei, X. (2016) A generalized model for wind turbine anomaly identification based on SCADA data. Appl Energy 168:550–67. doi: 10.1016/j.apenergy.2016.01.133.

[11] Schlechtingen, M., Santos, I.F., Achiche, S. (2013) Wind turbine condition monitoring based on SCADA data using normal behavior models. Part 1: System description. Appl Soft Comput 13:447–60. doi: 10.1016/j.asoc.2013.09.016.

[12] Wang, Y., Infield, D. (2012) Supervisory control and data acquisition data-based non-linear state estimation technique for wind turbine gearbox condition monitoring. IET Renew Power Gener 7:350–8. doi: 10.1049/iet-rpg.2012.0215.

[13] Tautz-Weinert, J., Watson, S.J. (2016) Comparison of different modelling approaches of drive train temperature for the purposes of wind turbine failure detection. J Phys Conf Ser 753:72014. doi: 10.1088/1742-6596/753/7/072014.

[14] Gray, C.S., Watson, S.J. (2010) Physics of Failure approach to wind turbine condition based maintenance. Wind Energy 13:395–405. doi: 10.1002/we.360.

# Adaptive Fault Detection and Tracking for a Wind Turbine Generator using Kalman Filter

***Raed Khalaf Ibrahim, Abdullahi Daniyan and Simon Watson***
*Wolfson School of Mechanical, Electrical and Manufacturing Engineering,*
*Loughborough University, UK.*
*R.Ibrahim@lboro.ac.uk, A.Daniyan@lboro.ac.uk, S.J.Watson@lboro.ac.uk*

***Abstract*—This paper describes a wind turbine (WT) condition monitoring technique that uses the measurement of stator current and rotational speed to derive a fault detection signal. The detection algorithm uses a Kalman filter (KF) to extract and track the strength of particular frequency components, characteristic of faults in the stator current signal. This has been done by an extensive simulation studies to develop an on-line detection and monitoring of mechanical faults in permanent magnet synchronous generators (PMSGs), recentlly used in modern variable-speed WTs. The model is developed and validated with operational data of five 2.5MW turbines were recorded by the supervisory control and data acquisition (SCADA) system over the period of 1 year. The simulation results show that the KF algorithm can provide a reliable indication of the presence of a fault with low computational times, from director indirect-drive fixed- or variable-speed WTs. The proposed algorithm can indicate the severity of the fault, where in contrast with traditional methods, they failed to extract the fault features from non-stationary current measurements, due to variable-speed operating conditions of WTs.**

***Index Terms*—Wind turbine, Generator, Condition monitoring, Current Signature, Fault signature, Fault detection, Diagnosis.**

## I. Introduction

Wind energy has been one of the fastest growing power sources in the world over the last two decades. The worldwide wind capacity reached 392.927 GW by the end of June 2015, out of which 21.678 GW were added in the first six months of 2015 [1]. The cost of operations and maintenance (OM) has been shown to be anything between 15% and 35% of the cost of energy from wind [2], and there is a great demand to reduce OM cost. The goal can be reached by detecting and identifying the fault of WTs in early stage which gives the operator sufficient time to make more informed maintenance decision. Traditionally, WTs condition monitoring method is supervised using vibration analysis but measuring such mechanical quantities is often expensive. Indeed, vibration sensors such as piezoelectric accelerometers and associated load amplifier are often expensive. Moreover, the ability of a clear detection of mechanical faults by vibration measurements potentially depends in the sensor locations [3]. For example, accelerometers need to be mounted near to each possible faulty component of the WT. The technique is also not ideally suited to all WT types and faults [4]. It has been reported in a recent reliability survey [5] that WT electrical components have a higher failure rate than the mechanical components. As the measurement of stator currents are already available for control purposes which means no additional sensors or data acquisition devices are needed [6], so the detection based on the measurement of stator currents would be beneficial and could be more comprehensive, simpler, and cheaper than other techniques. However, there are challenges in using current measurements for WT condition monitoring and fault detection. First, it is a challenge to extract WT fault signatures from non-stationary current measurements, due to variable-speed operating conditions of WTs [7]. Moreover, the useful information in current measurements for WT usually has a low signal to noise ratio, and thus very difficult to extract without a dedicated signal processing [8].

Generally, the majority of WT condition monitoring and fault diagnosis techniques have employed the Fourier Transform (FT) to detect a fault from the stator current [9]. The limitations of the direct application of the Fourier transform methods, and their inability to localize a signal in both the time and frequency domains, was realized very early on in the development of radar and sonar detection. Thus, a number of more advanced time-frequency analysis techniques were developed in recent years in order to extract fault signatures from the monitored signal. Among these newly developed methods, the short time Fourier transform (STFT) also known as windowed Fourier transform which has been widely used to compute the spectrogram from time signal which shows the spectral density of a signal varying with time [10]. Although the STFT can be used for analyzing transient signals using a time-frequency representation, it fails to give detailed information of the fault level because the STFT can only analyze the signal with a fixed sized window for all frequencies, which leads to poor frequency resolution. Wavelet transform is another well-known method for feature extraction in the area of fault detection and diagnosis [11]. Unlike the STFT with a fixed window function, the wavelet transform involves a varied time-frequency window and can provide good localization property in both the time and frequency domain, but it suffers from inevitable issues of low resolution, interference terms, border distortion, and energy leakage [12].

The KF algorithm is a relatively new method for time-frequency analysis that is able to track the instantaneous amplitude and frequency of nonlinear and non-stationary signals [13]. Unlike, short-time Fourier transform and wavelet transform, the KF is based on an adaptive algorithm and does not use any windowing technique. Therefore, no prior knowledge of the signal is required to implement the KF. Consequently, the trade-off between time and frequency resolutions is less controversial and can be used for real-time frequency tracking. Recently, the KF has been found to be powerful and successful in condition monitoring of permanent magnet synchronous machines operating under various speed and load conditions [14], and in detection of half- as well as full broken single rotor bar fault of a squirrel-cage induction machine under various loading conditions and speeds using stator current data [15].

This paper is a continuation of the preliminary investigation into the protection of PMSG-based WTs presented in [7]. The current work investigates the application of the KF to detect mechanical failures in WTs using generator stator current signals. Successful utilization of stator currents represents a cost-effective, non-intrusive condition monitoring and fault diagnosis technique for retrofitting existing condition monitoring methods for WTs. To verify the effectiveness of the proposed algorithm, a WT simulation model is developed and validated with operational data of five 2.5MW turbines were recorded by the SCADA system over the period of 1 year. The simulation results demonstrate that the proposed method is effective in detecting mechanical faults in a variable speed machine.

## II. Kalman Filter for Fault Detection and Tracking

A system whose physical process can be mathematically modelled as it changes or evolves over time is known as a dynamical system. In making inference for such a system, two models are usually considered, a state model and a measurement model. The problem of fault detection and tracking using electrical signals from a WT can be related to dynamical systems. This is so due to the fact that the operating state of a WT changes or evolves over time depending on whether the machine is operating at below the rated wind speed or above the rated, whether a fault occurs or not, whether the fault is transient or permanent and so on. The two dynamical system models mentioned above are used with the KF and applied to our problem.

The Kalman filter (KF) can be thought of as a sequential minimum mean square error (MMSE) estimator of a given signal (for example, electrical signals from a WT that is embedded in noise, where the signal is characterized by a state model [16]. The state and measurement models used in our problem are described next.

### A. State Model

The state model is otherwise known as the state evolution model. In our problem, it describes the motion model of a given frequency profile, i.e. how the amplitude of a frequency changes from an observation time $k$ to next $k+1$.

$$\mathbf{x}_k = \mathbf{F}\mathbf{x}_{k-1} + \mathbf{v}_k \tag{1}$$

where $\mathbf{x}_k$ denote a normal state with dimension $\mathbf{dx}_1$ and $\mathbf{x}_k = [f, A]^T$, where $f$ and $A$ denote frequency and amplitude respectively. $k$ = 1,2,... is the time instant of the discrete model. $\mathbf{F}$ is a $\mathbf{dx}_d$ matrix that define the linear function and is known as state transition matrix. $\mathbf{v}_k$ is a $\mathbf{dx}_1$ zero mean and an independent and identically distributed (i.i.d.) process noise vector with a $\mathbf{dx}_d$ covariance matrix $\mathbf{Q}_k$.

### B. Measurement Model

The measurement model maps the normal state from the state space onto the observation space. In our problem, it is given as:

$$\mathbf{z}_k = \mathbf{H}\mathbf{x}_k + \mathbf{n}_k \tag{2}$$

where $\mathbf{z}_k$ denote the measurement received at time $k$, $\mathbf{H}$ is a matrix that define the transformation function and is known as the transformation matrix. $\mathbf{n}_k$ is a zero mean and an i.i.d. measurement noise vector with covariance matrix $\mathbf{C}_k$.

In order to implement the KF in our fault detection and tracking problem, we assume that both the state and measurement models are linear and Gaussian as evident from (1) and (2). Following this assumption, we formulate the KF algorithm for our problem thus:

$$\mathbf{x}_{k|k-1} = \mathbf{F}\mathbf{x}_{k-1|k-1} \tag{3}$$

$$\mathbf{M}_{k|k-1} = \mathbf{Q}_k + \mathbf{F}\mathbf{M}_{k-1|k-1}\mathbf{F}^T \tag{4}$$

$$\mathbf{x}_{k|k} = \mathbf{x}_{k|k-1} + \mathbf{K}_k(-\epsilon_k) \tag{5}$$

$$\mathbf{x}_{k-1|k-1} = \mathbf{x}_k \tag{6}$$

$$\mathbf{M}_{k|k} = \mathbf{M}_{k|k-1} - \mathbf{K}_k\mathbf{H}\mathbf{M}_{k|k-1} \tag{7}$$

where

$$\epsilon_k = \mathbf{x}_k - \mathbf{z}_k \tag{8}$$

$$\mathbf{P}_k = \mathbf{H}\mathbf{M}_{k|k-1}\mathbf{H}^T + \mathbf{C}_k \tag{9}$$

$$\mathbf{K}_k = \mathbf{M}_{k|k-1}\mathbf{H}^T\mathbf{P}_k^{-1} \tag{10}$$

where $\mathbf{z}_k$ is the signal from the WT, and $\mathbf{x}_k$ is the expected normal state. $\epsilon_k$ denote the measurement innovation and $\mathbf{P}_k$ is covariance of the innovation term $\epsilon_k$, with $\mathbf{K}_k$ being the Kalman gain. For a matrix $\mathbf{B}$, $\mathbf{B}^T$ is its transpose. Equations (3) and (4) are the KF prediction equations and (5) and (7) are the update equations.

Notice in (5) that the Kalman gain, $\mathbf{K}_k$ is multiplied by the negative of the innovation term, $\epsilon_k$. This is because in our approach, we are interested in detecting whether a given normal state, $\mathbf{x}_k = [f, A]^T$ changes due to fault by tracking $\mathbf{x}_k$. When a fault occurs, it will be captured by the KF algorithm and both the fault frequency, $f$ and amplitude, $A$ as well as the time $k$ of the fault can be observed. The Implementation of the KF algorithm for fault detection and tracking is discussed next.

### C. Implementation

At time $k$, observed time series electrical signals obtained from the WT are converted to the frequency domain through Fourier transform. Various known and expected fault frequencies are selected along with their acceptable normal operating amplitudes to form the normal state vector, $\mathbf{x}_k^n = [f_n, A_n]^T$, where $n = 1, \cdots, N$ and $N$ is the number of frequency-amplitude pair selected for monitoring. $N$ banks of KF algorithms using (3) to (7) are deployed to perform the fault detection and tracking.

The fault detection and tracking for the $n$-th frequency-amplitude pair is captured in $\mathbf{x}^n_{k|k}$ of eqn. (5). A 2D plot of the amplitude, $A_n$ of the $n$-th frequency-amplitude pair against time, (i.e. $k$) from the tracked normal state, $\mathbf{x}^n_{k|k}$ can easily be used to visualize the fault profile of the $n$-th frequency-amplitude pair having frequency, $f_n$. A rise in amplitude from the normal state indicates the occurrence of a fault (of which the fault frequency, amplitude and time of occurrence are contained in $\mathbf{x}^n_{k|k}$). If this fault is transient, the observed rise will eventually fall and if the fault is permanent or fixed, the rise will remain constant or increase further depending on the severity of the fault.

## III. SIMULATION

In order to verify the performance of the fault detection and tracking algorithm, a general model for representation of variable speed WTs was implemented in MATLAB/Simulink, including wind speed, rotor, pitch control system, drivetrain and generator model [7]. The model has been developed to facilitate the investigation of condition monitoring and effective algorithm development for fault detection. The measured wind speed data recorded by 2.5MW WT SCADA system has been used as model input to validate the response of the WT model. Figure 1 shows the response of the model to measured generator speed. It is clear the model is in good agreement with the measured data.

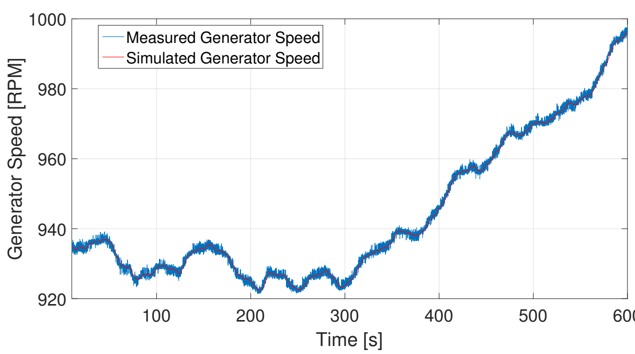


Fig. 1: Example of model validation considering generator speed.

Rotor eccentricity in a variable speed WT with a permanent magnet synchronous generator (PMSG) is used as an illustrative example to investigate the use of the KF algorithm with the aim of developing knowledge based fault detection method for performing online fault detection in variable speed WTs. During rotor eccentricity, certain sideband harmonics around the fundamental frequency in the machine current signal occur and their amplitude increases proportionally with the fault level. It was experimentally proven [6] that rotor eccentricity faults actually give rise to a sequence of such sidebands given by:

$$f_c = \left(1 \pm \frac{2k_p - 1}{p}\right).f_f \qquad (11)$$

Where $f_c$ and $f_f$ are the rotor fault and fundamental frequency components, respectively, $k_p$ is an integer ($k_p$=1, 2, 3, ...) and $p$ is the number of pole pairs. In order to observe the excitation of sideband harmonics, known as fault signature frequencies, due to the fault, the model was run at constant sub-synchronous, synchronous and super-synchronous speeds, respectively. Figure 2 shows the stator current spectra for the faulty machine operating at three operational points under faulty rotor conditions. One can notice components with frequencies at 60 Hz and 40 Hz, which are intentionally simulated to be present in the spectra as a dynamic eccentricity. Other spectral components given by the Equation (11) are generated by the fault. However, it is clear that the fault signature frequencies are not consistent across the results. This is mainly because the fundamental frequency in PMSGs is proportional to the rotational speed so that the fault signature frequencies are shifted respect to the rotational speed value, which means that the current signals acquired from the generator terminals of the WTs are always non-stationary.

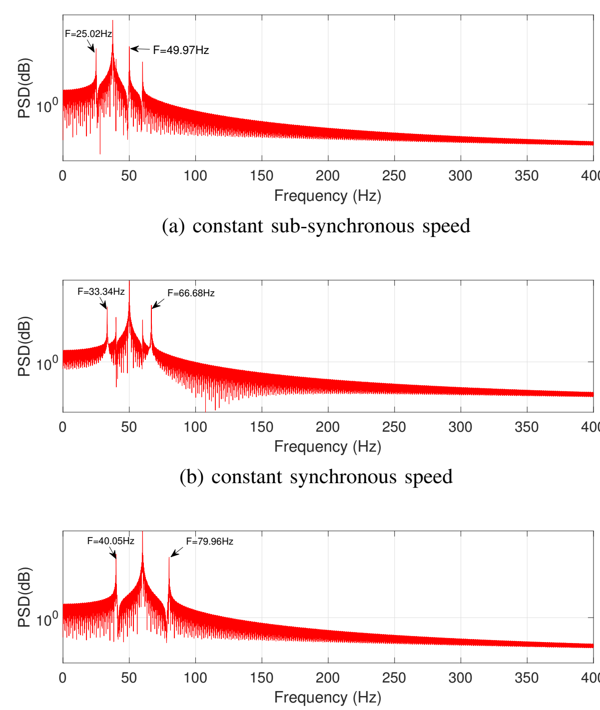


(a) constant sub-synchronous speed

(b) constant synchronous speed

(c) constant super-synchronous speed

Fig. 2: Stator current spectra for the healthy PMSG at three operational points.

Generally, WTs based PMSGs operate in variable-speed conditions owing to varying wind speeds. As a consequence, the fault signature frequencies are buried in wide-band dominant frequency components (i.e. harmonics due to variable rotational speeds) of the current signal that are irrelevant to the fault as shown in Figure 3. To solve this problem, the Kf algorithm is employed to track the magnitude of the lower fault signature frequency (LFSF) and upper fault signature frequency (UFSF),given by the Equation (11), over time form the non-stationary generator current signal.

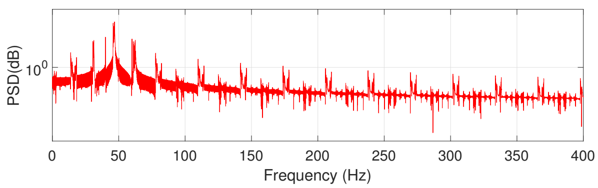


Fig. 3: Stator current spectra for the faulty PMSG at variable speed.

## IV. Fault Feature Extraction

A novel algorithm is developed to employ the KF for extracting the fault features among other wide-band dominant frequency components of the current signal that are irrelevant to the fault due to variable rotational speeds. To solve this problem, a non-stationary current signal which recorded for 300 seconds is firstly splitted into 2 second intervals leading to 150 data sets. The data sets are transformed to frequency domain using the Fast Fourier Transform (FFT) algorithm. The period of two seconds is chosen as the shortest possible interval with a sufficient resolution frequency domain to capture all frequency components of interest. Secondly, the fault-related features are then extracted from the FFT spectrum of the converted stationary current signal to reconstruct a new signal for quantitative health condition evaluation of the WT. After completing the previous steps, the 150 data sets have been applied to the KF algorithm at variable speeds at different fault conditions as follow:

- Permanent fault with a fixed level during the entire time simulation,
- Transient fault during the time period from 50sec to 100 sec,
- Variable fault level increasing linearly and proportionally with time simulation,

A process is developed to extract the maximum magnitude of particular frequency among fault signature frequencies for each data set. Then the magnitude of the frequencies of interest has been tracked over time as shown in Figure 5. By doing so, it is possible to create simple graphs tracking the fault signature frequencies over time as shown in Figure 5. The results can be visually inspected to verify the presence of the fault in question as well as to identify its severity. The KF algorithm innovatively explores the impacts of faults on stator current signatures, in the sense of variations in time domain over frequency ranges, rather than the changes at a specific frequency or several specific frequencies. The proposed algorithm is especially useful for cases where no specific frequency components are available in the measured signals, or when the characteristic frequencies are non-stationary, and thus not directly observable.

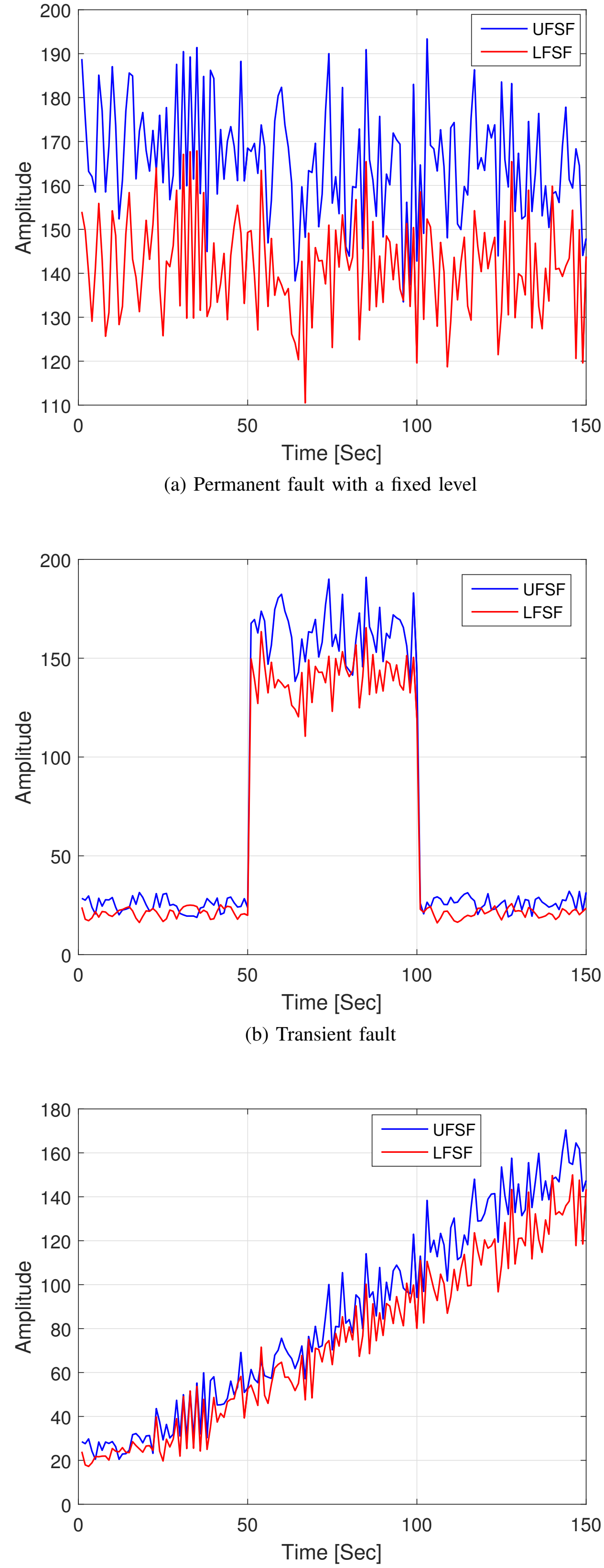


(a) Permanent fault with a fixed level

(b) Transient fault

(c) Variable fault level

Fig. 4: Extracting the magnitude of the fault signature frequencies over time at different fault conditions.

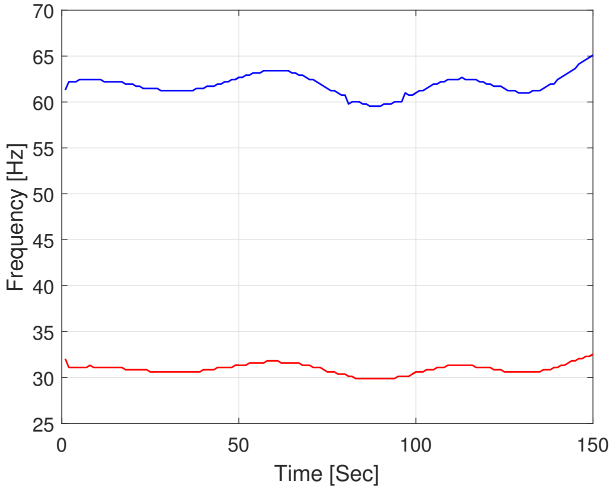


(a) Permanent fault with a fixed level

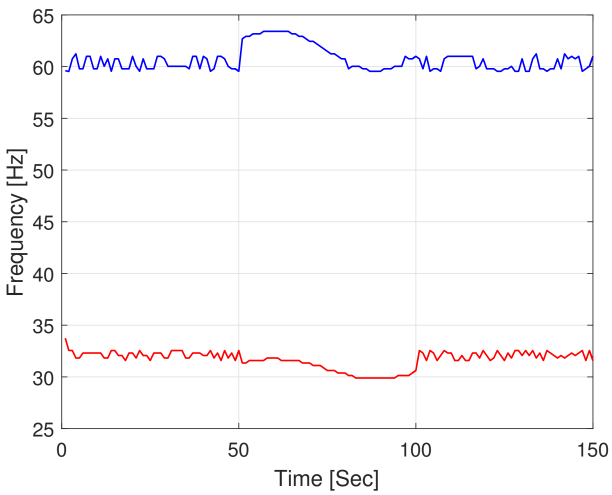


(b) Transient fault

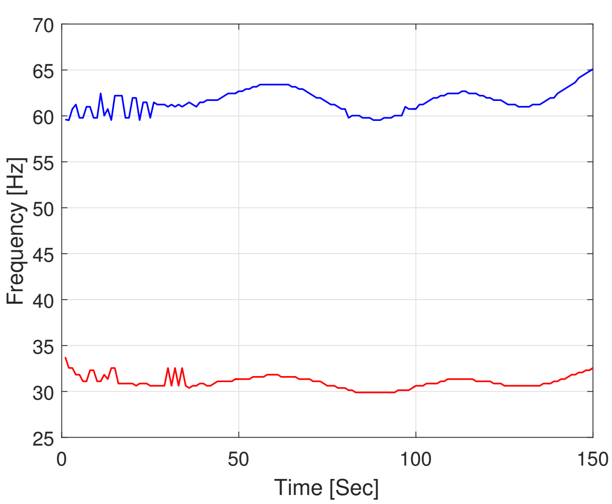


(c) Variable fault level

Fig. 5: Tracking the fault signature frequencies over time at different fault conditions.

## V. CONCLUSION

The KF-based algorithm is capable of detecting mechanical faults based on time-frequency analysis by tracking the instantaneous amplitude and frequency from the current signal. It can be directly applied to the nonlinear and non-stationary signals, without prepossessing to convert the characteristics frequencies to corresponding constant values. It overcomes the drawbacks of traditional frequency-based fault detection techniques that particular characteristic frequencies related to the faults should be pre-acquired.

## REFERENCES

[1] The World Wind Energy Association, WWEA BULLETIN SPECIAL ISSUE 2015, [Online]: http://www.wwindea.org/wwea-bulletin-special-issue-2015/.

[2] E. Wiggelinkhuizen, T. Verbruggen, H. Braam, L. Rademakers, J. Xiang, and S. Watson, "Assessment of condition monitoring techniques for offshore wind farms," *Journal of solar energy engineering*, vol. 130, no. 3, p. 031004, 2008.

[3] Y. Amirat, M. Benbouzid, B. Bensaker, and R. Wamkeue, "Condition monitoring and ault diagnosis in wind energy conversion systems: a review," in *Electric Machines & Drives Conference, 2007. IEMDC'07. IEEE International*, vol. 2, pp. 1434–1439, IEEE, 2007.

[4] W. Yang, P. Tavner, C. Crabtree, and M. Wilkinson, "Cost-effective condition monitoring for wind turbines," *Industrial Electronics, IEEE Transactions on*, vol. 57, pp. 263–271, Jan 2010.

[5] C. Crabtree, Y. Feng, and P. Tavner, "Detecting incipient wind turbine gearbox failure: a signal analysis method for on-line condition monitoring," in *Proceedings of European Wind Energy Conference (EWEC 2010), Warsaw, Poland*, pp. 20–23, 2010.

[6] X. Gong and W. Qiao, "Current-based mechanical fault detection for direct-drive wind turbines via synchronous sampling and impulse detection," *IEEE Transactions on Industrial Electronics*, vol. 62, no. 3, pp. 1693–1702, 2015.

[7] R. K. Ibrahim and S. Watson, "Wind turbine simulation model for the study of combined mechanical and electrical faults," in *Scientific Track Proceedings of European Wind Energy Association. EWEA*, 2015.

[8] R. K. Ibrahim and S. Watson, "Effect of power converter on condition monitoring and fault detection for wind turbine," in *Power Electronics, Machines and Drives, 2016. PEMD 2016. 8th IET Conference on*, IET, 2016.

[9] W. Jeffries, J. Chambers, and D. Infield, "Experience with bicoherence of electrical power for condition monitoring of wind turbine blades," *IEE Proceedings-Vision, Image and Signal Processing*, vol. 145, no. 3, pp. 141–148, 1998.

[10] B. Yazici and G. B. Kliman, "An adaptive statistical time-frequency method for detection of broken bars and bearing faults in motors using stator current," *IEEE Transactions on Industry Applications*, vol. 35, no. 2, pp. 442–452, 1999.

[11] S. J. Watson, B. J. Xiang, W. Yang, P. J. Tavner, and C. J. Crabtree, "Condition monitoring of the power output of wind turbine generators using wavelets," *Energy Conversion, IEEE Transactions on*, vol. 25, no. 3, pp. 715–721, 2010.

[12] Z. Peng, W. T. Peter, and F. Chu, "An improved hilbert–huang transform and its application in vibration signal analysis," *Journal of sound and vibration*, vol. 286, no. 1, pp. 187–205, 2005.

[13] H. Hajimolahoseini, R. Amirfattahi, H. Soltanian-Zadeh, and S. Gazor, "Instantaneous fundamental frequency estimation of non-stationary periodic signals using non-linear recursive filters," *IET Signal Processing*, vol. 9, no. 2, pp. 143–153, 2015.

[14] C. Wang, M. Delgado, L. Romeral, Z. Chen, F. Blaabjerg, and X. Liu, "Detection of partial demagnetization fault in pmsms operating under nonstationary conditions," 2016.

[15] F. Gu, T. Wang, A. Alwodai, X. Tian, Y. Shao, and A. Ball, "A new method of accurate broken rotor bar diagnosis based on modulation signal bispectrum analysis of motor current signals," *Mechanical Systems and Signal Processing*, vol. 50, pp. 400–413, 2015.

[16] S. Kay, *Fundamentals of Statistical Signal Processing: Estimation Theory*, vol. 1. Prentice-Hall PTR, 1993.

# Condition monitoring of wind turbine drive trains by normal behaviour modelling of temperatures

Jannis Tautz-Weinert*[1]
Simon J. Watson[1]

[1]Centre for Renewable Energy Systems Technology (CREST),
Wolfson School of Mechanical, Electrical and Manufacturing Engineering,
Loughborough University
Holywell Park, Loughborough, LE11 3TU, United Kingdom

# Contents

# 1 Abstract

Condition monitoring and early failure detection are needed to reduce operational costs of wind turbines, particularly for offshore farms where accessibility is restricted. Failure detection technologies should be simple and reliable in order to contribute to the overall aim of cost reduction. Operational data from the Supervisory Control And Data Acquisition (SCADA) system are a potential source of information for condition monitoring and have the advantage of being recorded at each turbine without the costs of additional sensors. Detection of drivetrain failures using these ten-minute data has been successfully demonstrated in the last five years. This paper summarises and evaluates different ways of so-called normal behaviour modelling of temperature using SCADA data, i.e. the prediction of a measured temperature under the assumption that the system is behaving normally. After training, the residual of modelled and measured temperature acts as an indicator for possible wear and failures. Multiple approaches are discussed: linear modelling, artificial neural networks in auto-regressive, feed-forward and layer recurrent configurations, adaptive neuro-fuzzy inference systems and state estimation techniques. A case study with real data reveals differences of approaches, sensitivity to training data and settings of algorithms. Early failure detection of a gearbox failure is demonstrated, although challenges in achieving reliable monitoring without many false alarms become apparent.

# 2 Introduction

Although wind energy costs have been dramatically decreased in the last decade, maintenance costs still contribute with up to 40 EUR/MWh for offshore farms [MIL14]. Traditional corrective maintenance strategies cannot be used for current projects in remote or offshore locations where limited accessibility would result in extended downtimes. Additionally, the financial losses per downtime are more critical nowadays due to dramatically increased turbine sizes and associated higher energy production. The advanced maintenance strategy of condition-based or predictive maintenance requires health statuses for all critical parts. Temperatures recorded by the Supervisory Control And Data Acquisition (SCADA) system are a cost-effective way to monitor the drive train health as these are commonly available for performance monitoring. In contrast, ‘dedicated’ condition monitoring systems, which are mainly based on vibration monitoring, are installed as an ‘add-on’ and may cost 11,000 EUR per turbine [YAN13]. Although SCADA data are usually sampled as low resolution 10 minute averages, slow wear related degradation can be tracked by finding changes in the temperature behaviour – i.e. how the temperature reacts in the transient interaction of turbine loading, cooling systems, heat convection and the environment. In contrast to monitoring of high absolute temperatures which commonly occur only shortly before a fault, the slight changes in the temperature behaviour can develop well in advance. First approaches investigated trends by visually comparing drive train temperatures as a scatter plot against the relative power [WIG08, FEN13] or building clusters of presumed healthy and faulty samples [KIM11, WIL14]. These attempts proved that analysis of SCADA data might help to detect imminent failures, but highly manual interpretation was required. For effective clustering of the condition, training data including faults has to be available, which is not feasible in practice. Recent research has focused on data-driven normal behaviour modelling (NBM), where temperatures are modelled using the history of the signal and / or information from other sensors while assuming normal behaviour, i.e. a healthy turbine [WIL14, SCH13, SUN16]. Further research has e.g. investigated more physical damage modelling or assessment of SCADA alarms. An overview of condition monitoring with SCADA data can be found in a recent review of the authors [TAU16a]. This paper focuses on different approaches of NBM of drive train temperature and ways to detect imminent failures. In a case study, data from a real wind farm are used to briefly demonstrate the functionality and assess the quality of modelling and monitoring.

# 3 Main section

NBM can be described as modelling a signal with information from the environment and from the process itself as sketched in Figure 1. In the case of the wind turbine considered as a process, the environment might consist of e.g. ambient temperature, wind speed etc. and process variables like turbine power output, rotational speed or temperatures acting as additional inputs. The model uses the information from the inputs to predict the target temperature by learning the relationship during a training phase. Different methodologies for modelling are discussed in chapter 3.1. After training, the residual of measured and modelled signal is expected to be approx. 0 for healthy conditions and different from 0 for faulty conditions. Several techniques to detect anomalies in the residual are discussed in chapter 3.2.

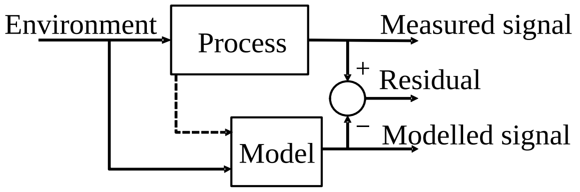


**Figure 1:** Sketch of NBM principle [TAU16b]

## 3.1 NBM modelling techniques

The different NBM modelling techniques can be assigned to two main approaches. If historic values of the target are used beside other inputs, the model can be termed auto-regressive with exogenous input (ARX). On the other hand,, full signal reconstruction (FSRC) avoids using the history of the target signal. The most promising FSRC modelling approaches derived from an earlier case study [TAU16b] are compared with three different ARX approaches.

### 3.1.1 FSRC – non-auto-regressive

FSRC is tested by using the two strongest signals from a cross-correlation analysis as inputs to predict a target temperature. Findings from a previous case study indicated that using more or lagged inputs does not necessarily improve the accuracy significantly [TAU16b].

One of the simplest ways of modelling the target temperature is building a weighted sum of the inputs. Although the assumption of linearity may not be true for drive train temperatures, successful failure detection based on linear NBM has been demonstrated [SCH10]. In this work, linear modelling with interactions (LINI) is tested, allowing linear terms, an intercept and products of the input pairs as inputs conducted with a least squares fit solver.

Artificial Neural Networks (ANN) can be applied to various non-linear problems. For NBM of drive train temperatures, feed-forward networks (ANN-FF) have been widely applied, e.g. [SCH10]. A network with one hidden layer of six neurons is trained with Levenberg-Marquard backpropagation. A layer recurrent architecture (ANN-LR) with a delay of two time-steps is investigated to consider the inertia of the system.

Adaptive Neuro-Fuzzy Inference System (ANFIS) as a combination of fuzzy inference and neural network learning has been demonstrated for failure detection [SCH13]. A setup with two Gaussian membership functions per input in combination with a linear output function is trained with a hybrid least squares and backpropagation algorithm.

### 3.1.2 ARX – auto-regressive

ARX modelling is investigated by using the same two exogenous inputs and historical values of the target temperature. Linear and ANN ARX modelling is supported by the last 20 time-steps of the target temperature.

Non-linear State Estimation Technique (NSET) as proposed by [WAN12] is also investigated with a memory matrix of training states and an estimation of the target via a weight matrix determined by the minimal Euclidean distance of observation and state matrix. NSET can be considered as similar to ARX, because the current observation is used to build the estimate. The number of states in the memory matrix is reduced with a selection algorithm [WAN12]; here an allowed distance to the grid of $\delta = 0.00015$ is used.

## 3.2 Prediction performance metrics and anomaly detection techniques

The accuracy of predicting a temperature signal can be described by statistical metrics related to the residual, i.e.: the mean absolute error (MAE), standard deviation of absolute error, the root mean squared error, mean absolute percentage error or the coefficient of determination $R^2$.

Different techniques to detect anomalies in the residual have been proposed for NBM of drive train temperatures. Obviously, a fixed threshold for the residual based on training experience (i.e. the residual distribution) is an easy way of detecting higher temperatures than expected. Averaging the residual for one day has been proven to be beneficial to increase certainty in results [SCH10, SCH13]. An exponentially weighted moving average control chart was proposed to account for cumulating effects [WAN16]. A Mahalanobis distance was suggested considering the training distribution and built for residual and target [BAN15]. A daily 'abnormal level index' was introduced with penalties for residuals based on their assignment to defined zones in the training distribution [SUN16]. Raising an alarm if several alarms in a week occurred has proved to be an efficient way to reduce false alarms [SCH13].

Table 1 gives the details of the investigated anomaly detection techniques in this work.

<table>
<tr><th>Technique</th><th>Details</th><th>Warning</th><th>Alarm</th></tr>
<tr><td>Raw residual (RAW)</td><td></td><td rowspan="2">$>$ $X$ % of a Normal distribution fitted to training residual</td><td rowspan="4">≥ 288 ten minute warnings in past 7 days</td></tr>
<tr><td>Daily residual [SCH10] (DAILY)</td><td>average of 144 samples</td></tr>
<tr><td>Mahalanobis distance [BAN15] (MAHAL)</td><td>distance is a function of residual and target referencing to training residual and target</td><td>$>$ $X$ % of a Weibull distribution fitted to training distance</td></tr>
<tr><td>Exponentially weighted moving average control chart [WAN16] (EWMA)</td><td>past observations weighting with $\lambda = 0.2$</td><td>$< \mu - X\sigma$ or $> \mu + X\sigma$ with $\mu$: mean, $\sigma$: standard deviation of the training residual</td></tr>
<tr><td>Abnormal level index [SUN16] (ALI)</td><td>penalty= $\begin{cases} 5, \text{if} > 97.5\% \\ 3, \text{if} > 75\% \\ 1, \text{else} \end{cases}$ of Normal distribution fitted to the training residual</td><td>fuzzy warning between 0 and 1</td><td>moving average of last 7 days' warnings</td></tr>
</table>

**Table 1:** Configuration of anomaly detection techniques (the warning threshold $X$ is calibrated, cp. chapter 3.3.2 and Table 2)

## 3.3 Case study for gearbox monitoring

Data from a Scottish wind farm with 12 turbines with a rated power of 2-3 MW are analysed. The maintenance records indicate 4 turbines with a gearbox exchange in the investigated 2.5 years of available data. Due to missing maintenance reports, the reasons for the exchanges are unclear. It is assumed that the gearboxes failed and, in general, gearbox bearing failures are the most likely cause. The SCADA data are preprocessed by filtering of non-operational times and checking for valid sensor ranges. NBM with 5 months of training is applied to detect gearbox failures in a drivetrain temperature.

### 3.3.1 Normal behaviour prediction performance

The prediction performance of the different modelling approaches is visualised in Figure 2 for all turbines in the farm which are not affected by gearbox exchanges. The results indicate that NSET outperforms all other approaches. ANNFF, ANNLR and ANFIS perform with similar accuracy. Using historic values in an ARX setup does not prove to be truly beneficial for ANN modelling. Linear ARX modelling results in poor performance and is excluded subsequently.

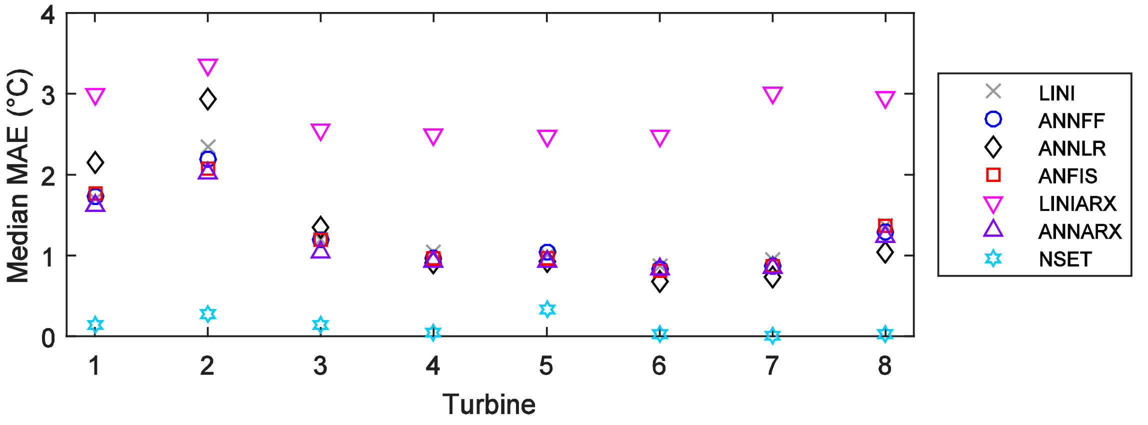


**Figure 2:** Median of monthly performance for turbines without gearbox exchange

### 3.3.2 Calibration of anomaly detection thresholds

The warning thresholds for the anomaly detection techniques are calibrated with modelling results of one turbine without gearbox exchange. In a simple optimisation the thresholds are decreased in steps of 0.05 as long as no alarms are issued. The resulting thresholds are summarised in Table 2. The parameters for the ALI calculation are not calibrated due to the higher complexity of this technique.

| | LINI | ANNFF | ANNLR | ANFIS | ANNARX | NSET |
|---|---|---|---|---|---|---|
| RAW (%) | 95.25 | 98.45 | 97.50 | 98.10 | 99.45 | 65.95 |
| DAILY (%) | 93.75 | 97.55 | 98.50 | 97.20 | 98.90 | 72.20 |
| MAHAL(%) | 87.85 | 93.35 | 95.40 | 92.15 | 97.35 | 85.90 |
| EWMA (-) | 3.00 | 3.70 | 3.75 | 3.55 | 4.35 | 0.70 |

**Table 2:** Calibrated warning threshold $X$ for different techniques (cp. Table 1)

### 3.3.3 Gearbox failure

Evaluation of the maintenance records indicate a gearbox failure and finally exchange in turbine A. From the daily residuals shown in Figure 3 it is difficult to visually identify the change in the behaviour before the failure. The sinusoidal variation of the residual indicates that the training has not learned this effect probably caused by seasonal temperature changes.

Application of the calibrated anomaly detection techniques resulted in the alarm patterns given in Figure 4. All alarms which are close to the end of the time axis can be considered as valid alarms for the gearbox degradation. Using LINI modelling, the earliest alarms which are not interrupted for more than two weeks until the end are raised approx. 25 days before failure for RAW, DAILY, MAHAL and EWMA anomaly detection. ANNFF modelling results in an early alarm 30 days before failure for RAW, MAHAL and EWMA and even 35 days in advance for DAILY. Similar results are obtained for ANNLR with 34, 23, 29 and 30 days for RAW, DAILY, MAHAL and EWMA, respectively. ANFIS modelling gives an early alarm (24 days) only for RAW anomaly detection (DAILY: no, MAHAL: 4, EWMA: 7 days). Failure detection with ANNARX and NSET and the discussed anomaly detection techniques does not work at all. LINI modelling and MAHAL anomaly detection are affected by alarms long before the fault, which could also indicate the gearbox degradation, but might be false alarms. The fuzzy alarm generated by the ALI technique shows an upward trend for all modelling techniques except NSET. However, it has to be noted that ALI levels of a similar magnitude occurred in the turbine used for calibration.

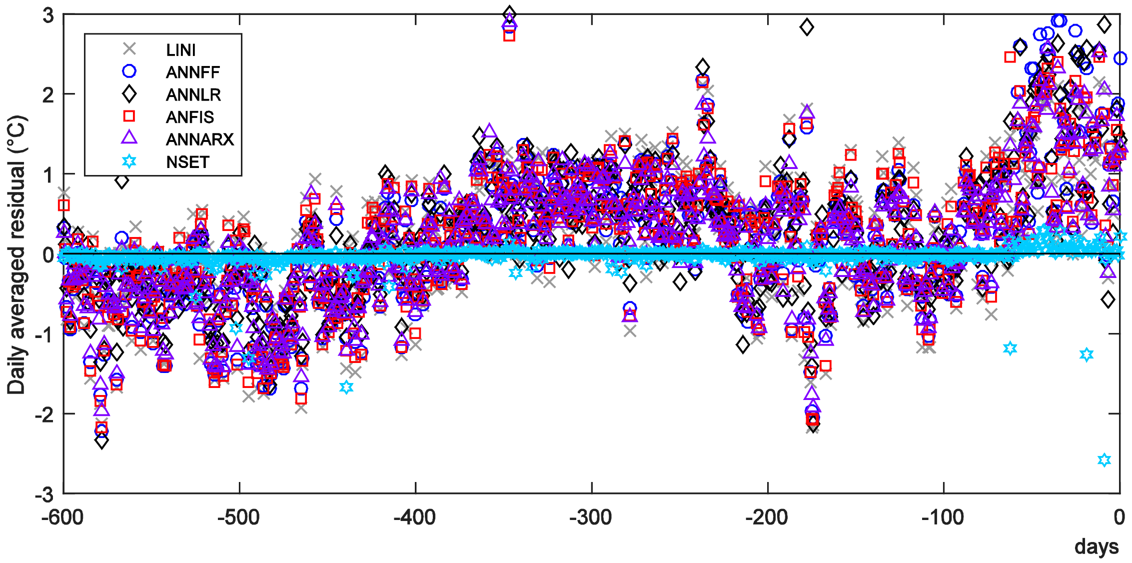


**Figure 3:** Residual of modelled and measured temperature before a gearbox failure

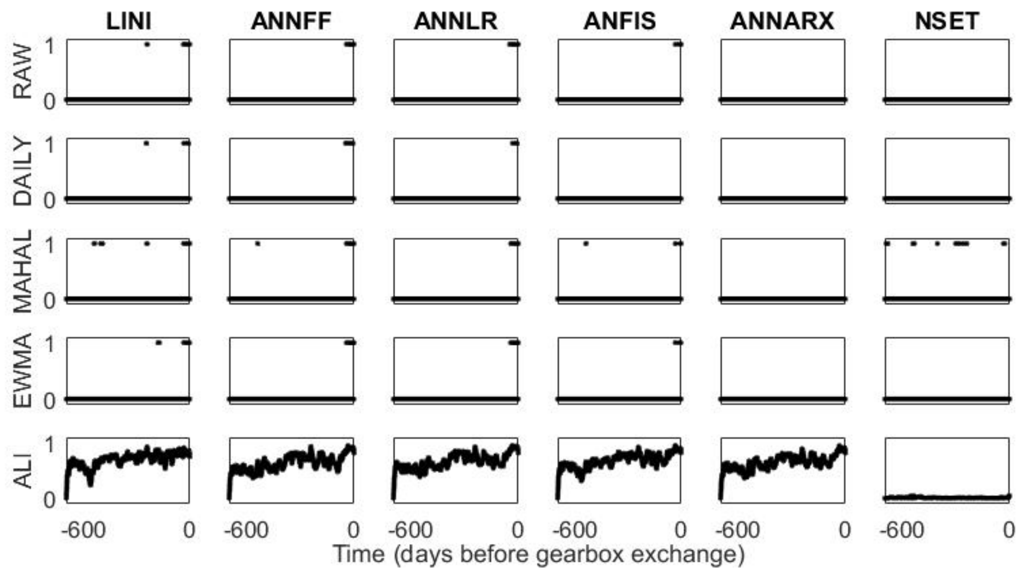


**Figure 4:** Alarms of different NBM modelling techniques and ways of anomaly detection

### 3.3.4 Validation with remaining turbines in farm

Application of the modelling and anomaly detection techniques on the other three turbines undergoing a gearbox exchange resulted in less clear and probably many false alarms. However, ANNFF and ANNLR modelling generated the best compromise of possible early alarms and minimal possible false alarms in two of three cases.

Testing the algorithms on the remaining turbines without noted gearbox exchanges revealed that the calibration did not work properly as high alarm levels occurred.

# 4 Conclusion

Different modelling techniques and anomaly detection techniques have been discussed and compared with the aim of condition monitoring of wind turbine drive trains.

The application of NBM algorithms in a case study shows that temperature prediction with a mean error of approx. 1° C is feasible with two model inputs for all investigated modelling techniques except linear ARX. Indeed, NSET performs with a prediction error approx. ten times smaller.

Using the residual of measured and modelled temperature for fault detection is not as straightforward as might be assumed. The calibration of the thresholds of the different anomaly detection techniques with one turbine in the farm did not result in reliable fault detection for all turbines. This might be due to various reasons including the unaccounted seasonal effect, suboptimal configuration of modelling techniques and anomaly detection algorithms or even incomplete maintenance records and poor data quality. However, the successful detection of a gearbox failure in one turbine up to 35 days in advance shows promise for LINI, ANNFF, ANNLR and ANFIS modelling, in particular using RAW and DAILY anomaly detection. The poor failure detection performance using ARX modelling techniques including NSET indicate, that although the target temperature is accurately predicted, the model parameters are adapting to new behaviour associated with incipient failure so no change in residual behaviour is observed. The ALI fuzzy alarm generation has not been implemented in a comparable manner to the other detection techniques, but the challenges of finding only true alarms have been visible here as well.

Further research needs to address the seasonal effect, optimal input selection, suitable calibration of anomaly thresholds, dedicated anomaly detection techniques for ARX techniques and additional ways to achieve reliable failure detection.

## Acknowledgement

This project has received funding from the European Union's Horizon 2020 research and innovation programme under the Marie Sklodowska-Curie grant agreement No 642108 (Advanced Wind Energy Systems Operation and Maintenance Expertise, http://awesome-h2020.eu/).

## Bibliography

[MIL14] Milborrow, David: The tide turns on offshore maintenance costs

http://www.windpoweroffshore.com/article/1314299/tide-turns-offshore-maintenance-costs

(2016-03-29)

[YAN13] Yang, Wenxian, Court, Richard and Jiang, Jiesheng: Wind turbine condition monitoring by the approach of SCADA data analysis.

In: Renewable Energy, 53, pp. 356-376

Elsevier, Amsterdam, 2013

[WIG08] Wiggelinkhuizen, Edwin, Verbruggen, Theo, Braam, Henk, Rademakers, Luc, Xiang, Jianping and Watson, Simon: Assessment of Condition Monitoring Techniques for Offshore Wind Farms.

In: Journal of Solar Energy Engineering, 130, 031004

ASME, New York, 2008

[FEN13] Feng, Yanhui, Qiu, Yingning, Crabtree, Christopher J., Long, Hui and Tavner, Peter J.: Monitoring wind turbine gearboxes.

In: Wind Energy, 16, pp. 728-740

Wiley, Hoboken, 2013

[KIM11] Kim, Kyusung, Parthasarathy, Girija, Uluyol, Onder, Foslien, Wendy, Sheng, Shuangwen and Fleming, Paul: Use of SCADA data for failure detection in wind turbines.

In: Proceedings of the ASME 2011 5th Int. Conf. Energy Sustain., Washington, DC, USA, pp. 2071-2079

ASME, New York, 2011

[WIL14] Wilkinson, Michael, Harman, Keir, van Delft, Thomas and Darnell, Brian: Comparison of methods for wind turbine condition monitoring with SCADA data.

In: IET Renewable Power Generation, 8, pp. 390-397

The IET, London, 2014

[SCH13] Schlechtingen, Meik, Santos, Ilmar Ferreira and Achiche, Sofiane: Wind turbine condition monitoring based on SCADA data using normal behavior models. Part 1: System description.

In: Applied Soft Computing, 13, pp.259-270

Elsevier, Amsterdam, 2013

[SUN16] Sun, Peng, Li, Jian, Wang, Caisheng and Lei, Xiao: A generalized model for wind turbine anomaly identification based on SCADA data.

In: Applied Energy, 168, pp.550-567

Elsevier, Amsterdam, 2016

[TAU16a] Tautz-Weinert, Jannis and Watson, Simon J.: Using SCADA Data for Wind Turbine Condition Monitoring - a Review.

In: IET Renewable Power Generation, in press

The IET, London, 2016.

[TAU16b] Tautz-Weinert, Jannis and Watson, Simon J.: Comparison of different modelling approaches of drive train temperature for the purposes of wind turbine failure detection.

In: Journal of Physics: Conference Series, 753, 072014

IOP Publishing, Bristol, 2016

[SCH10] Schlechtingen, Meik and Santos, Ilmar Ferreira: Comparative analysis of neural network and regression based condition monitoring approaches for wind turbine fault detection.

In: Mechanical Systems and Signal Processing, 25, pp. 1849-1875

Elsevier, Amsterdam, 2010

[WAN12] Wang, Yue and Infield, David: Supervisory control and data acquisition data-based non-linear state estimation technique for wind turbine gearbox condition monitoring.

In: IET Renewable Power Generation, 7, pp.350-358

The IET, London, 2012.

[WAN16] Wang, Long, Zhang, Zijun, Long, Huan, Xu, Jia and Liu, Ruihua: Wind Turbine Gearbox Failure Identification with Deep Neural Networks.

In: IEEE Transactions on Industrial Informatics, in press

IEEE, New York, 2016.

[BAN15] Bangalore, Pramod and Tjernberg, Lina Bertling: An Artificial Neural Network Approach for Early Fault Detection of Gearbox Bearings.

In: IEEE Transactions on Smart Grid, 6, 980-987

IEEE, New York, 2015

# Stator Winding Fault Diagnosis in Synchronous Generators for Wind Turbine Applications

***Raed Khalaf Ibrahim and Simon Watson***
*Centre for Renewable Energy Systems Technology (CREST),*
*Wolfson School of Mechanical, Electrical and Manufacturing Engineering,*
*Loughborough University, UK.*
*R.Ibrahim@lboro.ac.uk, S.J.Watson@lboro.ac.uk*

***Abstract*—Wind turbine manufacturers have introduced to the market a variety of innovative concepts and configurations for generators to maximize energy capture, reduce costs and improve reliability of wind energy. For the purpose of improving reliability and availability, a number of diagnostic methods have been developed. Stator current signature analysis (SCSA) is potentially an effective technique to diagnose faults in electrical machines, and could be used to detect and diagnose faults in wind turbines. In this study, an investigation was conducted into the application of SCSA to detect stator inter-turn faults in an excited synchronous generator and a permanent magnet synchronous generator. It was found from simulation results that, owing to disruption of magnetic field symmetry and imbalance between the current flowing in the shorted turn and the corresponding diametrically opposite turn in the winding, certain harmonic components in the stator current clearly increased as the number of shorted turns increased. The findings are helpful to detect faults involving only a few turns without ambiguity, in spite of the difference in the configuration of the generators. As expected, because of the different type, configuration and operational condition of the two generators studied, detecting faults through the generator current signature requires a particular approach for each generator type.**

***Index Terms*—Wind turbine, Generator, Condition monitoring, Current Signature, Fault signature, Fault detection, Diagnosis.**

## I. INTRODUCTION

Over the years, there has been much work to maximize energy capture, reduce costs and improve reliability of wind turbines [1]. With this work has come investment and the development of new technologies from wind turbine (WT) manufacturers. Among these technologies are the doubly fed induction generator (DFIG) with a three- stage gearbox which is the most common configuration at present, sharing the market with excited synchronous generators (EESGs) and the new arrivals, based on permanent magnet synchronous generators (PMSGs). Better design is of course one answer to increase the reliability and availability of WTs; the other is condition monitoring of the WT systems [2]. This allows for early detection of faults in wind turbines, allowing proactive decision making, minimizing downtime, and potentially forecasting the remaining useful life of ae component given a diagnosed fault.

A number of methods for WT condition monitoring have been proposed by researchers including the analysis of: vibration, oil quality, temperature, torque, acoustic emissions, fibre optics, and electrical output. However, each technique requires additional and expensive sensors or specialized tools. Moreover, there is a price to pay to access each WT in order to install the sensors, as well as lost revenue due to power outages associated with equipment installation and maintenance. Although SCSA is one of the preferred techniques to diagnose faults in electrical machines, it is not widely used by WT manufacturers. Many generator faults are bearing related and the lack of uptake could be because the physical link between rolling elements faults and fault signatures in electrical signals is not clearly identified. Also, it could be due to the difficulty in extracting fault signatures from the electrical signal which depends on the generator type, configuration and the operational condition. This paper considers two generator systems commonly used in WTs. Two models are implemented in MATLAB and simulated under a turn-to-turn short circuit fault as case studies to detect faults through the generator current signature. The first model represents a 2.0 MW WT with a PMSG (DeWind D9.1) and the second model represents a 2.0 MW WT with an EESG (DeWind D9.2). Both machine models are used to demonstrate fault detection capability for different generator configurations. The models allow for certain nonlinear and time-varying characteristics and take into account varying wind speeds similar to those experienced in WTs.

## II. GENERATOR CONFIGURATIONS IN WIND ENERGY CONVERSION SYSTEMS

Wind energy conversion configurations can be classified into fixed speed and variable speed. In the early 1990s, most of the installed WTs were designed using a squirrel cage induction generator running close to fixed speed and directly connected to the grid [3], meaning that whatever the wind speed would be, the rotational turbine speed is fixed and determined by the frequency of the supply grid, the gear ratio and the generator design. During the past few years, the variable-speed WT has become the dominant type among the installed WTs based on DFIGs, sharing the market with EESGs and the new arrivals, based on PMSGs. In this section, the essential properties of the PMSG and EESG are briefly described. For a detailed analysis of generator types, the reader is referred to the standard literature in this field [4].

*A. Electrically-Excited Synchronous Generator*

The EESG is the predominant generator in the electrical power industry [5]. The stator windings of EESGs are directly connected to the grid and, the rotor winding is supplied with DC currents that create the rotor magnetomotive force and the rotor flux so that the EESG does not need any further reactive power compensation system unlike an induction generator. In normal operating conditions, the rotor revolves synchronously with the stator field. The synchronous rotation of the rotor is the reason for this type to be called synchronous generators. The speed of the synchronous generator is determined by the frequency of the rotating field and by the number of pole pairs of the rotor. Figure1 shows a schematic of an EESG machine such as the DeWind D9.2 having a 93m rotor which drives a fixed speed EESG with a rated power of 2.0 MW. Due to its ability to generate at up to 13.8 kV, the generator can be directly connected to the grid through a synchronizing switch without the need of a power converter or a main power transformer. The fixed generator speed is achieved by converting the variable rotational speed from the WT rotor to a constant input speed by using a two stage helical /planetary gearbox and a variable speed Voith WinDrive hydrodynamic superimposed planetary gearbox. The heart of the WinDrive technology is a variable-speed hydrodynamic gearbox, and two main components of the WinDrive are the technique behind how it functions including a planetary gear combined and a hydrodynamic torque converter [6]. The planetary gear is designed as a superposition gear. It has the advantage that it does not need a power converter or a main power transformer. But the price to be paid for such a large, heavy and reliable gearbox design that has to provide the requirement for significant damping in the drive train.

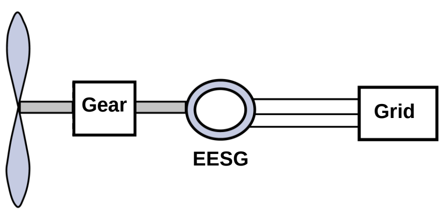


Fig. 1: Wind turbine system with EESG

*B. Permanent Magnet Synchronous Generator*

Instead of excitation windings, the rotor of a synchronous generator can have permanent magnets built into the rotor magnetic circuit. In this case, the rotor does not have any windings. PMSGs are favoured in WTs due to their light weight, high power density, and high efficiency [7]. The PMSG is often directly coupled with the rotor, eliminating the need for a gearbox and its associated cost and maintenance issues, whilst increasing the system reliability. They are not only used in small scale WTs but also in large MW applications. The PMSG is much more expensive than the DFIG of a similar size. However, it has one clear advantage compared with the DFIG: namely, it does not need reactive magnetizing current. Figure2 shows a scheme using a PMSG where the magnetic field inside the generator is produced by permanent magnets on the rotor. Because there is no field winding in this generator, there is no associated $I^2R$ loss so that this type of generator has a very high efficiency, well above 90%.

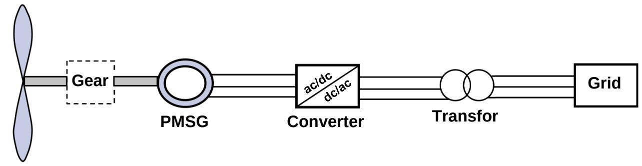


Fig. 2: Wind turbine system with PMSG

## III. DETECTION OF SHORT-CIRCUIT FAULT

When an internal fault occurs on the stator winding it can cause severe damage to the machine and the system to which it is connected so that early detection of turn to turn short circuit faults during operation is essential to eliminate consequential damage. Unless detected early enough, it might lead to fire, explosion, and even loss of personnel [8]. It has been reported that a turn to turn short circuit results in a disruption of the magnetic field symmetry in the winding region of the machine as well as increasing the magnitudes of certain harmonic components [9]. Turn-to-turn faults are difficult to detect with confidence. Overcurrent and differential relays are generally agreed to be inadequate for this purpose. However, turn-to-turn faults can be detected by analyzing the current spectrum in the electrical machine fault will introduce sideband harmonics in the current signal [8]. The following subsections will describe how the fault sideband harmonics may occur during a turn to turn short circuit in EESG and PMSG current signals, and potentially how they may deviate from a healthy state.

*1) Turn-to-turn fault in an EESG:* In the case of an EESG with stator turn-to-turn faults, turn-to-turn faults can be detected by the presence of a spectral component at twice the fundamental supply frequency $2f$, and the amplitude of this spectral component is directly related to the extension of the fault [10]. Other spectral components that can be observed in the stator line current are given by [11], [12].

$$f_c = kf \tag{1}$$

where $f_c$ and $f$ are detectable spectral components due to the fault and fundamental frequency components; $k$ is an even integer ($k$=2, 4, 6). For example, on a machine supplied at $f = 50Hz$, the stator spectrum exhibits 100, 200 and 300 Hz components because of turn-to-turn winding faults or supply unbalance, including single phasing.

*2) Turn-to-turn fault in a PMSG:* Current signature analysis has been studied extensively for fault detection in AC motors [13], [14]. According to [9], the occurrence of a turn-to-turn fault results in a disruption of magnetic field symmetry in the end winding region of the machine as well as increasing the magnitudes of certain harmonic components. This is because there is a severe imbalance between the current flowing in the shorted turn and the corresponding diametrically opposite turn in the winding. This type of fault will introduce sideband harmonics around the fundamental frequency in the machine current spectrum. It was later experimentally proven by Ebrahimi et al. [15] that turn-to-turn faults actually give rise to a sequence of such sidebands given by

$$f_c = \left(1 \pm \frac{2k_{sa}+1}{p}\right).f \tag{2}$$

where $f_c$ and $f$ are detectable spectral components due to the fault and fundamental frequency components, respectively, $k$ is a constant coefficient ($k$=0, 1, 2, 3, ...) and $p$ the number of pole pairs.

## IV. MODELLING AND SIMULATION

A WT model was implemented in MATLAB/Simulink, including wind speed, rotor, pitch control system, drivtrain and generator model (see previous work [16]-[17]). Accordingly, the models of the PMSG and EESG will be only described here briefly.

### A. EESG model

The detailed description and model equation derivation of EESGs can be found in most power system and electrical machine references [18]-[19]. Only the most important aspects of the modeling will be presented here. The system has been modeled and simulated in the Simulink toolbox extension of Matlab. Figure3 shows the complete equivalent circuit representation of a three-phase EESG. A dc power source supplies the rotor field circuit. The field current $I_f$ is controlled by a variable resistance connected in series with the field winding. Each phase has an internal generated voltage with series resistance $R_s$ and series reactance $X_s$. Assuming balanced operation of the machine, the rms phase currents are equal to each other and shifted by 120 electrical degrees. The same thing is also true for the voltages.

EESGs operate only at synchronous speed; a constant speed that can be determined by the number of poles and the frequency of alternation of the armature-winding voltage. EESGs are called synchronous because their speed is directly related to the stator electrical frequency. Therefore, the synchronous speed can be expressed in (rad/s) as:

$$\omega_s = \frac{\omega}{p} = \frac{2\pi f}{p} \tag{3}$$

or in (rev/min) as

$$n_s = \frac{60f}{p} \tag{4}$$

where $\omega_s$ is the angular speed of the magnetic field (which is equal to the angular rotor speed of the synchronous machine), $\omega$ is the angular frequency of the electrical system, $f$ (Hz) is the electrical frequency, $p$ pairs of poles and $n_s$ is the the synchronous speed in (rev/min) or rotational shaft speed.

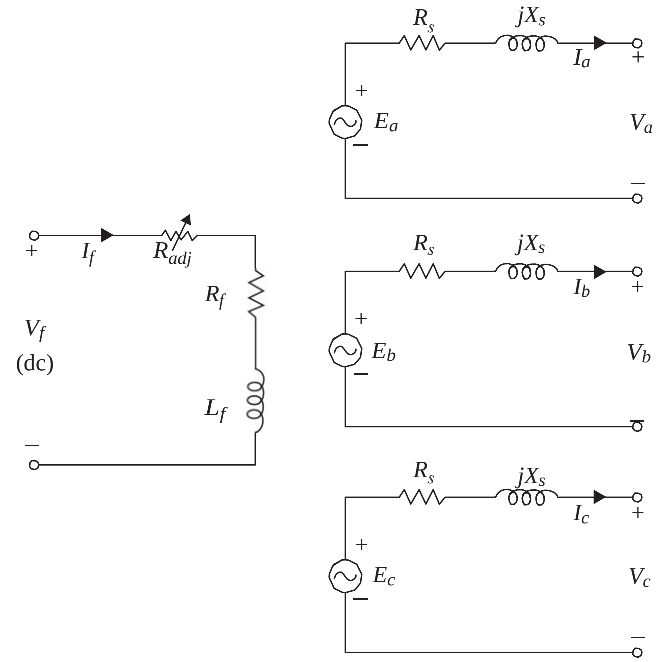


Fig. 3: Equivalent circuit representation of a three-phase EESG

According Faraday's Law the induced voltage in the stator winding can be expressed as:

$$\begin{aligned} e_a(t) &= E_{max}\sin\omega t \\ e_b(t) &= E_{max}\sin(\omega t - \frac{2\pi}{3}) \\ e_c(t) &= E_{max}\sin(\omega t + \frac{2\pi}{3}) \end{aligned} \tag{5}$$

The peak voltage in any phase of a three-phase stator is

$$E_{max} = \omega k N\phi = 2\pi f k N\phi \tag{6}$$

where $N$ is the number of turns in each phase winding; $\phi$ is the flux per pole due to the excitation current $I_f$; $k$ is the winding factor of the stator.

The voltage in RMS value is:

$$E_{max} = \frac{2}{\sqrt{2}}\pi f k N\phi = 4.44 f k N\phi \tag{7}$$

This voltage is a function of the frequency or rotational speed, the flux that exists in the machine, and, of course, the construction of the machine itself.

### B. PMSG model

A large number of papers describe the modeling of PMSGs [17]. PMSGs are ordinary synchronous machines with the field excitation provided by a permanent magnet. In other words, PMSGs provide the magnetic field so that there is no need for field windings, or supply current to the field. The PMSG operational principles are similar to that of EESGs, with the exception that they are run at different speeds, producing a variable-frequency output. Since the flux of the permanent magnet machine cannot be changed, they are not generally connected directly to the ac network. The power produced by the generator is initially variable voltage and frequency. This ac variable voltage should be rectified immediately to dc, and the resultant dc power then inverted to ac with a fixed frequency and voltage. Thus, the PMSG model has been implemented based on previous equations with the following assumptions:

- The flux ($\phi$) is fixed;
- The rotational speed $n_s$ is variable;
- The electrical frequency $f$ is proportional to the rotational speed;
- The induced voltages are proportional to the rotational speed;

As mentioned previously, the fundamental frequency in the PMSG is proportional to the rotational speed as explained in Equation (4) which clearly indicates that the current signals acquired from the generator terminals of the PMSG are always non-stationary so that it is essential to take into account the characteristic of the signal is varying with time. This will be briefly discussed in the results section.

The parameters for both generators used are detailed in Table 1.

TABLE I: The Parameters of PMSG and EESG.

| PMSG | |
|---|---|
| Cut-In, Rated, Cut-Out Wind Speed | 3 m/s, 12 m/s, 25 m/s |
| Rated Tip Speed | 80 m/s |
| Rotor Diameter | 93 m |
| Gearbox Ratio | 1:108 |
| Line-Line Voltage (RMS) | 690v |
| Grid Frequency | 50Hz |
| Pole Pairs | 2 |
| Generator Speed (RPM) | 200- 1500 |
| Stator phase resistance (ohm) | 0.026 |
| Stator phase inductance (H) | 0.02587 |
| EESG | |
| Cut-In, Rated, Cut-Out Wind Speed | 3 m/s, 12 m/s, 25 m/s |
| Rated Tip Speed | 80 m/s |
| Rotor Diameter | 93 m |
| Gearbox | planetary gearbox |
| Line-Line Voltage (RMS) | 690v |
| Frequency | 50Hz |
| Pole Pairs | 2 |
| Rated Generator Speed (RPM) | 1500 |
| Stator phase resistance (ohm) | 0.026 |
| Stator phase inductance (H) | 0.02587 |

## V. CASES

This section will present case study simulations of an EESG and PMSG. It may be interesting to analyze the behavior of the models during simultaneous stator faults. Thus, we proceed with a series of tests using a few short circuited inter turns (SCIT) or with a resistive contact of several ohms between a high number of inter turns in the same phase. The following tests were carried out for both machines:

- healthy machine,
- short-circuit of 1 inter turn on phase a,
- short-circuit of 3 inter turns on phase a,
- short-circuit of 5 inter turns on phase a,

In order to observe the faults level, stator windings were modified to access the intermediate tap points. These tap points are distributed over phase a with the aim being able to short-circuit a number of inter turns in a quasi-geometric progression. In other words, the EESG and PMSG models are implemented with intermediate terminals of the winding, in order to emulate (or introduce) short-circuit faults with a low number of shorted turns: (1, 3, and 5) turns on the phase a as shown in Figure 4. While different tests are introduced for the two generators, the rated stator current and the fault current flowing in shorted turns are recorded to observe how the stator current will change in relation to the number of short-circuiting turns. Figure 5 shows simulation results of the evolution of the fault current flowing in the shorted turns as a function of the number of turns in the short circuit of EESG stator winding. As the number of shorted turns increases, the fault current amplitude becomes higher, inevitably might lead to rapid overheating in the conductors, and accordingly, undetected turn-to-turn faults could grow and culminate into major ones such as phase-to-ground or phase-to-phase faults.

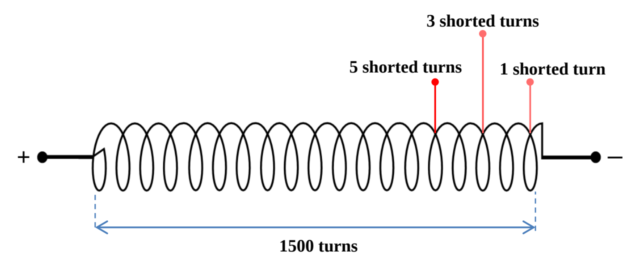


Fig. 4: Configuration of the access points of the stator windings of the EESG and PMSG models

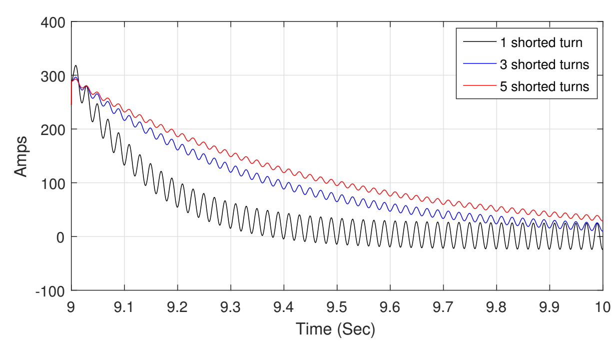


Fig. 5: Amplitude evolution in the fault current flowing in shorted turns in relation to the number of short-circuiting turns for an EESG.

## VI. RESULTS AT CONSTANT SPEED

Simulation results for a PMSG and EESG models under healthy condition and stator winding faults are discussed in this section. For each simulation result, data were recorded for 10 seconds at 5kHz sampling frequency and analysed using the fast Fourier transform (FFT) algorithm in MATLAB. Figure 6 shows the fundamental harmonic of the stator current spectrum of the EESG machine operating at constant speed. We can see components with frequencies at 63.33 Hz and 31.66 Hz, which are intentionally simulated to be present in the healthy machine spectrum as a dynamic eccentricity. Other spectral components given by the equation (1) are generated by the turn to turn faults in the EESG machine. The fault signature frequencies are labelled and identified as a function of the number of shorted turns. As the number of shorted turns increases, we notice a slight increase in the fault signature frequencies given by equation (1).

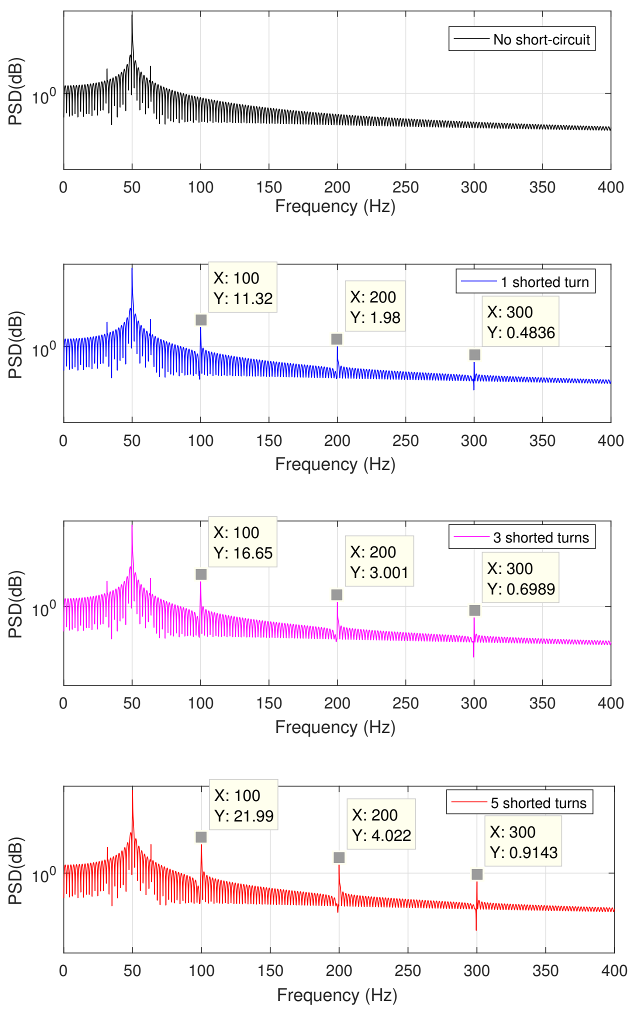


Fig. 6: Stator current spectrum around the fundamental harmonic for the EESG.

Figure 7 shows the stator current spectra of the PMSG after stator winding faults were applied, with the machine operating at constant speed. Turn to turn short circuit results in a disruption of the magnetic field symmetry in the winding region of the PMSG as well as increasing the magnitudes of certain harmonic components. The fault signature frequencies are clearly shown around the fundamental frequency and these frequencies are consistent for each case. These frequencies are defined by equation (2) and generated by the turn to turn faults in the PMSG machine. The amplitude of these frequencies are increased with the number of shorted turns. This might be a result of a severe imbalance between the current flowing in the shorted turn and the corresponding diametrically opposite turn in the winding.

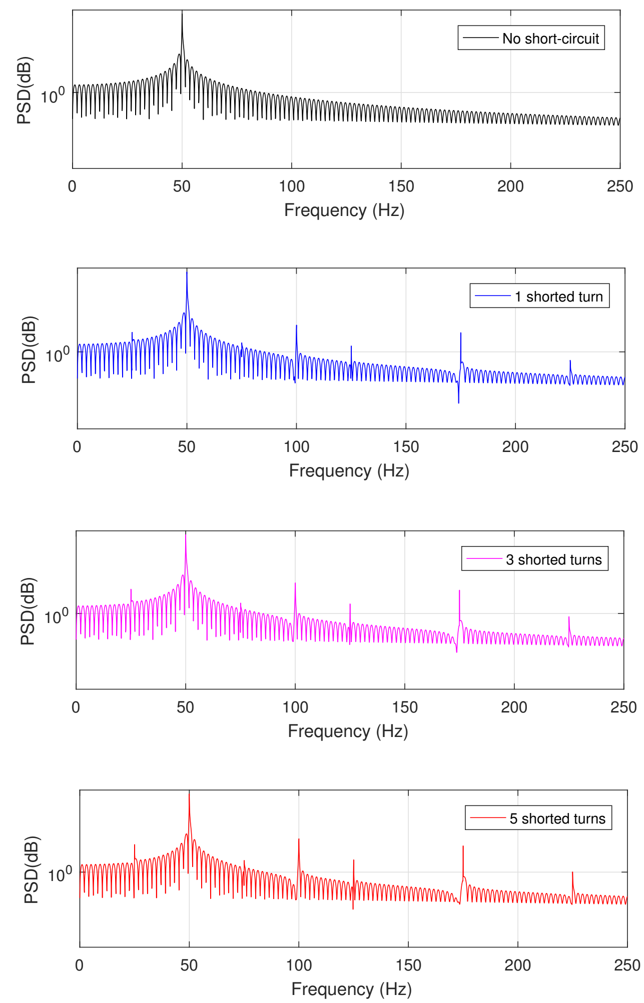


Fig. 7: Stator current spectrum around the fundamental harmonic for the PMSG operating at fixed speed.

Generally PMSGs operate at variable speed, therefore the model was run at variable speed to investigate the potential for fault frequency tracking. Figure 8 shows the stator current spectra for the healthy PMSG and with increasing shorted turn faults operating at variable speed. Although the fault signature frequencies are still seen in the spectrum, it is difficult to distinct between the fault levels in relation to the number of shorted turns, because the rotational speed in the PMSG is proportional to the wind speed so that the number of harmonics in the PMSG spectrum will increase with the rotational speed, as described by Equation (4). Consequently, the fault signature frequencies are buried in wide-band dominant frequency components (i.e. harmonics due to variable rotational speeds) of the current signal that are irrelevant to the fault.

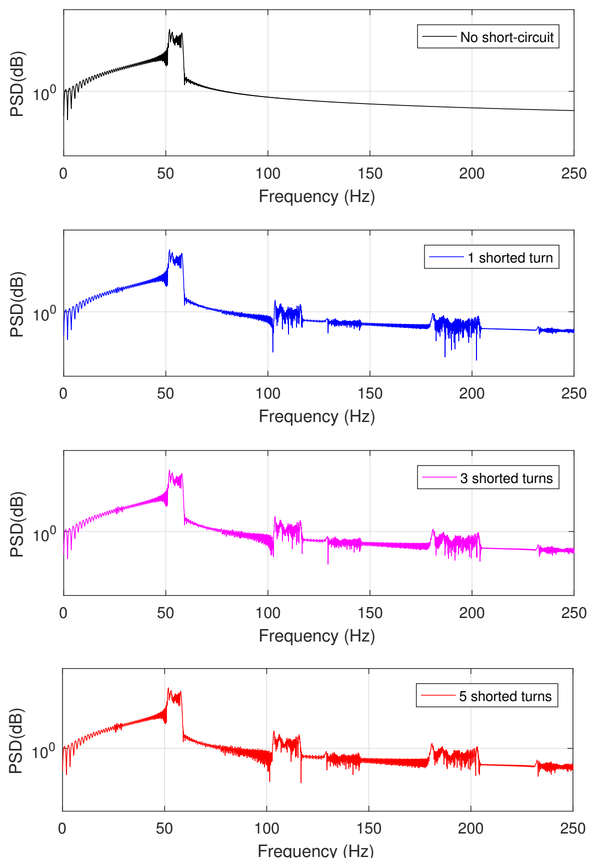


Fig. 8: Stator current spectrum around the fundamental harmonic for the PMSG operating at variable speed.

## VII. CONCLUSION

This paper analyzed the stator winding fault behavior of synchronous machines. Based on the analyses, approximate equations for the fault current flowing in shorted turns have been derived. The results obtained from the approximate equations have been compared to the results of time-domain and frequency-domain simulations. The results showed the frequencies inherent to shorted turn faults occur in the spectra of each machine. Although turn-to-turn faults have led to increase the amplitude of the fault current flowing in shorted turns, the rated current amplitude does not change so that it is difficult to detect with confidence using overcurrent and differential relays. However, we have noticed that the current analysis gives good results in the frequency-domain. It should be pointed out here that this type of fault is problematic to diagnose in time domain. Another important conclusion of this work is that stator winding faults have a particular signature that should be detectable in current signals in an EESG because this machine is operating at constant speeds, while the current signals in the PMSG includes harmonics, which are due to the variation of wind speed as well as those related to the presence of the electrical fault. Ultimately, stator current signature analysis could be used to detect and diagnose faults in a fixed speed WT. The technique can be used to detect faults in a variable speed machine but may require an alternative analysis technique (e.g wavelet or short-term Fourier transform analysis) to detect the magnitude of such faults.

## REFERENCES


[1] P. Tchakoua, R. Wamkeue, T. A. Tameghe, and G. Ekemb, "A review of concepts and methods for wind turbines condition monitoring," in *Computer and Information Technology (WCCIT), 2013 World Congress on*, pp. 1–9, IEEE, 2013.

[2] M. Wilkinson, B. Darnell, T. van Delft, and K. Harman, "Comparison of methods for wind turbine condition monitoring with scada data," *Renewable Power Generation, IET*, vol. 8, no. 4, pp. 390–397, 2014.

[3] H. Li and Z. Chen, "Overview of different wind generator systems and their comparisons," *Renewable Power Generation, IET*, vol. 2, pp. 123–138, June 2008.

[4] J. Machowski, J. Bialek, and J. Bumby, *Power system dynamics: stability and control*. John Wiley & Sons, 2011.

[5] T. Ackermann *et al.*, *Wind power in power systems*, vol. 140. Wiley Online Library, 2005.

[6] Voith Turbo Wind GmbH and Co. KG, A Unique Solution to Generating Electricity from the Wind. WinDrive Technology, [Online]: http://resource.voith.com/vt/publications/downloads/voith-windrive-for-wind-turbines.pdf.

[7] X. Yang, D. Patterson, and J. Hudgins, "Permanent magnet generator design and control for large wind turbines," in *Power Electronics and Machines in Wind Applications (PEMWA), 2012 IEEE*, pp. 1–5, IEEE, 2012.

[8] S. Nandi, S. Choi, and H. Meshgin-kelk, "Electric machines: Modeling, condition monitoring, and fault diagnosis," 2012.

[9] J. Penman, H. Sedding, B. Lloyd, and W. Fink, "Detection and location of interturn short circuits in the stator windings of operating motors," *Energy conversion, ieee transactions on*, vol. 9, no. 4, pp. 652–658, 1994.

[10] S. Cruz and A. M. Cardoso, "Stator winding fault diagnosis in three-phase synchronous and asynchronous motors, by the extended park's vector approach," *Industry applications, IEEE Transactions on*, vol. 37, no. 5, pp. 1227–1233, 2001.

[11] P. Tavner, "Review of condition monitoring of rotating electrical machines," *Electric Power Applications, IET*, vol. 2, no. 4, pp. 215–247, 2008.

[12] G. Singh *et al.*, "Experimental investigations on induction machine condition monitoring and fault diagnosis using digital signal processing techniques," *Electric Power Systems Research*, vol. 65, no. 3, pp. 197–221, 2003.

[13] S. Nandi and H. Toliyat, "Condition monitoring and fault diagnosis of electrical machines-a review," in *Industry Applications Conference, 1999. Thirty-Fourth IAS Annual Meeting. Conference Record of the 1999 IEEE*, vol. 1, pp. 197–204 vol.1, 1999.

[14] S. Nandi, H. Toliyat, and X. Li, "Condition monitoring and fault diagnosis of electrical motors-a review," *Energy Conversion, IEEE Transactions on*, vol. 20, pp. 719–729, Dec 2005.

[15] B. M. Ebrahimi and J. Faiz, "Feature extraction for short-circuit fault detection in permanent-magnet synchronous motors using stator-current monitoring," *Power Electronics, IEEE Transactions on*, vol. 25, no. 10, pp. 2673–2682, 2010.

[16] R. K. Ibrahim and S. Watson, "Effect of power converter on condition monitoring and fault detection for wind turbine," in *Power Electronics, Machines and Drives, 2016. PEMD 2016. 8th IET Conference on*, IET, 2016.

[17] R. K. Ibrahim and S. Watson, "Wind turbine simulation model for the study of combined mechanical and electrical faults," in *Scientific Track Proceedings of European Wind Energy Association. EWEA*, 2015.

[18] I. Tabatabaei, J. Faiz, H. Lesani, and M. T. Nabavi-Razavi, "Modeling and simulation of a salient-pole synchronous generator with dynamic eccentricity using modified winding function theory," *IEEE Transactions on Magnetics*, vol. 40, pp. 1550–1555, May 2004.

[19] I. Iglesias, L. Garcia-Tabares, and J. Tamarit, "A d-q model for the self-commutated synchronous machine considering the effects of magnetic saturation," *Energy Conversion, IEEE Transactions on*, vol. 7, no. 4, pp. 768–776, 1992.

# Challenges in Using Operational Data for Reliable Wind Turbine Condition Monitoring

*Jannis Tautz-Weinert, Simon J Watson*
Centre for Renewable Energy Systems Technology, Wolfson School, Loughborough University
Loughborough, Leicestershire, United Kingdom

ABSTRACT

Operational data of wind turbines recorded by the Supervisory Control And Data Acquisition (SCADA) system originally intended only for operation and performance monitoring show promise also for assessing the health of the turbines. Using these data for monitoring mechanical components, in particular the drivetrain subassembly with gearbox and bearings, has recently been investigated with multiple techniques. In this paper the advantages and drawbacks of suggested approaches as well as general challenges and limitations are discussed focusing on automated and farm-wide condition monitoring.

KEY WORDS: Wind Turbine; Condition Monitoring; SCADA; Drivetrain; Machine Learning.

## INTRODUCTION

Optimisation of maintenance is essential to further reduce the costs of offshore wind energy, where accessibility is restricted by weather conditions and the availability of transport vessels. Advanced maintenance strategies involve condition based decision-making while trying to predict the future maintenance needs before critical failures with significant downtimes occur. Continuous and reliable information of the condition of the different subassemblies and parts of the wind turbine are needed for effective prognosis of ongoing degradation and estimation of remaining life of critical parts.

Supervisory Control And Data Acquisition (SCADA) data have gained more attention in the last five years as they are usually available without any additional expense in contrast to dedicated condition monitoring systems which can cost approx. £14,000 per turbine (Yang et al., 2014). The operational data recorded in a SCADA system vary with the turbine type, but usually include at least wind speed, wind direction, yaw angle, pitch angle, active power, reactive power, generator current, generator speed, gearbox temperature, generator winding temperature and ambient temperature. Comparing parameters over time and in relation to the operational level has helped to identify changes in the behaviour related to developing failure (Wiggelinkhuizen et al., 2008; Feng et al., 2013). Based on that, the main idea has been the modelling of signals, mainly temperatures, assuming normal conditions and revealing problems via comparing modelled and measured temperatures. The focus of research has been on data-driven training of algorithms and machine learning tools adapted from computer science have been proposed, e.g. artificial neural networks (Garcia et al., 2006; Zaher et al., 2009; Bangalore and Tjernberg, 2015; Sun et al., 2016), adaptive-neuro fuzzy inference systems (Schlechtingen et al., 2013), nonlinear state estimation techniques (Wang and Infield, 2012) or multivariate adaptive regression splines (Tan and Zhang, 2016). An overview of the progress in the area of condition monitoring with operational data can be found in a recent review of the authors (Tautz-Weinert and Watson, 2016a).

Most publications on condition monitoring with operational data consist of a proposal for a new technique and a demonstration using one case study, whereas difficulties and challenges are rarely discussed. Yang et al. (2014) highlighted in their review of the current challenges in wind turbine condition monitoring that the sampling resolution of SCADA data is too low to monitor all aspects of a wind turbine and doubted the usefulness of SCADA monitoring in terms of early detection. The authors suggested the integration of SCADA-based monitoring in condition monitoring systems, however. Dienst and Beseler (2016) shared their lessons learned from monitoring of an offshore wind farm with operational data indicating e.g. that finding training data without errors is difficult, 2% of sensors are malfunctioning at any given time, using multiple models to predict a signal are beneficial and anomalies in models can indicate a defect but also unrepresentative training.

This work addresses the challenges in using operational data for wind turbine monitoring with the approach of normal behaviour modelling of temperatures based on experiences with real data from four wind farms. Drawbacks of the individual techniques are discussed and general challenges highlighted regarding data quality, pre-processing, input selection and alarm generation.

In the next section, the basic idea of normal behaviour modelling is introduced. The subsequent and third section summarises the properties of the data used. The fourth and main section addresses the challenges if failures are to be found retrospectively, whereas the fifth section gives a brief outlook if such an approach is used on-line. In the last section this work is concluded by summarising the key problems to be solved.

MONITORING BY NORMAL BEHAVIOUR MODELLING

Normal behaviour modelling is a way of building a virtual clone of a system which always represents the healthy state. The model generates a time series of the target signal, which can be compared with the measured signal to detect anomalies. Due to the complexity of wind turbine systems such models cannot be built analytically, but are data-driven. In a training period, where the turbine is assumed to operate normally, the relationship between input signals and the target signal is learnt by the algorithms.

Adequate target signals and corresponding inputs have to be selected to achieve a model which is useful in failure detection. Simple models predicting a signal with a sensor signal of the same type at the same location might help for monitoring the sensor itself. More advanced models can be used to monitor mechanical parts which are affected by wear: drivetrain bearings and gears. Wear will change the efficiency of a part and result in increased thermal losses which should become visible in the form of changed thermal behaviour (Feng et al., 2013). To monitor wear-related parts, temperature signals are commonly modelled with other temperatures of surrounding parts, signals describing the turbine's load level such as power output, electrical currents, rotational or wind speeds and/or signals representing the environmental background such as the nacelle or ambient temperature.

CASE STUDY

Records from four wind farms are used to highlight the challenges in condition monitoring with operational data. SCADA data are retrospectively analysed aiming to detect failures in advance. Although the turbines are from different manufacturers, all turbines are geared, variable speed and pitch controlled. The turbines cover the 1.5 MW and the 2-3 MW class. The investigated records range from only half a year to nearly five years and from 11 to 102 turbines in a farm. Reports of replacements are available for three of four farms. Although records from farm A are not supported by sufficient reports for failure detection analysis, normal behaviour modelling can be tested and compared based on the SCADA data. The key features of the data used are summarised in Table 1.

Table 1. Wind farm data used in this study

| Farm | Location | Power (MW) | Number of turbines | Length of data (years) | Service report |
|---|---|---|---|---|---|
| A | USA | 1.5 | 108 | 0.5 | Stoppages only |
| B | UK | 2-3 | 12 | 2.5 | Stoppages and replace-ments |
| C | Europe | 2-3 | 25 | 3.0 | Replace-ments |
| D | Europe | 2-3 | 11 | 4.7 | Replace-ments |

CHALLENGES IN RETROSPECTIVE ANALYSES

The challenges in using operational data for condition monitoring can be divided into: data quality, monitoring setup, proposed modelling techniques, comparing modelling techniques, modelling capabilities and alarm generation.

**Data quality**

Retrospective failure detection based on operational data is conducted with two main types of information: SCADA records available in a SQL database or spreadsheets and a service record in a spreadsheet.

***SCADA data.*** Although signals in SCADA records are usually named, the labelling of the signals is not necessarily sufficient for clear identification of the sensor properties. As there is neither a common set of available signals nor a generally accepted taxonomy, different SCADA systems use different names and abbreviations. Although unambiguous signals like the power output, wind speed, blade pitch angle etc. are always easily identifiable, other signals require more details for complete identification. In particular, the location of temperature sensors is often insufficiently described. In the investigated data the labelling ranged from only numbering all temperature sensors (e.g. temperature 2, farm B), giving the name of the subassembly (e.g. gearbox temperature, farm A), specifying a part type in a subassembly (e.g. gearbox bearing temperature, farm C) to providing approx. location of the sensor at a part (e.g. gearbox bearing high speed shaft gearbox [vicinity / side], farm D). Even in the farm with the most detailed labelling, the locations are open to interpretation: e.g. there are two generator bearing sensors labelled 1 and 2 or oil temperatures are labelled basis, level 1 and 2. Detailed knowledge of the turbine configuration or a technical drawing including the sensor locations would certainly ease the analysis but has not been available for this work. Reasons can be found in insufficient documentation and confidentiality issues applicable to academic studies with commercial data.

Although missing, invalid and poorly processed data hinder the analysis, the most serious problems are caused by inconsistencies. Any change in the behaviour of a sensor might be interpreted as a change of the monitored part. In data from farm D, several changes of the maximum occurring values can been observed as shown for example in Fig. 1. Sensor specifications or detailed information about the operation are not available. It is assumed that this event could be caused by a sensor drift, unreported maintenance or a change in control and operation. An actual change of the performance of the monitored part without any interaction by the operator is unlikely due to the rapid change. Additionally, the temperatures in the illustrated example are lower after the step, i.e. the losses would be reduced which is contrary to the effects of wear. To allow analysis if inconsistencies occur, data should be split into windows without steps which are investigated separately. A systematic way of detecting steps is required for automated splitting and applying the training and testing procedure of normal behaviour modelling. Comparing monthly maximums and percentiles resulted in adequate detection of steps.

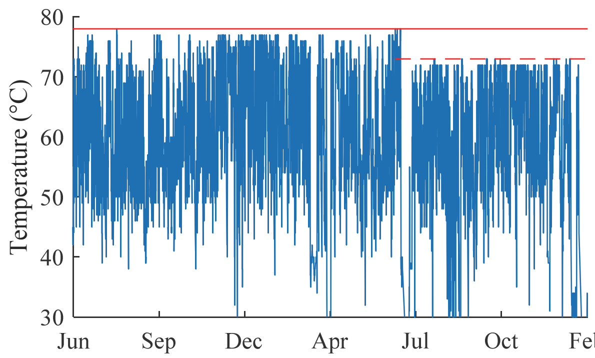

Fig. 1. Example of sensor inconsistency in a bearing temperature with a maximum temperature of 78° C before and 73° C after the step (farm D)

***Service record.*** Insufficient documentation plays a major role if monitoring techniques are evaluated with real data. The service record consisted in the investigated case study of a list of stoppages in the best case (farm B). Comments were added only for major replacements or occasionally for other maintenance actions describing the reason for the stoppage time. Assumed reasons for replacements and interpretations of alarms, stoppages and inspections were generally missing. Accordingly, the list of replacements is not a list of failures. Replacements could have been done as preventative interventions or after a failure which had caused the turbine to stop. Additionally, the time of replacement is not necessarily the time of the failure or the detection of the failure. For the other investigated data, the failure record consisted only of a list of replacements (farm C and D) or was not available at all (farm A).

Although it can be assumed that the operator or service provider has always full access to all reports, the shortcoming of incomplete or incomprehensible service reports is widely acknowledged. Accordingly, service providers are currently focussing on the digitisation of reporting and implementation of procedures to improve the data quality e.g. by using mobile devices for documentation.

Monitoring techniques based on operational data have to be developed and tested with real data. It is very rare to get data of good quality and complete information in terms of turbine and sensor specifications or operation and maintenance reports. As this will similarly be true for industrial application, any modelling technique has to cope with incomplete information. However, the impact of data quality problems should be carefully considered when findings are generalised.

**Monitoring setup**

The detailed configuration of the monitoring setup consists of multiple choices in terms of the model architecture, input selection, pre-processing and training length.

***Model architecture.*** A model using other signals to predict the target can be denoted as full signal reconstruction (FSRC) (Schlechtingen and Santos, 2010). Modelling could use the signal of the same time as the target or from previous time-steps to account for the inertia of the system. Using the latest history of the target itself could also be chosen to form an autoregressive model. If the history of the target is combined with other inputs, the model can be denoted as autoregressive with exogenous input (ARX). Although ARX models are more accurate in predicting the target, the prediction is likely to adapt to new behaviour, which might hinder failure detection.

***Input selection.*** Selecting the inputs for modelling has commonly been done based on the physical understanding of the system also called domain knowledge (Schlechtingen and Santos, 2010; Wang and Infield, 2012; Bangalore and Tjernberg, 2015; Sun et al., 2016) or by correlation analyses between possible inputs and the target (Zaher et al., 2009; Tautz-Weinert and Watson, 2016b). Although most domain knowledge approaches have been based on the basic idea of the heat transfer in the drive train, the reasons for the manual choices of inputs have not been documented thoroughly. The limitation of possible inputs is additionally in contrast to the idea of using machine learning to find complex relationships. Using automated correlation analyses to build the model has the risk of selecting multiple similar inputs, e.g. generator currents 1-3.

The case studies show that e.g. for an ambient temperature a low correlation with a bearing temperature results in an exclusion as input, but less seasonal error is observed if the ambient temperature is selected as input. Selecting inputs only based on their correlation to the target is accordingly not necessarily the best option. Using all possible inputs and an algorithm to select inputs based on their relevance for accurate prediction has been proposed by Dienst and Beseler (2016) in applying the Least Absolute Shrinkage and Selection Operator (LASSO).

***Pre-processing.*** Pre-processing of inputs should include a validity check to exclude data acquisition errors and time-steps with missing or erroneous data have to be removed completely. Additionally, scaling and lag removal might be necessary depending on the modelling technique and input selection (Schlechtingen and Santos, 2010). Focussing on data when the turbine is operating might ease the modelling and failure detection and can be implemented by filtering with a power threshold (Sun et al., 2016).

***Training length.*** There is no consensus about the necessary training time under (assumed) healthy conditions. The proposed lengths range from 3 (Schlechtingen and Santos, 2010) to 14 months (Bach-Andersen et al., 2016). A length of one year is obviously beneficial to cover the full seasonal variation, but such a long training time is probably not always achievable. Other work has tried to concentrate data from a longer period in a shorter, representative training set (Wang and Infield, 2012; Bangalore and Tjernberg, 2014; Tan and Zhang, 2016), although there is not necessarily a benefit in terms of the modelling accuracy.

Tests in the case study reveal that the required training length depends on the turbine specific operation and behaviour. Even one month training results in acceptable accuracy for some turbines. Future work should address the sensitivity to the training length in more detail.

**Proposed modelling techniques**

Several models have been proposed for the required regression task of normal behaviour modelling.

***Multi-linear regression (LIN).*** LIN trained by a least square algorithm is a simple way of modelling the system. Although this assumes linearity, the prediction can have a similar level of accuracy compared with more complex tools (Schlechtingen and Santos, 2010; Tautz-Weinert and Watson, 2016b). Slight improvements have been proposed such as allowing selected polynomial terms up to ninth order (Wilkinson et al., 2014), interactions, i.e. products of the inputs (Tautz-Weinert and Watson, 2016b) or added features such as squares, roots and logarithms (Dienst and Beseler, 2016).

***Artificial Neural Networks (ANNs).*** ANNs have been widely applied to extend the modelling capabilities to non-linearity. A basic setup uses a feed-forward backpropagation network with one input, one hidden layer with a small number of neurons and one output layer with a single linear output. Past research has involved a range of configurations, though authors do not always describe in detail the set up used, Zaher et al. (2009) found that 3 neurons in one hidden layer provide the best results in an ARX approach to model the gearbox bearing. In contrast, Bangalore and Tjernberg (2014) use two hidden layers with 13 neurons in the first layer and one neuron in the second layer in a FSRC approach for gearbox monitoring. Sun et al. (2016) state that the number of neurons has to be selected for each turbine individually ranging from 2 to 10. L. Wang et al. (2016) claim that so called deep ANNs are better with three hidden layers of 100 neurons. Tan and Zhang (2016) highlight the difficulty in selecting a configuration when randomly varying the number of neurons and the type of transfer function and trying to select the best of 200 ANNs.

Tests in the case study show that using more neurons generally improves the accuracy, but there is no significant advantage of deep ANNs with three layers of 100 neurons. Varying the number of neurons and their transfer function randomly does not counterbalance the worse performance of some turbines if using a fixed configuration.

***Adaptive Neuro-Fuzzy Inference Systems (ANFIS).*** ANFIS as a way of learning a fuzzy system with ANN approaches have been proposed by Schlechtingen, Santos and Achiche (2013). Two inputs were used per target with generalised normal distribution membership functions and hybrid gradient descent and least squares estimation learning. The main advantage over straight ANNs was given as the reduced training time.

***Nonlinear State Estimation Technique (NSET)***. NSET has been proposed by Y. Wang and Infield (2012) as a way of modelling based on a state matrix and a weighting vector determined by a least square approach and a Euclidean distance operator. NSET includes the target signal in the state matrix and for determining the weighting vector. It is accordingly comparable to an ARX approach. To find a good compromise of better accuracy for more states and reasonable computational effort for fewer states, a data selection algorithm was proposed. The algorithm selects states, if they are less than the defined distance $\delta$ away from a regular grid of 100 sections of the normalised input. However, the algorithm allowed multiple states for the same grid point which resulted in a high numbers of states. Reproducing the approach in the case studies shows that it was impossible to get a similar number of states for different turbines with one selected $\delta$. However, Guo, Infield and Yang (2012) defined the algorithm to select only one state per grid point. Testing this approach results in a dramatically lower, but more regular number of states for different turbines.

***Multivariate Adaptive Regression Splines (MARS).*** MARS have been applied to wind turbine normal behaviour modelling by Tan and Zhang (2016) allowing a maximum of 21 basis functions. Each basis function can be a constant (for the intercept), a hinge function or a product of hinge functions.

Further well known techniques such as Gaussian Process and Support Vector Machine could also be used for the regression task. However, first case study results could not demonstrate any advantage in using these techniques (Tautz-Weinert and Watson, 2016b).

**Comparing modelling techniques**

The proposed modelling techniques and different input choices are compared with configurations as detailed in Table 2. A comparison of different modelling techniques should consider two main features: effort and accuracy.

The evaluation of the effort can be expressed in the simplicity of the model and the computational effort in training. The simplicity is here evaluated based on the subjective experience of implementing the technique in MATLAB 2015b. Computational effort is easily comparable in terms of the runtime. Example numbers are given using a common desktop PC (64-bit operating system with a four core CPU with 2.8 GHz clock rate and 32 GB memory).

Table 2. Modelling setups for comparison

| Technique | Properties |
|---|---|
| General | - Data from farms A-D, pre-processed including non-operation filtering, turbines with known failures excluded.<br>- Modelling target: Gearbox (bearing) temperature<br>- Modelling inputs:<br>a) 2 inputs, b) 3 inputs selected based on correlation c) power and rotational speed, d) power, rotational speed and ambient temperature<br>- 3 months training, 3 months' blind testing |
| LIN | Linear terms and interactions. |
| ANN | FSRC feed-forward network with 20 neurons in hidden layer. |
| ANFIS | 2 generalised normal distribution membership functions per input. |
| NSET | One state per grid point, $\delta = 0.001$. |
| MARS | Maximum of 21 basis functions. |

There are internal MATLAB functions for all discussed methods, except MARS for which a toolbox is available online (Jekabsons, 2016) and NSET which has been implemented according to Wang and Infield (2012). LIN does not require any detailed configuration and is consequently the easiest method to implement. In contrast, settings have to be chosen for ANNs, ANFIS and MARS. The default settings and main approaches in the literature might be useable for configuring MARS and ANFIS, but in particular the choice of the architecture of ANNs appears to be surprisingly random.

The major advantage of linear models is the low computational effort required as shown in Table 3. Training of ANNs also requires relatively low computational effort with approx. 1-3 s per turbine, but training deep ANNs or repeating the training hundreds of times is highly time consuming. ANFIS modelling is done in about five seconds for up to three inputs, but can take up 30 min per turbine if seven inputs are used. Training NSET in this configuration requires usually 1-12 s with longer runtime for more inputs. MARS training is more expensive and can take more than a minute per turbine depending on the complexity of the model.

Evaluating the accuracy is feasible if the normal operation prediction is assessed. The error of prediction and actual measurement should be as small as possible and mean absolute errors, root mean squared errors, standard deviations or the coefficient of determination ($R^2$) can be used as metrics.

Table 4 compares the normal behaviour modelling accuracies based on the mean absolute error for the different modelling techniques, input selection cases a)-d) and the farms A-D. Due to the limitations in the service reports, the turbines in the study might be affected by further problems which could change the modelling performance, but the selection of the median value from all turbines should give a good indication of the accuracy. It can be seen, that NSET modelling is most accurate with mean absolute errors as low as 0.10 °C. This is due to the autoregressive nature of this technique. Using fewer inputs is better here, which can be explained by the stronger impact of the target signal in this case. All FSRC techniques are similarly accurate with slight advantages of ANN, ANFIS and MARS over LIN modelling. Using three instead of two inputs based on correlation usually improves the performance for FSRC techniques. Using only power and rotational speed to predict the drive train temperature is less accurate. Adding the ambient temperature as a third input improves the prediction in most cases. Comparing the different farms, prediction is most accurate in farm D, but similar low errors can be found in farms B and C. Prediction in farm A is less accurate, in particular in input case c). Possible reasons are manifold, but most likely the differences in the measurement setup and turbine operation of different manufacturers play a major role.

Table 3. Training time in seconds given as median values of all evaluated turbines and cases a) – d)

| Technique | Farm A | Farm B | Farm C | Farm D |
|---|---|---|---|---|
| LIN | 0.02 – 0.02 | 0.02 – 0.02 | 0.01 – 0.02 | 0.02 – 0.02 |
| ANNs | 1.73 – 3.02 | 1.41 – 2.00 | 1.58 – 1.99 | 1.70 – 2.93 |
| ANFIS | 4.42 – 5.70 | 4.40 – 5.42 | 4.39 – 5.43 | 4.40 – 5.48 |
| NSET | 1.27 – 1.94 | 2.40 – 6.64 | 1.90 – 5.09 | 3.00 – 11.52 |
| MARS | 23.81 – 71.82 | 5.44 – 25.42 | 1.37 – 18.77 | 0.78 – 11.00 |

Table 4. Accuracy in modelling normal behaviour given as median value of the mean absolute error (°C) of all evaluated turbines

| Technique | Case | Farm A | Farm B | Farm C | Farm D |
|---|---|---|---|---|---|
| *Used turbines* | | *102* | *8* | *18* | *6* |
| LIN | a) | 2.24 | 1.22 | 0.98 | 1.07 |
| | b) | 2.03 | 0.96 | 0.91 | 0.85 |
| | c) | 11.41 | 1.62 | 1.39 | 1.53 |
| | d) | 3.07 | 1.29 | 1.06 | 1.45 |
| ANNs | a) | 2.27 | 1.12 | 0.87 | 0.89 |
| | b) | 2.00 | 0.89 | 0.86 | 0.82 |
| | c) | 9.47 | 1.58 | 1.39 | 1.19 |
| | d) | 3.21 | 1.27 | 1.41 | 1.49 |
| ANFIS | a) | 2.16 | 1.14 | 0.93 | 0.97 |
| | b) | 1.94 | 0.88 | 0.88 | 0.82 |
| | c) | 10.65 | 1.60 | 1.39 | 1.16 |
| | d) | 2.92 | 1.22 | 1.20 | 1.19 |
| NSET | a) | 0.23 | 0.33 | 0.38 | 0.91 |
| | b) | 0.25 | 0.27 | 0.35 | 1.09 |
| | c) | 0.18 | 0.10 | 0.10 | 0.13 |
| | d) | 0.25 | 0.77 | 1.53 | 0.52 |
| MARS | a) | 2.18 | 1.08 | 0.87 | 0.93 |
| | b) | 2.11 | 0.86 | 0.85 | 0.82 |
| | c) | 10.23 | 1.58 | 1.39 | 1.15 |
| | d) | 3.07 | 1.26 | 1.09 | 1.14 |

Accurate normal behaviour prediction does not necessarily imply good failure detection in terms of early and reliable alarms. Comparing the residual of modelled and measured temperatures before a known failure should give an insight in possible early warnings. However, displaying unfiltered residuals from a long period is not feasible due to the high number of samples per month and strong fluctuations.

In Fig. 2 – Fig. 6 the fortnightly moving averages of the residuals are given for 1.5 years' period before a gearbox replacement in farm B for LIN, ANN, ANFIS, NSET, MARS, respectively. Although most techniques and input selection cases show rising values in the last three months before the replacement, trends of a similar magnitude can be seen during the previous year. It is obvious that the smoothed residual is not an ideal indicator for failures and dedicated alarm generation techniques are required (which will be discussed below). However, ANN, NSET and MARS modelling with input case a) seem to give the most prominent increase directly before the replacement. Noticeably, case d) shows a trend from June to December which differs from the other cases in four of five modelling techniques. Future studies are required to better understand the impact of the input selection.

**Modelling capabilities**

These types of models are unlikely to be able to predict uncommon features in a signal. It has been observed that some abrupt increases in a bearing temperature in farm C cannot be modelled by any of the modelling techniques. These spikes occur only when the turbine power is rapidly increasing as shown in Fig. 7.

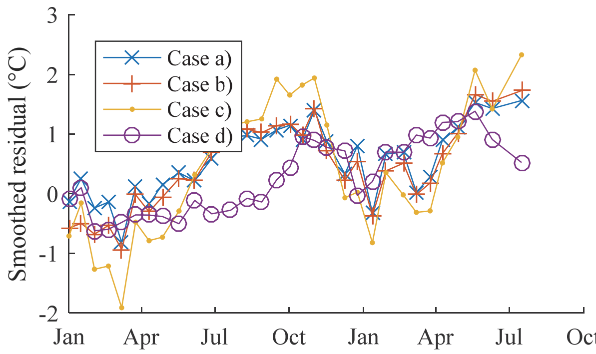

Fig. 2. Residuals from LIN modelling before a gearbox replacement

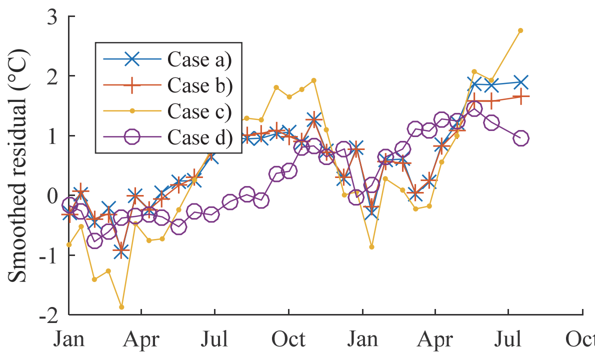

Fig. 3. Residuals from ANN modelling before a gearbox replacement

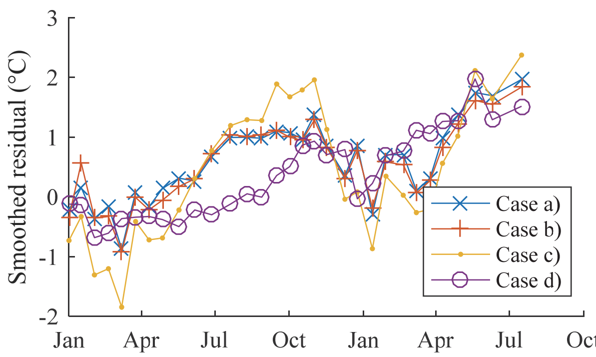

Fig. 4. Residuals from ANFIS modelling before a gearbox replacement

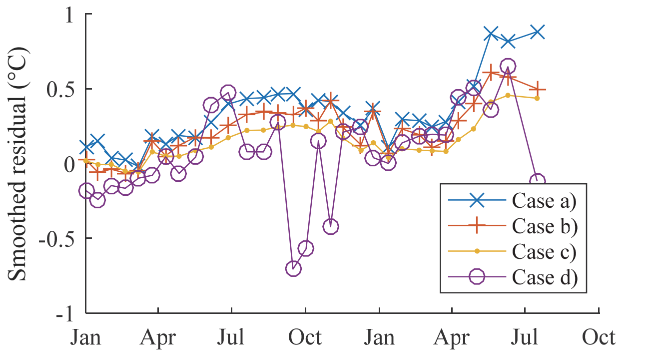

Fig. 5. Residuals from NSET modelling before a gearbox replacement

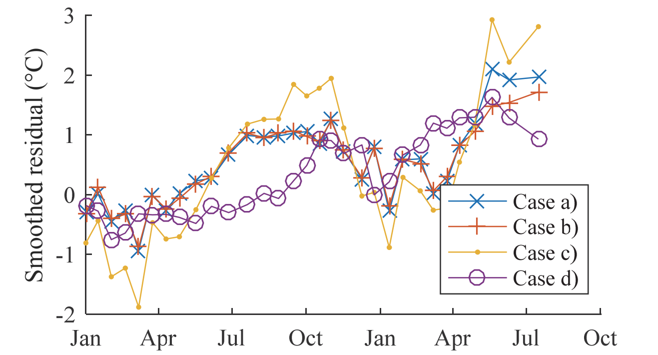

Fig. 6. Residuals from MARS modelling before a gearbox replacement

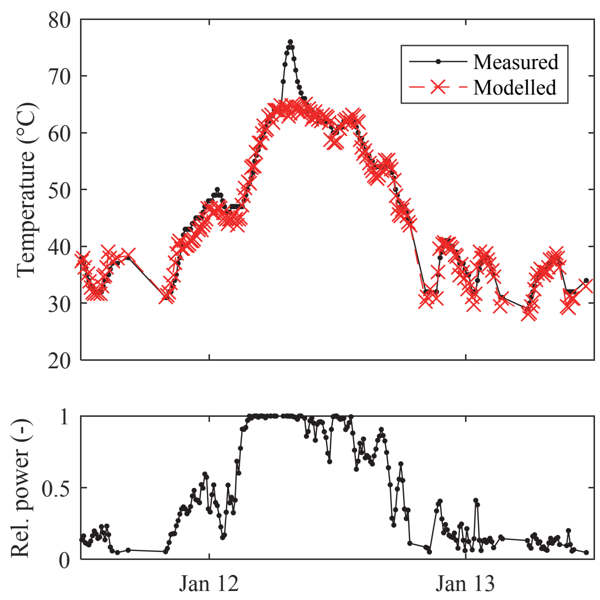

Fig. 7. Example of unpredicted spike in a bearing temperature when power is rapidly increasing (farm C, modelling with ANNs)

**Alarm generation**

The idea behind normal behaviour modelling is the use of the residual of measured minus modelled temperature to act as an indicator of potential failure. Different approaches have been proposed for generating alarms based on the residual time series.

***Absolute threshold.*** The simplest way of generating alarms is by defining an absolute threshold for the residual. This can be by confidence bands (Garcia et al., 2006), with a defined threshold based on experience (Schlechtingen and Santos, 2010; Wilkinson et al., 2014) or a certain probability to occur derived from the error distribution in training, as e.g. less than 0.01 % (Schlechtingen et al., 2013). The reliability of the absolute threshold can be increased by using a daily average (Schlechtingen and Santos, 2010).

***Mahalanobis distance.*** A Mahalanobis distance is a metric to condense the correlation of multiple variables and their distribution to a single number. Bangalore and Tjernberg (2015) proposed using a Mahalanobis distance of the residual and target referenced to the training distribution to detect anomalies. Alarms were raised if averages of three days were smaller than a distance with a probability of 1 % defined by a Weibull distribution fitted to the training results.

***Exponentially weighted moving average control chart (EWMA).*** EWMA has been proposed to consider cumulating effects by Wang et al. (2016). Compared to the simple absolute threshold for the error, here a recursive statistic is built from the current error and the statistic in the previous time-step. A weighting of 0.2 for the current error and 0.8 for the previous statistic was used.

***Abnormal level index (ALI).*** Sun et al. (2016) developed a numeric index to describe the abnormality of monitored signals. The index is calculated as a daily sum of penalties for residuals significantly bigger than the expected based on the training period. The penalty was defined as 5 and 3 for a penalty exceeding 97.5 and 75 % cumulative probability, respectively, or 1 else. After normalising, the index provided values between 0 and 1, with smaller values for less abnormality.

***Discussion.*** Failure detection accuracy can be assessed in terms of the true positive and false positive alarms compared to the number of failures. Additionally, the advance time of detection before failure is a key measure. Comparing the failure detection capabilities is hindered by the above mentioned difficulties with the service reports. A thorough comparison of the modelling and the alarm generation techniques is out of the scope of this paper.

As an example, the detection of the above discussed gearbox failure in farm B modelled with ANNs in case a) is given in Fig. 8. All alarm generation techniques require a defined threshold for raising the alarm. The proposed probabilities of occurrence determined from the training data are not necessarily the optimal choice for new cases. A threshold defined by a probability of > 0.01 % for the residual leads to vanishing alarms in the investigated case studies. The limits are defined with a > 2 % probability of occurrence for the absolute daily threshold, > 1 % probability for the Mahalanobis distance, $6\sigma$ in the EWMA and the ALI as proposed. It can be seen that this selection of thresholds results in an increasing number of alarms in the two months before the replacement.
However, a significant number of alarms occur far ahead of the replacement, in particular with the Mahalanobis distance. These alarms have to be considered as false alarms. The number of false alarms can be reduced by requiring several alarms in a row or in a specific time window as e.g. a week (Schlechtingen et al., 2013). By applying a limit of at least two days of alarms in one week and adapted thresholds the number of possibly false alarms can be reduced, as shown in Fig. 9. In this example, there is no significant difference between the first reliable detection of the different alarm generation techniques. However, the Mahalanobis distance and EWMA technique have a higher number of alarms after the first alarm than the absolute threshold and can be seen

as more reliable accordingly. The fuzzy indicator provided by ALI shows a clear upward trend, but has two previous peaks which have to be assumed to be false alarms. A calibration of alarm thresholds with one turbine in the farm without replacements has been tested, but resulted in unsatisfactory results as many false alarms occurred.

The comparison of alarm generation techniques highlights that the adequate definition of thresholds has a higher impact than the differences in the detection approach. Future work has to address this problem in more detail.

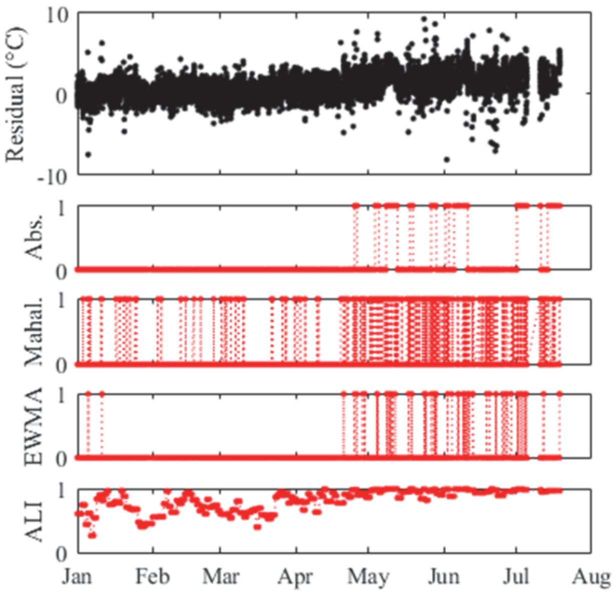


Fig. 8. Testing different alarm generation techniques (gearbox replacement at the end of time axis, ANNs modelling, case a), farm B)

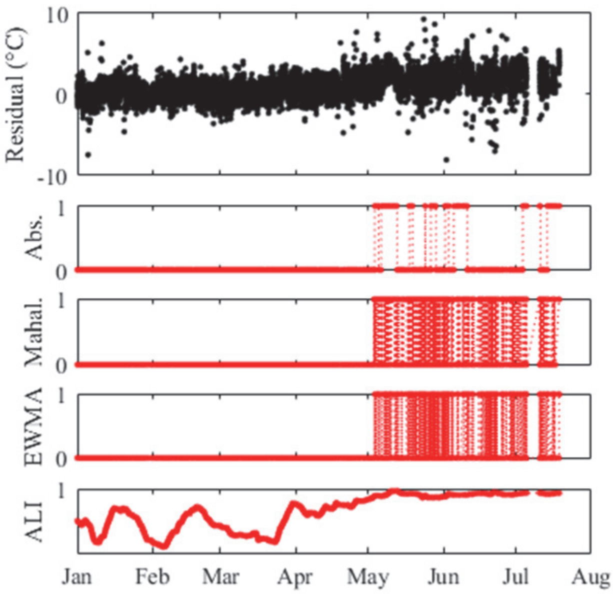


Fig. 9. Using a weekly filter for different alarm generation techniques (gearbox replacement at the end of time axis, ANNs modelling, case a), farm B)

## FUTURE CHALLENGES IN ON-LINE MONITORING

Retrospective analyses of failures are of interest in an academic project of finding suitable tools for monitoring, but in industrial reality wind turbines are to be monitored on-line. Depending on the data management system this could be with new data every day, every ten minutes or even more frequently.

Most challenges which occur in retrospective analyses are also valid here, as e.g. SCADA data quality problems and model definitions. Problems with missing maintenance information are probably less severe in industrial on-line monitoring as a wind farm operator is aware of ongoing maintenance. However, insufficient or misleading maintenance reports occur in industrial practice too. The requirement for minimal computational effort for modelling will be even greater for on-line monitoring. Additionally, computational environments other than MATLAB are common in industry and will require adapted implementations. On-line monitoring will require adequate re-training of models after significant changes in the system or operation, as briefly discussed by Bangalore and Tjernberg (2013).

The main challenge of on-line monitoring is the required accuracy of monitoring in to allow decisions to be made about whether or not to send a maintenance team. A balance needs to be struck between providing early warnings whilst avoiding false alarms in order to minimise maintenance costs and maximise turbine availability. In the first months of operation of a new farm, there should be an iterative process of training and model evaluation until confidence in the results is achieved.

A combination of monitoring based on operational data and common vibration-based condition monitoring systems might be desirable to increase the reliability.

## CONCLUSIONS

Based on analyses of case studies on four wind farms, the challenges in using operational data for wind turbine condition monitoring can be summarised as:

- Poor SCADA data documentation and quality,
- Insufficient maintenance documentation,
- The absence of best practice in selecting modelling techniques and settings,
- Isolated behavioural features which are difficult to model,
- The difficulty in defining sensible alarm thresholds which give sufficient notice of early genuine problems but minimise false alarms.

First findings indicate that ANN, ANFIS and MARS are similar accurate FSRC modelling techniques with the least computational effort for ANN. However, linear modelling is only slightly less accurate and possibly preferable due to its simplicity. NSET modelling is more accurate than all other techniques because of its autoregressive nature.

A brief comparison of smoothed residuals from all techniques before a gearbox replacement indicated that good modelling accuracy does not necessarily coincide with straightforward failure detection. Selecting inputs based on correlation or based on the physics seem to result in different residual trends, which are not fully understood yet.

If the different proposed alarm generation techniques are compared, no clear advantage of any approach is directly visible. A weekly filter of alarms is desirable to increase the certainty of results.

Future work will address the challenges in more detail and thoroughly evaluate the capabilities of failure detection with operational data.

ACKNOWLEDGEMENTS

This project has received funding from the European Union's Horizon 2020 research and innovation programme under the Marie Sklodowska-Curie grant agreement No 642108 (Advanced Wind Energy Systems Operation and Maintenance Expertise, http://awesome-h2020.eu/).
We would like to thank the industrial partner in the AWESOME project, DNV GL, for sharing anonymised wind farm data.

REFERENCES

Bach-Andersen M, Rømer-Odgaard B, Winther O (2016). "Flexible non-linear predictive models for large-scale wind turbine diagnostics," *Wind Energy*, 17, 657–669.

Bangalore P, Tjernberg LB (2015). "An Artificial Neural Network Approach for Early Fault Detection of Gearbox Bearings," *IEEE Trans Smart Grid*, 6, 980–987.

Bangalore P, Tjernberg LB (2014). "Self Evolving Neural Network Based Algorithm for Fault Prognosis in Wind Turbines : A Case Study," *PMAPS*, 1–6.

Bangalore P, Tjernberg LB (2013). "An approach for self evolving neural network based algorithm for fault prognosis in wind turbine," In: 2013 IEEE Grenoble Conference. IEEE, pp 1–6.

Dienst S, Beseler J (2016). "Automatic Anomaly Detection in Offshore Wind SCADA Data," In: WindEurope Summit 2016. .

Feng Y, Qiu Y, Crabtree CJ, et al (2013). "Monitoring wind turbine gearboxes," *Wind Energy*, 16, 728–740.

Garcia MC, Sanz-Bobi MA, del Pico J (2006). "SIMAP: Intelligent System for Predictive Maintenance Application to the health condition monitoring of a windturbine gearbox," *Comput Ind*, 57, 552–568.

Guo P, Infield D, Yang X (2012). "Wind Turbine Generator Condition-Monitoring Using Temperature Trend Analysis," *Sustain Energy, IEEE Trans*, 3, 124–133.

Jekabsons G (2016). "ARESLab: Adaptive Regression Splines toolbox for Matlab/Octave," http://www.cs.rtu.lv/jekabsons/ (accessed 2016-03-24).

Schlechtingen M, Santos IF (2010). "Comparative analysis of neural network and regression based condition monitoring approaches for wind turbine fault detection," *Mech Syst Signal Process*, 25, 1849–1875.

Schlechtingen M, Santos IF, Achiche S (2013). "Wind turbine condition monitoring based on SCADA data using normal behavior models. Part 1: System description," *Appl Soft Comput*, 13, 447–460.

Sun P, Li J, Wang C, Lei X (2016). "A generalized model for wind turbine anomaly identification based on SCADA data," *Appl Energy*, 168, 550–567.

Tan M, Zhang Z (2016). "Wind Turbine Modeling With Data-Driven Methods and Radially Uniform Designs," *IEEE Trans Ind Informatics*, 12, 1261–1269.

Tautz-Weinert J, Watson S (2016a). "Using SCADA Data for Wind Turbine Condition Monitoring - a Review," IET Renew Power Gener.

Tautz-Weinert J, Watson SJ (2016b). "Comparison of different modelling approaches of drive train temperature for the purposes of wind turbine failure detection," *J Phys Conf Ser*, 753, 72014.

Wang L, Zhang Z, Long H, et al (2016). "Wind Turbine Gearbox Failure Identification with Deep Neural Networks," *IEEE Trans Ind Informatics*, 3203, 1–1.

Wang Y, Infield D (2012). "Supervisory control and data acquisition data-based non-linear state estimation technique for wind turbine gearbox condition monitoring," *IET Renew Power Gener*, 7, 350–358.

Wiggelinkhuizen E, Verbruggen T, Braam H, et al (2008). "Assessment of Condition Monitoring Techniques for Offshore Wind Farms," *J Sol Energy Eng*, 130, 31004-1-31004–9.

Wilkinson M, Harman K, van Delft T, Darnell B (2014). "Comparison of methods for wind turbine condition monitoring with SCADA data," *IET Renew Power Gener*, 8, 390–397.

Yang W, Tavner PJ, Crabtree CJ, et al (2014). "Wind turbine condition monitoring: technical and commercial challenges," *Wind Energy*, 17, 673–693.

Zaher A, McArthur SDJ, Infield DG, Patel Y (2009). "Online wind turbine fault detection through automated SCADA data analysis," *Wind Energy*, 12, 574–593.

# Comparison of different modelling approaches of drive train temperature for the purposes of wind turbine failure detection



2016 J. Phys.: Conf. Ser. 753 072014

(http://iopscience.iop.org/1742-6596/753/7/072014)

# Comparison of different modelling approaches of drive train temperature for the purposes of wind turbine failure detection

**J Tautz-Weinert and S J Watson**

Centre for Renewable Energy Systems Technology, Wolfson School of Mechanical, Electrical and Manufacturing Engineering, Loughborough University, Loughborough, LE11 3TU, UK

j.tautz-weinert@lboro.ac.uk

**Abstract**. Effective condition monitoring techniques for wind turbines are needed to improve maintenance processes and reduce operational costs. Normal behaviour modelling of temperatures with information from other sensors can help to detect wear processes in drive trains. In a case study, modelling of bearing and generator temperatures is investigated with operational data from the SCADA systems of more than 100 turbines. The focus is here on automated training and testing on a farm level to enable an on-line system, which will detect failures without human interpretation. Modelling based on linear combinations, artificial neural networks, adaptive neuro-fuzzy inference systems, support vector machines and Gaussian process regression is compared. The selection of suitable modelling inputs is discussed with cross-correlation analyses and a sensitivity study, which reveals that the investigated modelling techniques react in different ways to an increased number of inputs. The case study highlights advantages of modelling with linear combinations and artificial neural networks in a feed-forward configuration.

## 1. Introduction

Onshore wind turbines are now able to compete with fossil fuel powered plants in terms of the levelised cost of energy achieving 74 EUR/MWh [1]. But unscheduled maintenance, particularly offshore, results in high costs as accessibility is restricted by weather and availability of vessels. Studies of recent offshore projects reported operation and maintenance costs of 40-44 EUR/MWh [2]. Advanced maintenance strategies based on actual condition rather than using corrective or preventive maintenance can reduce these costs. Evaluation of operational data recorded by the Supervisory Control And Data Acquisition (SCADA) system of a wind turbine shows promise for the purposes of condition monitoring as the high cost of additional sensors in a common dedicated condition monitoring system is avoided.

Increased temperatures in bearings or the gearbox can indicate reduced performance or imminent failure as mechanical faults are usually accompanied by increased heat loss [3]. Thresholds of absolute values are generally implemented in control systems to avoid overheating. But wear-related changes in the temperature trends are often hidden by normal operational fluctuations in temperature due to the variable speed nature of modern large-scale wind turbines as shown for a simulated fault in figure 1. Some of the first approaches of condition monitoring using SCADA temperature data used manual trending against power [3–5] or clustering [6,7] to find anomalies. These techniques succeeded for single turbines in historic analyses, but feasible detection in real time is difficult due to the required manual interpretation of results. Another recent approach is normal behaviour modelling, i.e. the prediction of a temperature while assuming that the component is behaving normally [8–17]. This approach appears to be more suitable for automated failure detection due to an easily interpretable indicator, i.e. the residual of measured minus modelled temperature.

In this paper, different approaches for normal behaviour modelling are investigated using historic SCADA data. Extensive tests are conducted to gain not only the most accurate temperature prediction for a single turbine and modelling target, but also the average prediction performance and the robustness of each approach using automated training and testing. Two different drive train temperatures are modelled for more than 100 turbines in a wind farm.

In section 2 of this paper the methodology is presented. Section 3 provides details of the case study. The modelling results are discussed in section 4. The final section summarises the findings and addresses future work.

## 2. Methodology

In this section the idea of normal behaviour modelling is explained and the settings of the different modelling approaches described. Cross-correlation and performance metrics are introduced for input selection and prediction evaluation, respectively.

### *2.1. Normal behaviour modelling*

Temperature signals in recorded SCADA data can give information about the changing performance of mechanical parts. Temperatures of drive trains fluctuate due to the rapidly changing operation of variable speed turbines as shown in figure 1. Normal behaviour modelling is a way to reveal hidden trends in temperature signals. This type of model can be used to estimate temperature using information from sensors external to the component being monitored. Figure 2 shows the idea of modelling a measured variable by using environmental signals (e.g. ambient temperatures, wind speed etc.) and process parameters (e.g. rotational speeds, other temperatures) as inputs to predict the target temperature. The model learns normal behaviour by training with input and desired output data under healthy conditions. After training, the residual of measured minus modelled temperature acts as a potential indicator of failure: if a fault occurs, the residual will increase. An alarm can be raised if a fixed threshold or confidence band is violated [8,12–14], if a Mahalanobis distance considering temperature and residual distributions from training exceeds a probability threshold [16] or based on an abnormal level index which weights residuals according to their probabilities [17]. Generating warnings on the basis of residuals of one or more days of data has been proposed to provide more confidence in alarms [11,13,17]. Further evaluation of alarms with fuzzy inference systems has been applied [8,13,15,17].

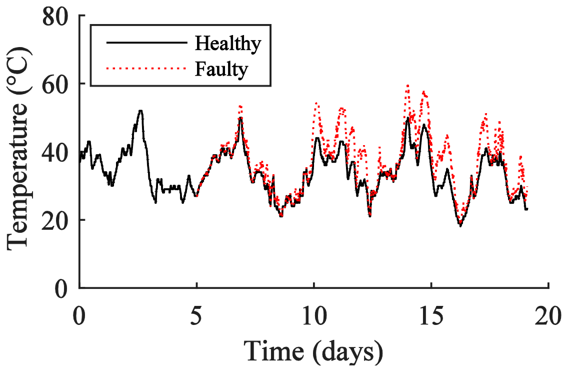


**Figure 1.** Example of a bearing temperature time series. A time series of a simulated fault is added for visualisation of the detection difficulty.

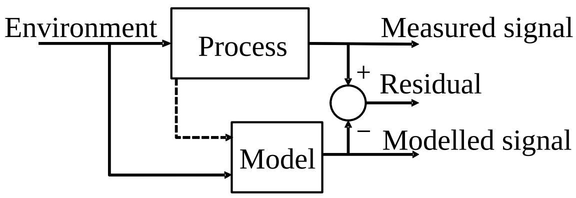


**Figure 2.** Normal behaviour modelling sketch.

The quality of the failure indicator depends on the accuracy of the modelling. In this study, modelling based on linear combinations ([9,11,14,15]) is compared with artificial neural networks ([8,11,12,15–17]) and adaptive neuro-fuzzy inference systems ([13]). Two novel techniques for modelling of SCADA temperatures are added: support vector machine regression and Gaussian process regression.

Autoregressive modelling approaches and state estimation techniques ([18]) are not considered due to their more likely adaption to new behaviour in the case of a failure as a result of using the target temperature itself for prediction. This is not necessarily desirable for condition monitoring when changes in a physical state which may be an indicator of failure need to be detected through an increased residual. Due to this reason all approaches are here applied in a strictly non-autoregressive way without using any historic values of the target signal (in contrast to approaches in [8–10,16,17]).

### *2.2. Cross-correlation*

The sample cross-correlation (CC) gives a measure of the similarity of two signals and can be used as a basis for selecting suitable inputs for modelling. CC at lag $k$ is defined for two (real-valued) signals $x$ and $y$ as:

$$\mathrm{CC}(k) = \sum_i (x_{i+k} - \bar{x})(y_i - \bar{y}) \tag{1}$$

with an over-bar denoting the mean value. The summation uses all possible samples for the particular lag of interest. Usually CC is normalised to a value of one for auto-correlation at lag zero, i.e. the correlation of the target with itself at zero lag.

### *2.3. Model approaches*

Linear modelling is conducted with a least squares fit of first order polynomials. Simple linear modelling (LIN) uses a linear regression model consisting of a sum of all inputs with individual weights and an interceptor. Linear modelling with interactions (LIN-I) uses a model with intercept, linear terms and products of pairs of inputs (without squared terms).

Artificial neural networks (ANNs) are applied in two configurations: feed-forward (ANN-FF) and layer recurrent (ANN-LR). ANN-FF describes a network with only connections from inputs and layers to the next layer without any feedback or recurrence and has been used in [11,12] for normal behaviour modelling. In contrast, ANN-LRs have a delayed feedback from layer outputs to the input of the layer and are used as a novel way to include system inertia in SCADA normal behaviour modelling. For both configurations a hyperbolic tangent sigmoid (tansig) transfer function is used for neurons in the hidden layer and a linear transfer function for the output layer. Initial tests resulted in an architecture consisting of one hidden layer with six neurons. ANN-LRs are set up with a delay of two steps for the recurrence. Training of neural networks is conducted by Levenberg-Marquardt backpropagation and the mean squared error as performance function. Convergence criteria are minimum performance gradient of $10^{-7}$, 1000 epochs or 6 successive iterations with validation performance failing to decrease. Selected training data are randomly split using 80% for real training and the rest for validation.

Gaussian process regression (GPR) [19] is configured with a squared exponential kernel for the covariance function and a constant basis matrix. Standardisation of inputs is applied. Fitting uses a subset of data points approximation.

Linear epsilon-insensitive Support Vector Machine (SVM) [20] regression is applied with a Gaussian kernel. A Sequential Minimal Optimisation solver is used with training until a feasibility gap of $10^{-3}$, a zero gradient or $10^{6}$ iterations are reached.

Adaptive Neuro-Fuzzy Inference System (ANFIS) modelling is conducted in a similar manner to [13]. Two Gaussian membership functions are associated with each input. A linear membership function is used for the output. Training uses a hybrid algorithm utilising backpropagation and least squares in 20 epochs.

For easier comparison of the modelling accuracy, a 'trivial' modelling approach is added, where the target temperature is set to the mean value of the training period. The prediction is constant and unaffected by any input signals.

### *2.4. Evaluation metrics*

Modelling is conducted in Matlab 2015b on a 64-bit operating four core CPU with 2.8 GHz clock rate and 32 GB memory. The runtime for training and testing of each model is recorded to compare the computational effort of the investigated approaches.

Performances of the modelling approaches are evaluated in terms of the mean absolute error (MAE), the root mean squared error (RMSE), standard deviation of error (STDE) and the Coefficient of Determination ($R^2$), as defined in equations (2)-(6) with $n$ as the number of samples, $y$ as the measured and $\hat{y}$ as the modelled target temperature. Results of the individual models for all turbines are summarised for the farm by calculating the median of the metric values as a measure for the average performance ignoring extreme outliers. Although outliers will be of interest in the condition monitoring stage, here the focus lies on the average performance of normal behaviour modelling. Residual distributions of all turbines are merged by selecting the median for each bin count.

$$\mathrm{MAE} = \frac{1}{n}\sum_{i=1}^{n}|\hat{y}_i - y_i| \tag{2}$$

$$\mathrm{RMSE} = \left(\frac{1}{n}\sum_{i=1}^{n}(\hat{y}_i - y_i)^2\right)^{\frac{1}{2}} \tag{3}$$

$$\mathrm{STDE} = \sigma(\hat{y} - y), \text{ with standard deviation } \sigma(x) \text{ as:} \tag{4}$$

$$\sigma(x) = \left(\frac{1}{n-1}\sum_{i=1}^{n}(x_i - \bar{x})^2\right)^{\frac{1}{2}} \tag{5}$$

$$R^2 = 1 - \frac{\sigma(\hat{y}-y)^2}{\sigma(y)^2} \tag{6}$$

## 3. Case study

The different approaches are tested with data from a US wind farm with more than 100 turbines. Six months of SCADA data from variable speed turbines with a rated power of 1.5 MW are analysed. The data consist of temperatures as well environmental and control parameters in 10 minute averages.

Two different drive train temperatures are selected to be modelled: a bearing temperature and a generator winding temperature. Due to a lack of maintenance information, all turbines are assumed to operate normally with only short stops for minor repairs. Distributions of operational status are analysed to exclude turbines with significantly long downtimes. The analysis is carried out by visual interpretation of status codes and distributions of power output. Six turbines are excluded from modelling due to unusually high frequencies of non-operational status codes and downtime.

The investigated SCADA data are not always of a high quality. Unfeasible sensor values are found to occur and temperature records show a non-physically high frequency of discrete whole numbers. Although this is a limitation to achieving good modelling accuracy, the aim of comparing different approaches is not hindered. Pre-processing of data is conducted in terms of applying valid sensor ranges similar to [13]. Detailed investigations of SCADA uncertainties by means of sensitivity studies are left for future research.

### *3.1. Cross-correlation results*

All possible inputs for predicting the two chosen target temperatures are analysed with a cross-correlation (CC) calculation up to a maximum lag of $\pm$ 20 ten-minute time-steps. The results in table 1 indicate that the Bearing A temperature correlates with the other bearing, the ambient and generator temperature. Power, currents, wind and rotational speeds have a delayed impact on the bearing temperature. Blade angles and generator voltages do not correlate with the bearing temperature. A comparison of the maximum CC with the CC without any lag reveals the most significant difference for the ambient temperature with a value of 0.82 for a signal lagging 17 time-steps behind compared to 0.76 for the simultaneous signals. The results for the Generator 1 temperature as the target show that the two generator temperatures are statistically identical. The target temperature is highly correlated with the Bearing B temperature, the power, phase currents and wind and rotational speeds. The ambient temperature has a low cross-correlation value of 0.48. Power, currents and wind speed have a delayed correlation with the generator temperature.

**Table 1.** Highest normalised cross-correlation (CC) (as a function of lag) with Bearing A (a) and Generator 1 (b) temperature. Median of all turbines for first 7500 samples.

(a)

| Signal | CC(best lag) | | CC(0) |
|---|---|---|---|
| Bearing A temperature | 1.00 | (0) | |
| Bearing B temperature | 0.86 | (1) | 0.86 |
| Ambient temperature | 0.82 | (-17) | 0.76 |
| Generator 1 temperature | 0.76 | (0) | |
| Generator 2 temperature | 0.76 | (0) | |
| Power | 0.45 | (-5) | 0.42 |
| Phase current A | 0.45 | (-5) | 0.42 |
| Phase current B | 0.45 | (-5) | 0.42 |
| Phase current C | 0.45 | (-5) | 0.43 |
| Wind speed | 0.45 | (-5) | 0.42 |
| Generator speed | 0.36 | (-3) | 0.35 |
| Rotor speed | 0.36 | (-3) | 0.35 |

(b)

| Signal | CC(best lag) | | CC(0) |
|---|---|---|---|
| Generator 1 temperature | 1.00 | (0) | |
| Generator 2 temperature | 1.00 | (0) | |
| Bearing B temperature | 0.95 | (3) | 0.94 |
| Power | 0.83 | (-2) | 0.80 |
| Phase current A | 0.83 | (-2) | 0.80 |
| Phase current C | 0.83 | (-2) | 0.80 |
| Phase current B | 0.82 | (-2) | 0.80 |
| Wind speed | 0.81 | (-3) | 0.79 |
| Bearing A temperature | 0.76 | (0) | |
| Generator speed | 0.72 | (-3) | 0.71 |
| Rotor speed | 0.72 | (-3) | 0.71 |
| Ambient temperature | 0.48 | (-20) | 0.39 |

### *3.2. Model input sensitivity study*

The selection of inputs for the normal behaviour modelling is based on CC results. However, for condition monitoring purposes not only the prediction accuracy is important, but also the visibility of a fault in the residual [13]. Therefore, previous temperature measurements of the target component are excluded from the model as inputs, as these would be affected by any change in condition of the component. As the premise of normal behaviour modelling is that the system is not changing then including previous measurements may mask systematic changes in the residuals.

A basic configuration (1a) is defined by selecting the two strongest signals in the CC as inputs without any lag. Using more inputs and the optimal lag could increase the prediction accuracy. Therefore, a sensitivity study is conducted in which the signal lag is changed and further inputs are added according to their CC value. Table 2 summaries the input selection for the configurations with different inputs and their sub-variations a-c with different lags.

### *3.3. Training and testing selection*

Models are trained with 7,500 samples, which is equivalent to 52 days. A further 10,000 samples (69 days) are used for blind testing of the models. A two-fold cross validation is applied by partitioning of the measured SCADA time series into a training period and a testing period. These are then reversed for a second run. It has to be emphasised that down times and start or stop manoeuvres are not excluded in order to test the robustness of the approaches.

**Table 2.** Inputs and lags for modelling the different configurations.

| Configuration | Target: Bearing A temperature | | | | | | | | | Target: Generator 1 temperature | | | | | | | | |
|---|---|---|---|---|---|---|---|---|---|---|---|---|---|---|---|---|---|---|
| | 1 | | | 2 | | | 3 | | | 1 | | | 2 | | | 3 | | |
| | a | b | c | a | b | c | a | b | c | a | b | c | a | b | c | a | b | c |
| Generator 1 temperature (t) | x | x | x | x | x | x | x | x | x | | | | | | | | | |
| Ambient temperature (t) | x | | x | x | | x | x | | x | | | | | | | | | |
| Ambient temperature (t-17) | | x | x | | x | x | | x | x | | | | | | | | | |
| Bearing B temperature (t) | | | | | | | | | | x | x | x | x | x | x | x | x | x |
| Power (t) | | | | x | | x | x | | x | x | | x | x | | x | x | | x |
| Power (t-2) | | | | | | | | | | | x | x | | x | x | | x | x |
| Power (t-5) | | | | | x | x | | x | x | | | | | | | | | |
| Phase current A (t) | | | | | | | x | | x | | | | x | | x | x | | x |
| Phase current A (t-2) | | | | | | | | | | | | | | x | x | | x | x |
| Phase current A (t-5) | | | | | | | | x | x | | | | | | | | | |
| Wind speed (t) | | | | | | | | | | | | | | | | x | | x |
| Wind speed (t-3) | | | | | | | | | | | | | | | | | x | x |

## 4. Results
The results of the case study confirmed that modelling of a temperature with information from other sensors results in a time series signal, which reliably follows the transient trends of the measured signal, as shown for an example in figure 3.

### *4.1. Baseline results*
The results of the bearing temperature modelling with the baseline configuration (1a), table 3, indicate that linear, ANN and ANFIS approaches perform each with a similar small error. The best approach cannot be found as different approaches perform differently for each of MAE, RMSE, STDE and $R^2$ metrics and for the two tests. GPR and SVM techniques, however, do not perform as accurately as the other models. The results in table 4 for the generator temperature modelling show a similar pattern, although the ANN approaches give the least errors for all metrics.

Figure 4 gives an insight into the distribution of model performance across the wind farm. Although ANN-LR modelling results in the lowest minimum and median MAE, more than 20 % of the turbines have a distinctly larger MAE compared with the other approaches. A model with an inferior minimum accuracy, but more constant prediction errors for the whole farm will be preferred for failure detection purposes. Maximum errors in the farm should be interpreted with care, as they could also denote a problem in the particular turbine, since normal operation is not guaranteed.

An analysis of the median distribution of the residual time series for the two tests, as given in figure 5 and figure 6 for the generator temperature, reveals bell shaped distributions with a slightly skewed behaviour. The residuals of nearly all approaches are shifted to negative values for the chronological training and test sequences (test 1), but to positive values for the reversed sequence (test 2). The residual distributions of the linear modelling are skewed in an ambiguous way. If the modelling approaches are compared, it can be noted that linear modelling results in the broadest and ANN-LR in the sharpest peaks. The skewness trends of the residual distributions are reversed for the bearing temperature modelling, i.e. positively skewed for test 1 and negatively skewed for test 2. A seasonal influence is assumed to cause the skewness, which is already visible for the trivial model. However, the effect cannot be explained completely by this hypothesis.

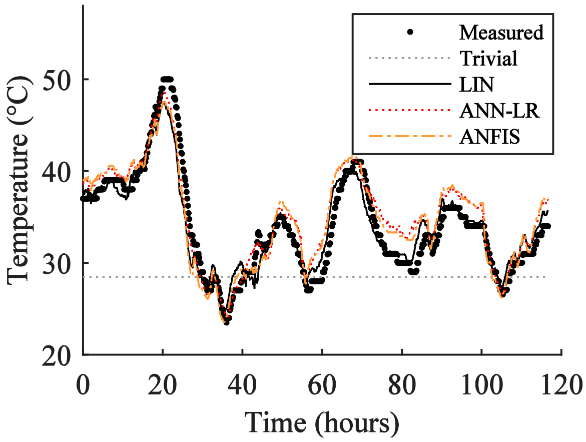


**Figure 3.** Bearing temperature modelling example.

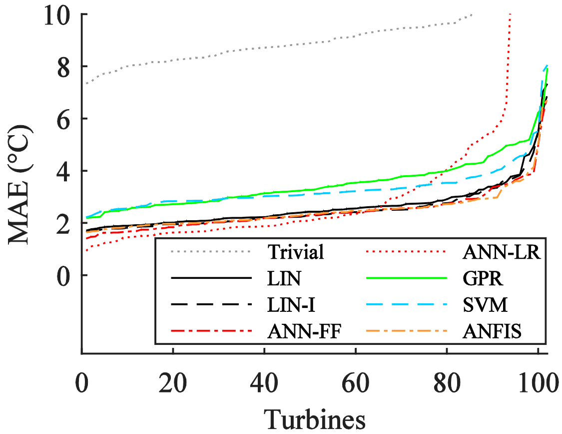


**Figure 4.** Sorted MAE of all turbines for bearing temperature modelling in configuration 1a, test 1.

**Table 3.** Performance of different approaches for bearing temperature modelling in basic configuration (1a). Median values are given from all turbines' models.

| | MAE (°C) | | RMSE (°C) | | STDE (°C) | | $R^2$ (-) | |
|---|---|---|---|---|---|---|---|---|
| | Test 1 | Test 2 | Test 1 | Test 2 | Test 1 | Test 2 | Test 1 | Test 2 |
| Trivial | 8.92 | 8.78 | 10.89 | 10.62 | 8.37 | 7.37 | 0.00 | 0.00 |
| LIN | 2.43 | **2.22** | 3.30 | **2.93** | 2.96 | **2.88** | **0.88** | **0.85** |
| LIN-I | 2.30 | 2.28 | **3.16** | 3.08 | **2.89** | 2.99 | **0.88** | 0.83 |
| ANN-FF | 2.32 | 2.34 | 3.28 | 3.24 | 3.08 | 3.04 | **0.88** | 0.84 |
| ANN-LR | **2.15** | 2.35 | 3.34 | 3.82 | 3.02 | 3.52 | 0.87 | 0.78 |
| GPR | 3.30 | 3.26 | 5.28 | 5.83 | 4.89 | 5.32 | 0.65 | 0.46 |
| SVM | 3.12 | 3.15 | 5.02 | 5.69 | 4.53 | 5.32 | 0.72 | 0.48 |
| ANFIS | 2.36 | 2.27 | 3.19 | 3.01 | 2.94 | 2.89 | **0.88** | **0.85** |

**Table 4.** Performance of different approaches for generator temperature modelling in basic configuration (1a). Median values are given from all turbines' models.

| | MAE (°C) | | RMSE (°C) | | STDE (°C) | | $R^2$ (-) | |
|---|---|---|---|---|---|---|---|---|
| | Test 1 | Test 2 | Test 1 | Test 2 | Test 1 | Test 2 | Test 1 | Test 2 |
| Trivial | 16.02 | 16.42 | 20.27 | 19.81 | 18.75 | 18.43 | 0.00 | 0.00 |
| LIN | 3.56 | 3.42 | 4.69 | 4.57 | 4.60 | 4.38 | 0.94 | **0.95** |
| LIN-I | 3.44 | 3.36 | 4.58 | 4.42 | 4.52 | 4.21 | 0.94 | **0.95** |
| ANN-FF | 3.04 | 2.90 | 4.30 | **4.26** | 4.19 | **4.11** | **0.95** | **0.95** |
| ANN-LR | **2.49** | **2.38** | **4.25** | 4.68 | **4.10** | 4.55 | **0.95** | 0.94 |
| GPR | 3.16 | 3.25 | 4.77 | 5.25 | 4.64 | 5.09 | 0.94 | 0.93 |
| SVM | 3.40 | 3.44 | 5.20 | 5.91 | 5.05 | 5.83 | 0.93 | 0.90 |
| ANFIS | 3.35 | 3.30 | 4.83 | 4.37 | 4.68 | 4.31 | 0.94 | **0.95** |

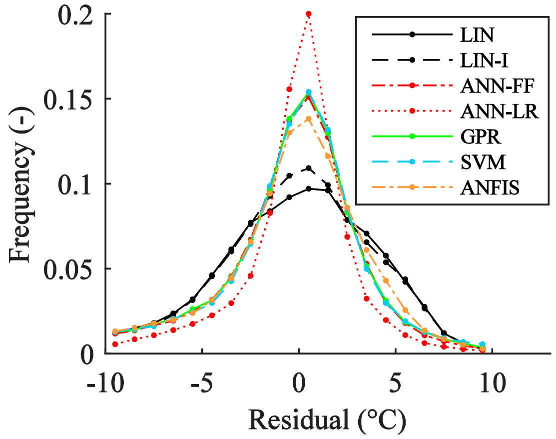


**Figure 5.** Median residual distribution for generator temperature prediction for test 1.

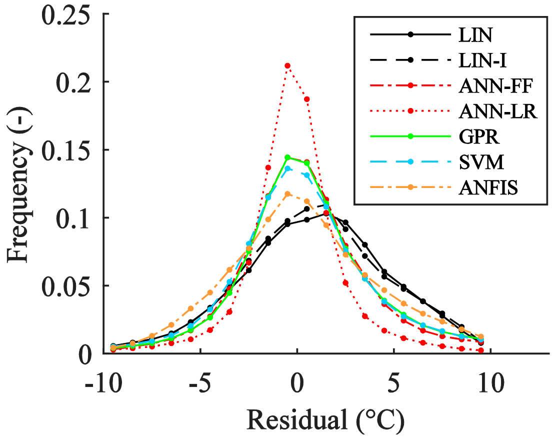


**Figure 6.** Median residual distribution for generator temperature prediction for test 2.

### *4.2. Sensitivity to input selection*

The RMSE is plotted for the different input configurations in figure 7 and figure 8 for bearing and generator temperature prediction, respectively. For simplification, results from test 1 and 2 are merged by presenting the inferior value from both tests. Using the optimal lag from the CC instead of simultaneous inputs is not beneficial in general. Also, more inputs do not lead to higher accuracy for all approaches. A moderate RMSE reduction trend is visible for linear and ANN modelling approaches if more inputs are used. SVM and ANFIS tend to have larger errors with more inputs. If both simultaneous and lagged inputs are used, the error is only smaller for all results in linear and ANN-FF modelling. There is no clear trend for the other approaches. The optimal setting is found for the RMSE metric in configuration 3c and ANN-FF modelling, although LIN, LIN-I and ANN-LR show very similar accuracy. A detailed comparison for this configuration is given in table 5 and table 6 for bearing and generator temperature prediction, respectively. For the bearing temperature modelling ANN-FF performs best in all median values of the metrics. However, LIN-I shows similar accuracy for the median value and is generally a better performer in terms of the mean values of the metrics, suggesting that it is less affected by outliers. ANN-LR performs well in terms of the median metric, but significantly less well with respect to mean values. The results of the generator temperature modelling show that both ANN approaches perform most accurately here if the median metric values are compared. For ANN-LR the inferior performance in terms of the mean indicates again that the approach performs poorly for some turbines.

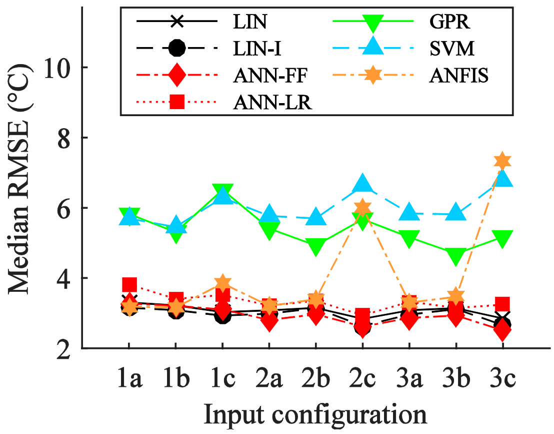


**Figure 7.** Input sensitivity study for bearing temperature prediction.

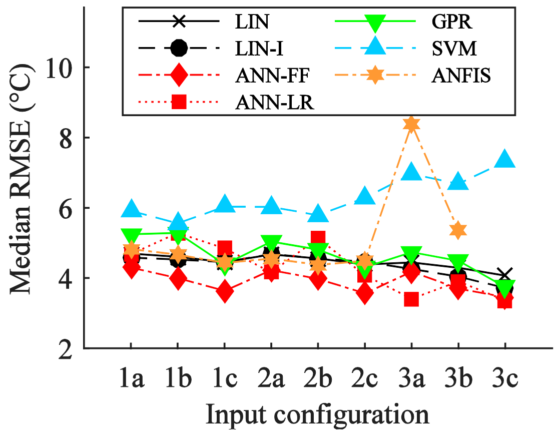


**Figure 8.** Input sensitivity study for generator temperature prediction. ANFIS modelling was not completed for configuration 3c due to excessive runtimes.

**Table 5.** Performance for bearing temperature modelling in configuration 3c.

| | MAE (°C) | | RMSE (°C) | | STDE (°C) | | $R^2$ (-) | |
|---|---|---|---|---|---|---|---|---|
| | Median | Mean | Median | Mean | Median | Mean | Median | Mean |
| LIN | 2.04 | 2.31 | 2.85 | 3.16 | 2.62 | 2.90 | 0.87 | 0.86 |
| LIN-I | 1.84 | 2.09 | 2.66 | **2.88** | 2.48 | **2.69** | 0.89 | **0.87** |
| ANN-FF | **1.68** | **1.99** | **2.51** | 3.00 | **2.39** | 2.81 | **0.90** | 0.84 |
| ANN-LR | 1.83 | 2.87 | 3.24 | 4.89 | 2.98 | 4.34 | 0.84 | 0.04 |
| GPR | 2.67 | 2.93 | 5.18 | 5.47 | 4.99 | 5.09 | 0.56 | 0.52 |

**Table 6.** Performance for generator temperature modelling in configuration 3c.

| | MAE (°C) | | RMSE (°C) | | STDE (°C) | | $R^2$ (-) | |
|---|---|---|---|---|---|---|---|---|
| | Median | Mean | Median | Mean | Median | Mean | Median | Mean |
| LIN | 3.19 | 3.41 | 4.07 | 4.37 | 4.00 | 4.23 | 0.96 | 0.95 |
| LIN-I | 2.50 | 2.80 | 3.71 | 4.01 | 3.64 | 3.87 | 0.96 | **0.96** |
| ANN-FF | 2.33 | **2.61** | 3.46 | **4.00** | 3.29 | **3.85** | **0.97** | 0.95 |
| ANN-LR | **2.05** | 3.45 | **3.37** | 6.29 | **3.22** | 5.77 | **0.97** | 0.47 |
| GPR | 2.31 | 2.64 | 3.74 | 4.09 | 3.60 | 3.96 | 0.96 | 0.95 |

### *4.3. Comparison of computational effort*

Table 7 gives the training and testing runtimes for the different modelling approaches and different configurations. The computational effort is insignificant for linear modelling. SVM and ANN-FF are trained in about two seconds, but ANN-LR and GPR require 10 and 20 seconds, respectively. The runtime for ANFIS increases significantly with the number of inputs with less than a second for a configuration with 2 inputs and nearly 30 minutes per turbine for 7 inputs.

**Table 7.** Average runtime for model training and testing per turbine in seconds.

| Configuration | Bearing, 1a, test 1 | Generator, 1a, test 1 | Bearing, 2a, test 2 | Bearing, 2b, test 1 | Bearing, 2c, test 1 | Generator, 3a, test 2 | Bearing, 3c, test 1 |
|---|---|---|---|---|---|---|---|
| Inputs | 2 | 2 | 3 | 3 | 5 | 4 | 7 |
| LIN | 0.02 | 0.02 | 0.02 | 0.02 | 0.02 | 0.02 | 0.02 |
| LIN-I | 0.02 | 0.02 | 0.02 | 0.02 | 0.03 | 0.02 | 0.05 |
| ANN-FF | 2.36 | 2.28 | 2.17 | 2.26 | 2.43 | 2.24 | 2.61 |
| ANN-LR | 11.84 | 10.14 | 15.42 | 10.99 | 14.38 | 11.10 | 18.63 |
| GPR | 18.86 | 19.86 | 17.42 | 17.99 | 17.50 | 21.05 | 17.94 |
| SVM | 2.49 | 1.92 | 2.51 | 2.52 | 3.12 | 2.18 | 3.54 |
| ANFIS | 0.67 | 0.65 | 1.60 | 1.62 | 32.93 | 6.41 | 1702.63 |

## 5. Conclusion

Normal behaviour modelling of two wind turbine drive train temperatures has been investigated with modelling approaches based on linear systems, ANNs, ANFIS, SVM and GPR. In a case study with real SCADA data from more than hundred turbines' inputs for modelling were selected following a detailed correlation analysis. All investigated approaches predict the target temperatures with good accuracy. Best results are obtained for linear, ANN and ANFIS modelling in a basic configuration with two input signals. GPR modelling works well for the generator temperature prediction, but less well for the bearing temperature prediction. Modelling with SVM results in distinctly higher errors for both targets. Results of a two-fold cross-validation indicate that there is a seasonal impact in the modelling since the residuals are differently skewed for different training periods. In a sensitivity study, the impact of adding inputs and introducing time lagged signals is investigated. The results indicate that most approaches perform better with more inputs, except for SVM and ANFIS. The computational effort is significant for ANN-LR and GPR independent of the number of inputs and for the ANFIS model if five or more inputs are used. If the different variants of approaches are compared, it can be noted that adding interactions to linear models is beneficial, whereas introducing recurrence in the ANN model seems to be only helpful for some turbines, but leads to inferior performance for others. Adequate input selection with appropriate delay may be a better way to increase the accuracy, although the simple selection of delay based on averaged correlation analysis results does not work in general.

Investigations of filtering out non-operational times (similar to [17]) and a sensitivity study of the training length and number of neurons in an ANN have been the subjects of preliminary investigation, but are not included in this paper due to length limitations. Further research will continue to find suitable approaches for optimal selection of inputs for temperature modelling. In particular ANN-FF and linear modelling will be investigated with more inputs using approaches such as stepwise adding and removing of inputs. Finally, the failure detection capabilities of the normal behaviour models developed in this research need to be tested with real data containing recorded failures. It is intended to compare the approaches with auto-regressive and state estimation techniques to evaluate the differences in failure detection in more detail. Different advanced alarm concepts like the Mahalanobis distance [16] and abnormal level index [17] will be compared.

**Acknowledgement**

This project has received funding from the European Union's Horizon 2020 research and innovation programme under the Marie Sklodowska-Curie grant agreement No 642108 (Advanced Wind Energy Systems Operation and Maintenance Expertise, http://awesome-h2020.eu/).

**References**

[1] Bloomberg New Energy Finance 2015 [cited 2016-04-28] *Wind and solar boost cost-competiveness versus fossil fuels* [Internet] available from: http://about.bnef.com/press-releases/wind-solar-boost-cost-competitiveness-versus-fossil-fuels/

[2] Milborrow D 2014 [cited 2016-03-29] *The tide turns on offshore maintenance costs* [Internet] available from: http://www.windpoweroffshore.com/article/1314299/tide-turns-offshore-maintenance-costs

[3] Feng Y, Qiu Y, Crabtree C J, Long H and Tavner P J 2013 Monitoring wind turbine gearboxes *Wind Energy* **16** 728–40

[4] Wiggelinkhuizen E, Verbruggen T, Braam H, Rademakers L, Xiang J and Watson S 2008 Assessment of Condition Monitoring Techniques for Offshore Wind Farms J. *Sol. Energy Eng.* **130** 031004–1 – 031004–9

[5] Yang W, Tavner P J and Court R 2013 An online technique for condition monitoring the induction generators used in wind and marine turbines *Mech. Syst. Signal Pr.* **38** 103–12

[6] Catmull S 2011 Self-Organising Map Based Condition Monitoring of Wind Turbines *EWEA Annu. Conf. 2011*

[7] Kim K, Parthasarathy G, Uluyol O, Foslien W, Sheng S and Fleming P 2011 Use of SCADA data for failure detection in wind turbines *ASME 5th Int. Conf. Energy Sustain.* 2071–9

[8] Garcia M C, Sanz-Bobi M A and del Pico J 2006 SIMAP: Intelligent System for Predictive Maintenance Application to the health condition monitoring of a windturbine gearbox *Comput. Ind.* **57** 552–68

[9] Garlick W G, Dixon R and Watson S J 2009 A Model-based Approach to Wind Turbine Condition Monitoring using SCADA Data *20th Int. Conf. Syst. Eng.*

[10] Zaher A, McArthur S D J, Infield D G and Patel Y 2009 Online wind turbine fault detection through automated SCADA data analysis *Wind Energy* **12** 574–93

[11] Schlechtingen M and Santos I F 2010 Comparative analysis of neural network and regression based condition monitoring approaches for wind turbine fault detection *Mech. Syst. Signal Pr.* **25** 1849–75

[12] Kusiak A and Verma A 2012 Analyzing bearing faults in wind turbines: A data-mining approach *Renew. Energy* **48** 110–6

[13] Schlechtingen M, Santos I F and Achiche S 2013 Wind turbine condition monitoring based on SCADA data using normal behavior models. Part 1: System description *Appl. Soft Comput.* **13** 259–70

[14] Wilkinson M, Harman K, van Delft T and Darnell B 2014 Comparison of methods for wind turbine condition monitoring with SCADA data *IET Renew. Power Gen.* **8** 390–7

[15] Cross P and Ma X 2015 Model-based and fuzzy logic approaches to condition monitoring of operational wind turbines *Int. J. Autom. Comput.* **12** 25–34

[16] Bangalore P and Tjernberg L B 2015 An Artificial Neural Network Approach for Early Fault Detection of Gearbox Bearings *IEEE Trans. Smart Grid* **6** 980–7

[17] Sun P, Li J, Wang C and Lei X 2016 A generalized model for wind turbine anomaly identification based on SCADA data *Appl. Energy* **168** 550–67

[18] Wang Y and Infield D 2012 Supervisory control and data acquisition data-based non-linear state estimation technique for wind turbine gearbox condition monitoring *IET Renew. Power Gen.* **7** 350–8

[19] Rasmussen C E and Williams C K I 2006 *Gaussian Processes for Machine Learning* (London: MIT Press)

[20] Smola A J and Scholkopf B 2004 A tutorial on support vector regression *Stat. Comput.* **14** 199–222

# Neural Networks for Wind Turbine Fault Detection via Current Signature Analysis

Raed K Ibrahim, Jannis Tautz-Weinert, Simon J Watson

Centre for Renewable Energy Systems Technology (CREST)
Wolfson School of Mechanical, Electrical and Manufacturing Engineering
Loughborough University, Loughborough, LE11 3TU, United Kingdom

R.Ibrahim@lboro.ac.uk, J.Weinert@lboro.ac.uk, S.J.Watson@lboro.ac.uk

**Abstract** – Cost-effective condition monitoring techniques are required to optimise wind turbine maintenance procedures. Current signature analysis investigates fault indications in the frequency spectrum of the electrical signal and is thereby able to detect mechanical faults without additional sensors. Due to the modern variable speed operation of wind turbines, fault frequencies are hidden in the non-stationary frequency spectra. In this work, artificial neural networks are applied to identify faults under transient conditions. The feasibility of the detection algorithm is demonstrated with a wind turbine SIMULINK model, which has been validated with experimental data. A framework is proposed for developing and training the algorithm for different rotational speeds. A simulation study demonstrates the ability of the algorithm not only to detect faults, but also to identify the strength of the faults as required for fault prognosis.

**Keywords** – Wind Turbine, Condition Monitoring, Fault Detection, Current Signature Analysis, Neural Networks, Variable Speed.

## 1 Introduction

With an increasing number of wind turbines (WTs) being installed in offshore and remote locations, there is a need for cost-effective maintenance. Predictive maintenance aims to detect condition changes early and enables maintenance teams to schedule the required work considering other limiting factors as e.g. weather conditions. For this reason, a reliable condition monitoring system (CMS) is required to detect and diagnose WT failures in their early stages.

In order to develop an effective CMS, the best solution for two characteristics of the system must be found:

- A signal providing information to describe the state of the monitored component.
- A technique to extract the condition state from the signal.

The most simple, but sufficient accurate solution has to be determined to reduce maintenance costs by giving reliable results and avoiding unnecessary equipment. Generally, the signals used in common WT CMSs include vibration, acoustic emission, strain, torque, temperature, lubrication oil quality, electrical output, and supervisory control and data acquisition (SCADA) system signals [1]-[2]. Among them, vibration is the most well-known signal used in a WT CMS [3]-[4]. However, analysis of electrical signals from the generator has been shown to have advantages over vibration signals for condition monitoring as the costs and complexity involved in current measurements are significantly lower [5-6]. Additional installation costs are avoided because current signals are already continuously measured in WTs [7].

Current Signature Analysis (CSA) utilises the knowledge that mechanical faults as rotor unbalance show up in increased amplitudes in the sidebands of harmonics of the fundamental frequency. However, it is a challenge to extract WT fault signatures from current measurements under variable speed operation. Moreover, the useful information in current measurements from a WT usually has a low signal to noise ratio, and thus it is very difficult to extract this information in a reliable way.

Extracting the fault signature from a monitored signal is commonly done by the well-known fast Fourier transform (FFT) and the short–time Fourier transform (STFT) [9]-[10]. However, in the case of variable speed WTs, FFT and STFT often fail to extract the required information which can vary in the time-domain, since the operation is predominately non-stationary due to variations in the wind speed.

The attractive feature of Artificial Neural Networks (ANNs) for condition monitoring is their ability to represent complex, nonlinear relationships through learned pattern recognition or signal regression. ANNs have been successfully used to identify changes in the relationships between SCADA signals that indicate the development of a failure [10].

In this work, the possibility of detecting mechanical faults in wind turbines by CSA is investigated. The application of Artificial Neural Networks (ANN) for detecting mechanical faults is proposed to automate the fault detection in the light of the limitations of spectral analysis in processing signals subject to transient effects. The diagnosis of rotor unbalance in a WT is used as an illustrative example. The simulation results demonstrate that the proposed method is effective in detecting mechanical faults in a variable speed machine.

## 2 Methodology

This research aims to develop a reliable technique to detect mechanical faults in a WT via the generator current signal. An ANN technique is proposed to automate the fault detection in a variable speed machine. The main purpose of using an ANN is to identify changes in the current signal which have non-stationary characteristics due to the variable-speed operating conditions of WTs, and to provide online fault detection in advance of catastrophic failures.

The data used in this work is based on a WT simulation model. The model is developed and validated with operational data of five 2.5MW turbines recorded by the SCADA system over the period of 1 year. The measured data recorded at 32Hz sampling frequency included wind speed, wind direction, pitch angle, rotational speed and three-phase power output. The model parameters used are detailed in Table 1.

The required phases of the algorithm development and testing for an online fault detection tool are given in Table 2.

**Table 1: Model parameters.**

| Parameter | Value |
|---|---|
| Cut-In, Rated, Cut-Out Wind Speed | 3 m/s, 12 m/s, 25 m/s |
| Rated Tip Speed | 80 m/s |
| Rotor Diameter | 90 m |
| Gearbox Ratio | 1:77.4 |
| Line-Line Voltage (RMS) | 690V |
| Frequency | 50Hz |
| Pole Pairs | 3 |
| Rated Generator Speed (RPM) | 1000 |

**Table 2: Phases of the project.**

| Phase | Task |
|---|---|
| 1 | Development of simulation tool providing current signal |
| 2 | Validation of simulation with experimental data |
| 3 | Training and testing of automated fault detection with simulation |
| 4 | Validation of fault detection with experimental current signal |
| Final | Online fault detection with current signal |

In the following, the methodology behind the simulation model, CSA and the ANN fault detection are presented.

### 2.1 Wind turbine SIMULINK model

A general model for representation of variable speed wind turbines was implemented in MATLAB/Simulink, including wind speed, rotor, pitch control system, drivetrain and generator model [11]. The model has been developed to facilitate the investigation of condition monitoring and effective algorithm development for fault detection. The measured wind speed recorded by a wind turbine SCADA system has been used as model input to validate the response of the wind turbine model. Figure 1 shows the response of the model compared with measured generator speed. It is visible that the model is in good agreement with the measured data.

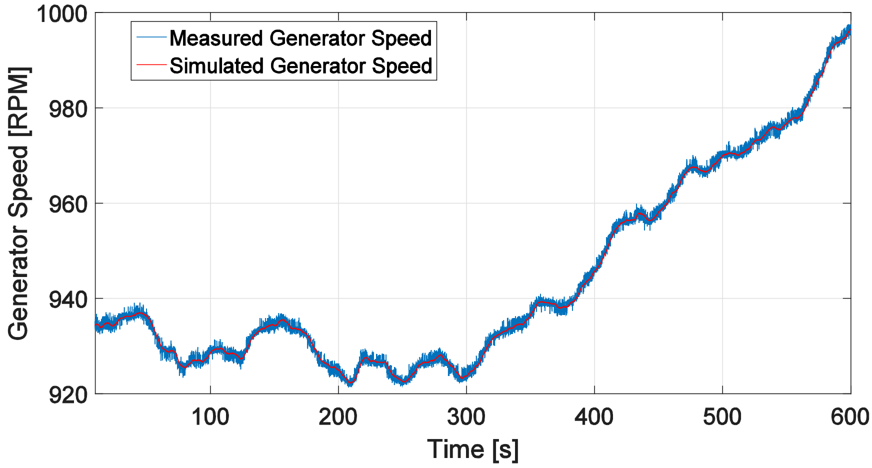


**Figure 1: Model validation considering generator speed.**

Rotor eccentricity is used as an illustrative example to investigate the use of the proposed fault detection algorithm in variable speed WTs. During rotor eccentricity, certain sideband harmonics around the fundamental frequency in the machine current signal occur with increased amplitudes proportionally to the fault level. It was experimentally proven [5] that rotor eccentricity faults give rise to a sequence of such sidebands given by:

$$f_C = \left(1 \pm \frac{2k-1}{p}\right) f \tag{1}$$

where $f_C$ and $f$ are the rotor fault and fundamental frequency, respectively, $k$ is an integer $(k = 1, 2, 3, \ldots)$ and $p$ is the number of pole pairs. The fundamental frequency in a variable speed WT with a permanent magnet synchronous generator (PMSG) is proportional to the rotational speed, i.e. the characteristic of the signal is varying with time.

Figure 2 shows the stator current spectra for a faulty and healthy machine for fixed rotational speed. Components with frequencies at 60 Hz and 34Hz are intentionally induced in the healthy machine spectrum to represent machine-specific noise close to the fault frequencies. The fault frequencies identified by the equation (1) are labelled in Figure 2.

## 2.2 Automated fault detection with Artificial Neural Networks

A simple detection threshold for the fault frequencies is not feasible due to the variable speed operation and accordingly shifting frequencies.

ANNs are useful for automated processing and finding non-linear relationships. With data-driven training, ANNs learn to weight different inputs in a way to deliver the required output. Problem-specific settings have to be found in particular for the number of neurons and the amount of training required.

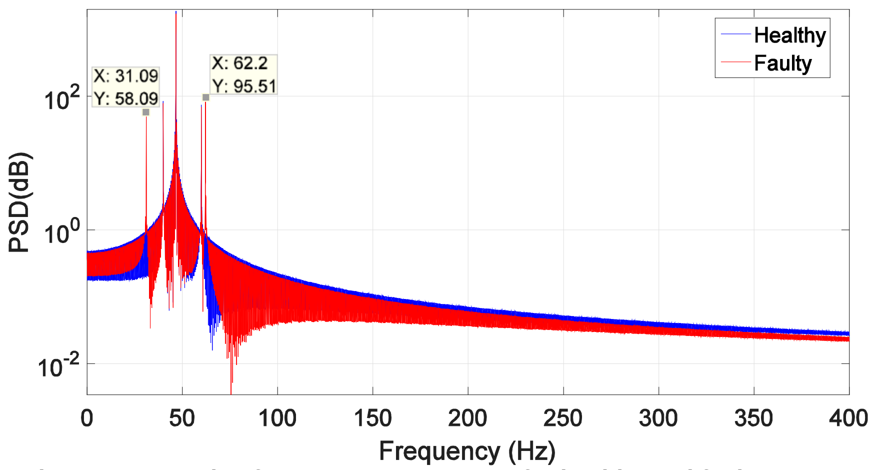


**Figure 2: Example of stator current spectra for healthy and faulty states.**

The rotational speed $\omega$ of a PMSG turbine varies significantly. Fault detection for all possible rotational speeds is not feasible with a single ANN. A framework is proposed, in which different networks are used for different ranges of rotational speeds, as sketched in the workflows in Figure 3 and Figure 4. In the training phase, $n$ sets of different rotational speeds ($\Omega$) with defined limits $\omega_{\min}$ and $\omega_{\max}$ are used for simulation of the current signals. The sets are selected in a way that all possible speeds are covered. For each of the sets, an ANN is trained to detect a fault. In the detection phase, maximum (max), minimum (min) and-standard deviation ($\sigma$) are calculated for each two second record. If the variation in the rotational speed is relatively high, the frequency spectrum becomes indistinct. Accordingly, the standard deviation of the set has to go below a defined limit $\sigma_L$ to allow further processing. The appropriate ANN for fault detection with the FFT of the current signal is selected with the information of the rotational speed extrema.

In this paper, the feasibility of the framework is discussed by investigating the training of one network for a limited rotational speed variation.

## 2.3 Simulation study

In a first simulation study the ability to differentiate between healthy and faulty stages is tested. The second study investigates fault degree detection with different fault strengths where the fault level has been simulated by increasing the magnitude of the sideband harmonics as an indication to the fault with higher level.

### 2.3.1 Fault classification

The WT model is run for healthy and faulty condition with a selected variable speed variation between 924 and 937 rpm as shown in Figure 5. Analysis of the real SCADA data suggested such a variation in 5 minutes.

For each condition, the current signal is recorded for 300 seconds at 5 kHz sampling frequency. Periods of two seconds of data are selected for analysis using the Fast Fourier Transform (FFT) algorithm. This window length is identified as the shortest possible with a sufficient resolution to capture all harmonics of interest. The frequency spectrum of each window consisting of 250 amplitudes acts as a 'sample' for ANN fault detection. All samples from healthy and faulty stages are mixed and randomly split in training and testing. A classification as 'healthy' or 'faulty' is trained with scaled conjugate gradient backpropagation. The number of neurons and training samples are varied in a sensitivity study. Network training is repeated a number of times to investigate the impact of the random selection of training samples.

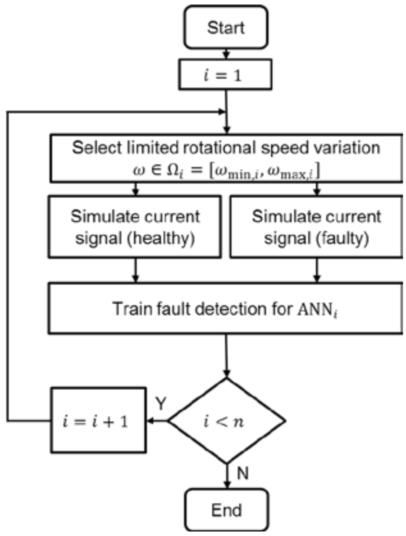


**Figure 3: Workflow for training of fault detection algorithm.**

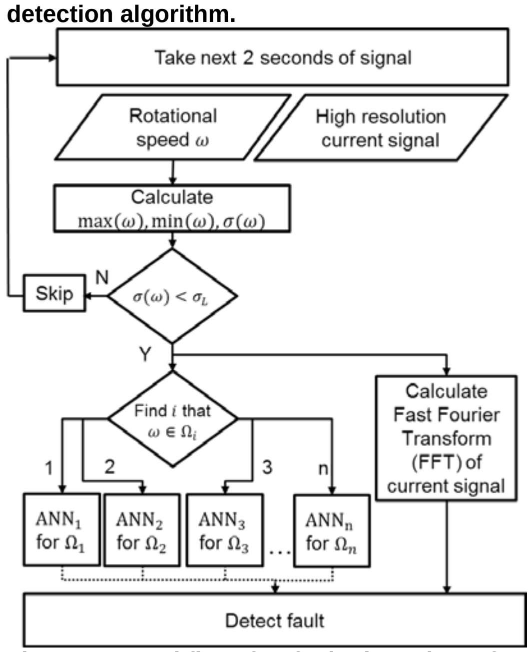


**Figure 4: Workflow for fault detection after training.**

### 2.3.2 Fault degree detection

Additional to the above described two simulations representing permanent healthy and faulty condition, two further runs are used to investigate fault development. The first simulation applies a linear increasing fault during 300 seconds. In the second run a fault occurs only at a certain point in the simulation.

A fitting neural network with a tansig transfer function in the output layer is used to predict a fault degree between 0 and 1. All samples from the first simulation plus 100 randomly selected samples of the linear increasing fault simulation are used for training the ANN. Network training is repeated with identical data to illustrate differences resulting from suboptimal training.

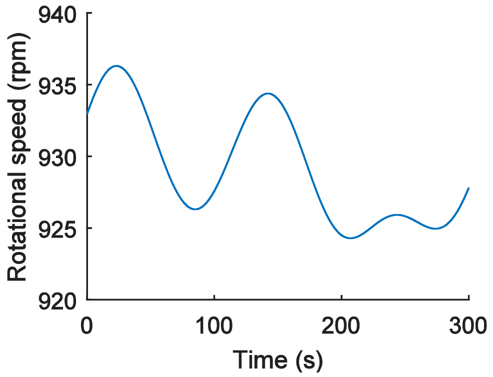


**Figure 5: Rotational speed variation in simulation study.**

# 3 Results of simulation study

## 3.1 Fault classification

The results of the simulation study with current signals from healthy and faulty conditions are presented in Table 3 considering accuracy as correct classification of both 'healthy' and 'faulty' stages. The median detection accuracy between 93.5 and 98 % for different ANN and training length configurations distinctly higher than random classification (50 % accuracy) shows that ANN fault detection using current signals under non-stationary conditions is feasible.

**Table 3: Accuracy of ANN condition detection from frequency spectrum given as median percentage from 250 training repetitions.**

| Number of neurons used: | Training with 100 samples, testing with 200 samples | Training with 150 samples, testing with 150 samples | Training with 200 samples, testing with 100 samples |
|---|---|---|---|
| 2 | 93.5 | 96.7 | 98.0 |
| 5 | 94.5 | 96.7 | 98.0 |
| 10 | 95.5 | 97.3 | 98.0 |
| 25 | 95.5 | 97.3 | 98.0 |
| 50 | 95.0 | 97.3 | 98.0 |

## 3.2 Transient and variable fault detection

Results of the transient and variable fault detection are presented in Figure 5 and 6. Although the significant differences between three ANNs trained with the same input indicate that further optimisation of training and algorithm settings might be reasonable, the general fault development is successfully detected. Unsurprisingly, the fault degree detection is less accurate than the simple healthy or faulty classification. Regardless, even the rough detection of the strength of a fault enables better monitoring of condition changes.

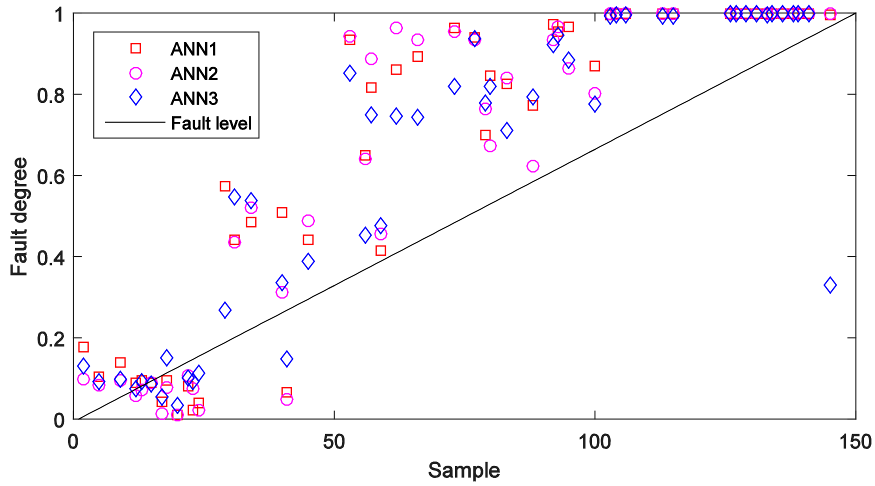


**Figure 5: ANN fault degree detection of a linear increasing fault.**

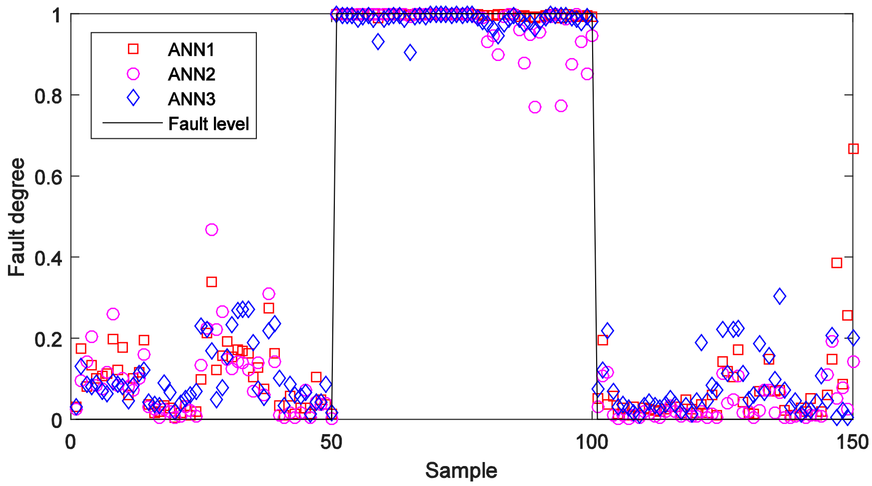


**Figure 6: ANN fault detection of a transient fault.**

# 4 Conclusion

A technique to detect mechanical faults in variable speed WTs via the CSA and ANN is proposed. A framework is discussed for training of fault detection with simulated signals from faults for later online detection in real WTs. For each set of limited rotational speed variation a separate ANN will detect the fault.

In a simulation study of a rotor imbalance under varying rotational speed as expected in 5 minutes operation the feasibility of the fault detection approach is demonstrated. Simple classification of healthy or faulty condition is achieved with a high accuracy. In a further step towards fault prognosis, the severity of the fault is successfully detected.

Future work has to be done to validate the fault detection algorithm with experimental data. A full test of the proposed framework has to be conducted including different sets of rotational speed variation. In terms of fault prognosis, optimisation of the ANN settings might increase the fault degree detection accuracy.


# Acknowledgement

This project has partly received funding from the European Union's Horizon 2020 research and innovation programme under the Marie Sklodowska-Curie grant agreement No 642108 (Advanced Wind Energy Systems Operation and Maintenance Expertise, http://awesome-h2020.eu/).


# References


[1] B. Lu, Y. Li, X. Wu, and Z. Yang, "A review of recent advances in wind turbiine condition monitoring and fault diagnosis," in Proc. *2009 IEEE symposium on Power Electronics and Machines in Wind Applications*, Lincoln, NE, 2009, p p. 1-7.

[2] Z. Hameed, Y. S. Hong, Y. M. Cho, S. H. Ahn, and C. K. Song, "Condition monitoring g and fault detection of wind turbines and related algorithms: A review," *Renewable and Sustainable Energy Reviews*, vol. 13, pp. 1-39, 2009.

[3] Qiao, Wei, and Dingguo Lu. "A Survey on Wind Turbine Condition Monitoring and Fault Diagnosis—Part II: Signals and Signal Processing Methods," in *IEEE Transactions on Industrial Electronics,* vol. 62, no. 10, pp. 6546-6557, Oct. 2015.

[4] Tchakoua, P., Wamkeue, R., Ouhrouche, M., Slaoui-Hasnaoui, F., Tameghe, T.A. and Ekemb, G., "Wind turbine condition monitoring: State-of-the-art review, new trends, and future challenges." *Energies* 7, no. 4 (2014): 2595-2630.

[5] Gong, Xiang, and Wei Qiao. "Current-based mechanical fault detection for direct-drive wind turbines via synchronous sampling and impulse detection." *Industrial Electronics, IEEE Transactions* on 62.3 (2015): 1693-1702.

[6] S. Djurovic, C. J. Crabtree, P. J. Tavner and A. C. Smith, "Condition monitoring of wind turbine induction generators with rotor electrical asymmetry," in *IET Renewable*

*Power Generation*, vol. 6, no. 4, pp. 207-216, July 2012.

[7] J. P. Barton and S. J. Watson, “Analysis of electrical power data for condition monitoring of a small wind turbine,” *IET Renewable Power Generation*, vol. 7, no. 4, pp. 341–349, 2013.

[8] W. Yang, P. Tavner, and M. Wilkinson, “Condition monitoring and fault diagnosis of a wind turbine synchronous generator drive train,” *IET Renewable Power Generation*, vol. 3, no. 1, pp. 1–11, 2009.

[9] Z. Hameed, Y. Hong, Y. Cho, S. Ahn, and C. Song, “Condition monitoring and fault detection of wind turbines and related algorithms: A review,” *Renewable and Sustainable energy reviews*, vol. 13, no. 1, pp. 1–39, 2009.

[10] P. Bangalore and L. B. Tjernberg, “An Artificial Neural Network Approach for Early Fault Detection of Gearbox Bearings,” *IEEE Trans. Smart Grid*, vol. 6, no. 2, pp. 980–987, Mar. 2015.

[11] R. K. Ibrahim and S. Watson, “Wind turbine simulation model for the study of combined mechanical and electrical faults,” in *Scientific Track Proceedings of European Wind Energy Association. EWEA*, 2015.